CR 86309

DESIGN OF THE ADVANCED REMOTE OCULOMETER

By John Merchant and Ronald Wilson

September 1969

Prepared Under Contract No. NAS12-531
Honeywell Radiation Center
Lexington, Massachusetts 02173

ELECTRONICS RESEARCH CENTER
NATIONAL AERONAUTICS AND SPACE ADMINISTRATION
575 Technology Square
Cambridge, Massachusetts 02139

Matthew Hillsman
Technical Monitor
NAS 12-531
Electronics Research Center
575 Technology Square
Cambridge, Massachusetts 02139

Requests for copies of this report should be referred to:

NASA Scientific and Technical Information Facility
P.O. Box 33, College Park, Maryland 20740

DESIGN OF THE ADVANCED REMOTE OCULOMETER

By John Merchant and Ronald Wilson

September 1969

Prepared Under Contract No. NAS12-531
Honeywell Radiation Center
Lexington, Massachusetts 02173

ELECTRONICS RESEARCH CENTER
NATIONAL AERONAUTICS AND SPACE ADMINISTRATION
575 Technology Square
Cambridge, Massachusetts 02139

TABLE OF CONTENTS

TABLE OF CONTENTS (cont.)

APPENDICES

LIST OF ILLUSTRATIONS

LIST OF ILLUSTRATIONS (cont.)

APPENDICES

LIST OF TABLES

LIST OF SYMBOLS

W_{pc} = main photocathode signal

x_n, y_n = noise levels

N_1 = number of electrons/ms collected in present case

N_2 = number of electrons/ms collected in reference 2

D_2 = aperture diameter in reference 2

D_1 = aperture diameter in present case

T = minimum frame time in seconds

N = number of lines/frame

W = fraction of line width subtended by a minimum dia. pupil

S = detection level threshold in electrons/s

θ = angular mirror motion

α = angular acceleration

T_{FE} = minimum frame time

β = out-of-focus blur diameter

x = lens displacement

M = mass of the lens and carriage

p = pitch of the screw

T = torque applied to screw

F = force transmitted by screw

u, v = image and object distances for lens

K_r = effective reflectivity of retina

τ = transmission factor of eye

d = diameter of eye pupil

ρ = apparent pupil reflectivity

a = anterior focal length of eye

F_β = reciprocal of effective angular size of blur circle caused by accommodation error

δD = accommodation error due to ametropia

ρ_o = iris reflectivity

R = range

ψ = angle of rotation

DESIGN OF THE ADVANCED REMOTE OCULOMETER

By John Merchant and Ronald Wilson

Honeywell Radiation Center
Lexington, Massachusetts

SUMMARY

The Oculometer is a device that measures eye direction without attachment* to the subject, without causing interference to the subject and which can operate at up to several feet from the subject.

The development of the Oculometer has been supported by NASA to provide a much needed means of accurately monitoring eye fixations without subject interference, and also as a possible new means of human control - eye control. With eye control the subject will perform a pointing or tracking task by eye, instead of by manual control.

This report presents a design of the optomechanical part of a remote Oculometer intended for laboratory or simulator use, and capable of being easily developed (by careful packaging design) into a flight unit which would fit into the space normally occupied by a standard 3-inch instrument panel. As part of this design effort, experimental work has been performed to provide certain optical design information. The principal results of the present design program are:

1) Detailed characteristics of the optical signal received by the Oculometer from the eye.

2) Optimized optical design allowing for operation with almost all subjects under almost all conditions.

* In most applications of the remote Oculometer the subject will be required to wear a 1-inch diameter, 0.2 inch thick, head marker.

3) Development of a new fail safe xenon arc illumination system, for improved ambient discrimination.

4) Development of an accommodation sensing technique that is incorporated into the new Oculometer design.

5) Design of an automatic focussing system to permit axial head motions.

6) Specification of all optical elements, and their relative placement in the new remote Oculometer.

THE OPTICAL-MECHANICAL SUBSYSTEM

The remote Oculometer optical-mechanical subsystem consists of:

1) a source of near IR radiation.
2) an optical system to direct this radiation at the eye.
3) an optical system to image the IR illuminated eye onto the electro-optical sensor system.
4) an electro-optical sensor system
5) a servo controlled moving mirror system to allow for gross x and y axis head motion.
6) a servo controlled autofocussing system to allow for gross z axis head motion.

The optical-mechanical subsystem is constructed out of three units.

1) the lamp house unit (plus lamp power supply).
2) the main unit (sensor tubes and most of the optics).
3) the moving mirror box (attached to, but demountable from, the main unit).

The lamp house unit is connected to the main unit by a flexible fiber optics relay. An electronics subsystem (not described in this report) will connect with the optical-mechanical subsystem to constitute the complete, operating, instrument. The interconnection of the two subsystems is shown in Figure 1.

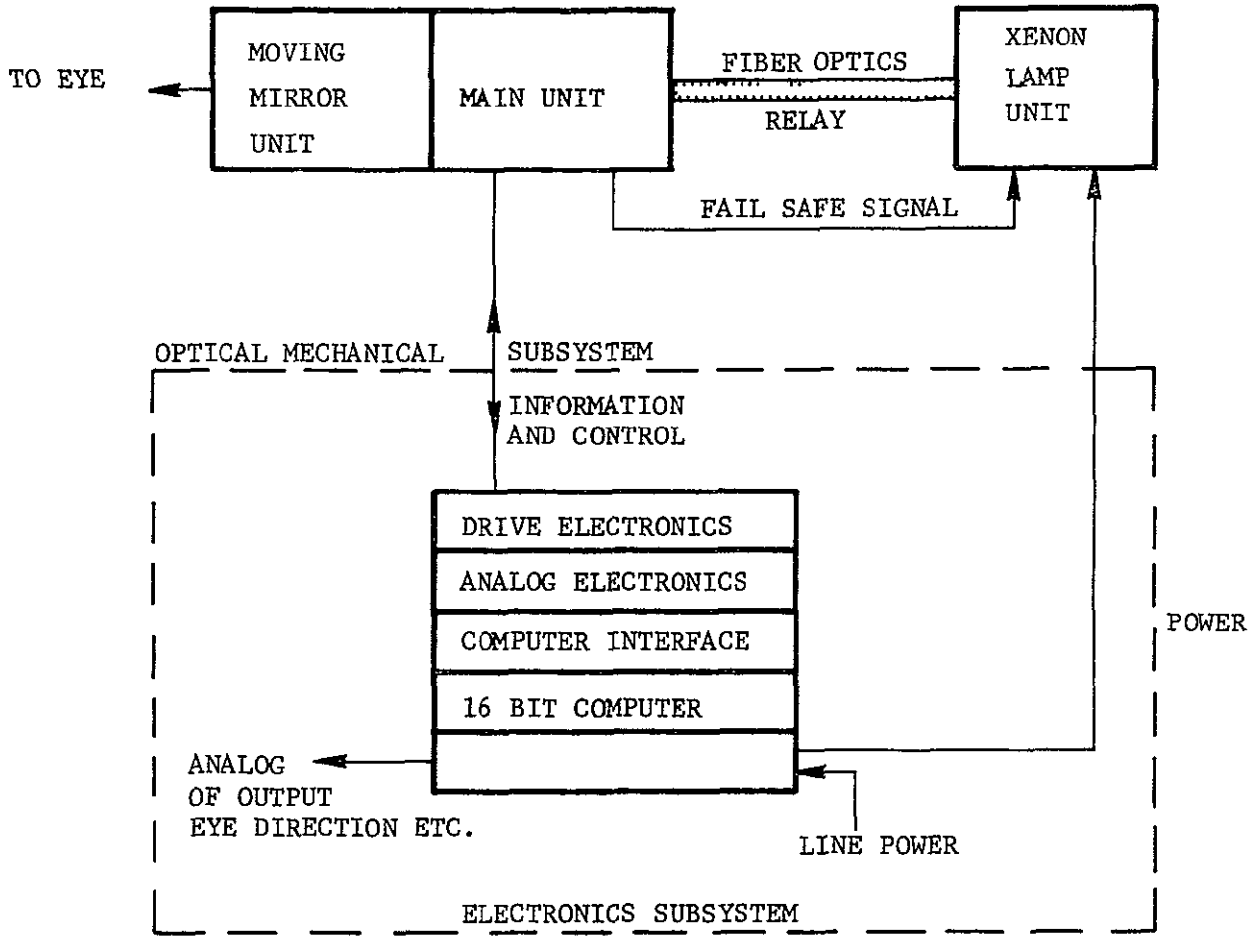

Figure 1.--Overall System Interconnection

A cutaway illustration of the remote Oculometer optical-mechanical unit is shown in Figure 2.

Optical-Mechanical Subsystem Components

A xenon short arc lamp is located in the lamp house unit. This unit is connected to the main unit by an incoherent fiber optics relay. The lamp radiation is filtered to remove all radiation outside the band 8250 ± 50 Å. The filtered radiation is collected by an aspheric condenser and focussed onto the fiber optics faceplate.

The other end of the fiber optics relay is located in the main unit. Radiation is collected from the output faceplate by an aspheric condenser. A telephoto lens system, consisting of a servo controlled movable positive lens and a manually controlled negative lens, directs the radiation to the eye. An identical telephoto lens combination images the illuminated eye onto the photocathode of a 1-inch image dissector tube. The illuminator telephoto lens system images a 0.75-inch diameter area of the aspheric condensor collecting lens onto a 1-inch diameter region at the eye onto a 0.75-inch diameter area of the photocathode.

The positive lenses, in the two identical telephoto systems, are carried on the same movable carriage and can be moved together, over a range of about 2 inches by means of a motor driven lead screw. The negative lenses are also mechanically ganged together and are moved manually by turning an external knob.

A fraction of the illuminating radiation is directed onto a silicon detector which monitors the level of the illuminating radiation to provide:

a) automatic lamp shutdown in the event of an increase above a preset threshold.
b) visual monitoring (via a meter) of lamp intensity to indicate when the lamp is aging.

The illuminator optical path joins with the collection optical path at the system beam splitter. The path to the eye from this point is via an adjustable iris diaphragm which is used to set the correct system f/number and a two-axis moving mirror system. The moving mirror allows the 1-inch diameter instantaneous eye space region to be deployed over a 12-inch x 12-inch region.

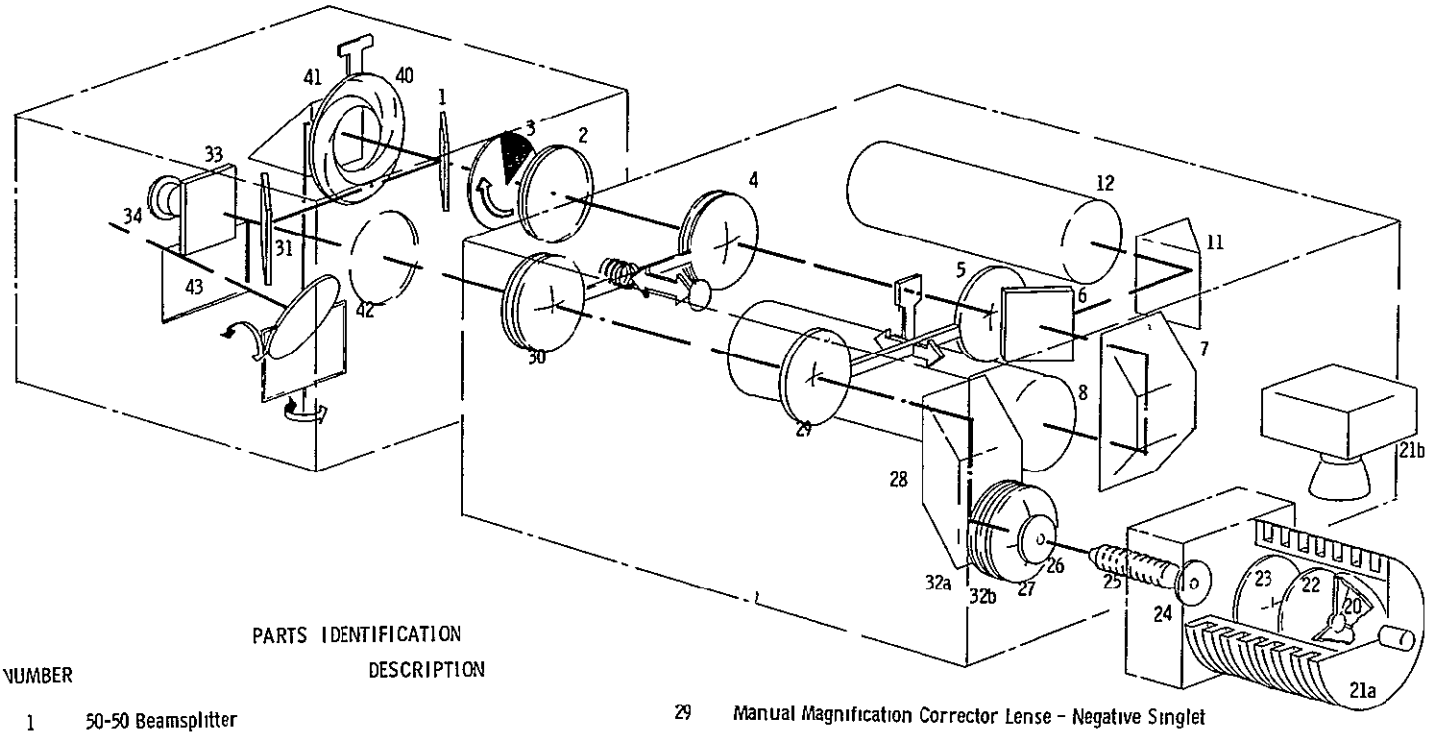

PARTS IDENTIFICATION

NUMBER	DESCRIPTION
1	50-50 Beamsplitter
2	Narrow Band Infrared Filter
3	Rotating Occluded Aperture
4	Automatic Focussing Lense Positive Doublet
5	Manual Magnification Corrector Lense Negative Singlet
6	75-25 Beamsplitter
7	Trapezoidal Prism-Specialized Use
8	Image Dissector 5 Mil Aperture
11	Right Angle Prism
12	Scanning Photomultiplier
20	Xenon Arc Source Varian X6163S
21	Cooling Fins And Blower
22	Narrow Band Infrared Filter
23	Aspheric Condensing Lense
24	Aperture
25	Totally Incoherent Fiber Optics Bundle
26	Aperture
27	Aspheric Condensing Lense
28	Rhomboidal Prism-Specialized Use
29	Manual Magnification Corrector Lense - Negative Singlet
30	Automatic Focussing Lense Positive Doublet
31	Narrow Band Hot Mirror
32	Broad Band Filter
33	Narrow Band Hot Mirror
34	Silicon Detector
40	Manually Variable Iris Diaphram
41	Right Angle Prism
42	Scanning Mirror - Dual Axis
43	Exit Window

Figure 2.--Remote Oculometer - Cutaway

A special rotating aperture is located in the collector optical path, just before the beam splitter (Figure 2). It consists of a 90° opaque wedge, the apex of which is on the optical axis. The wedge is rotated at about 4,000 rpm by a motor/tachometer combination. This rotating aperture generates focus error information. It also provides, as described later, a means of sensing accommodation information.

The telephoto lens system in the collector path forms an image of a 1-inch region of eye space on the 0.75-inch active area of the photocathode of a 1-inch image dissector tube. A fraction (about 25%) of the radiation being directed to the image dissector tube is split off after the negative lens and this fraction is used to form an identical eye space image on the photocathode of a 1-inch scanning photomultiplier tube. The reason for having two tubes is that a small scanning aperture is desirable (in the image dissector) for accurate tracking whereas a large scanning aperture (in the scanning photomultiplier) is desirable for rapid acquisition.

To provide for rapid acquisition, the subject being monitored by the Oculometer will wear a small piece of silver coated corner reflecting material near his eye. A silver coated hemisphere lens will be fixed to the center of the reflector, as shown in Figure 3, to provide a small point source (by convex reflection) against a dark background for preliminary focus information.

The optical-mechanical subsystem is defined in more detail in the set of Oculometer optomechanical subsystem drawings:

F2100-3109 Drawing	Side view, collection optics.
F2100-3111 Drawing	Side view, illumination optics.
F2100-3112 Drawing	Top view, collection and illumination optics.
F2100-3116 Drawing	Lens, and lens slide, arrangement.
F2100-3114 Drawing	Two-axis mirror.
F2100-3113 Drawing	Rotary aperture detail.
F2100-3117 Drawing	Xenon lamp detail.
F2100-3115 Drawing	Head marker detail.
F2100-3108 Drawing	Fail safe circuit.
F2100-3008 Drawing	Motor Assembly.

Additional information is contained in the specification sheets associated with the drawings, (see Appendix B).

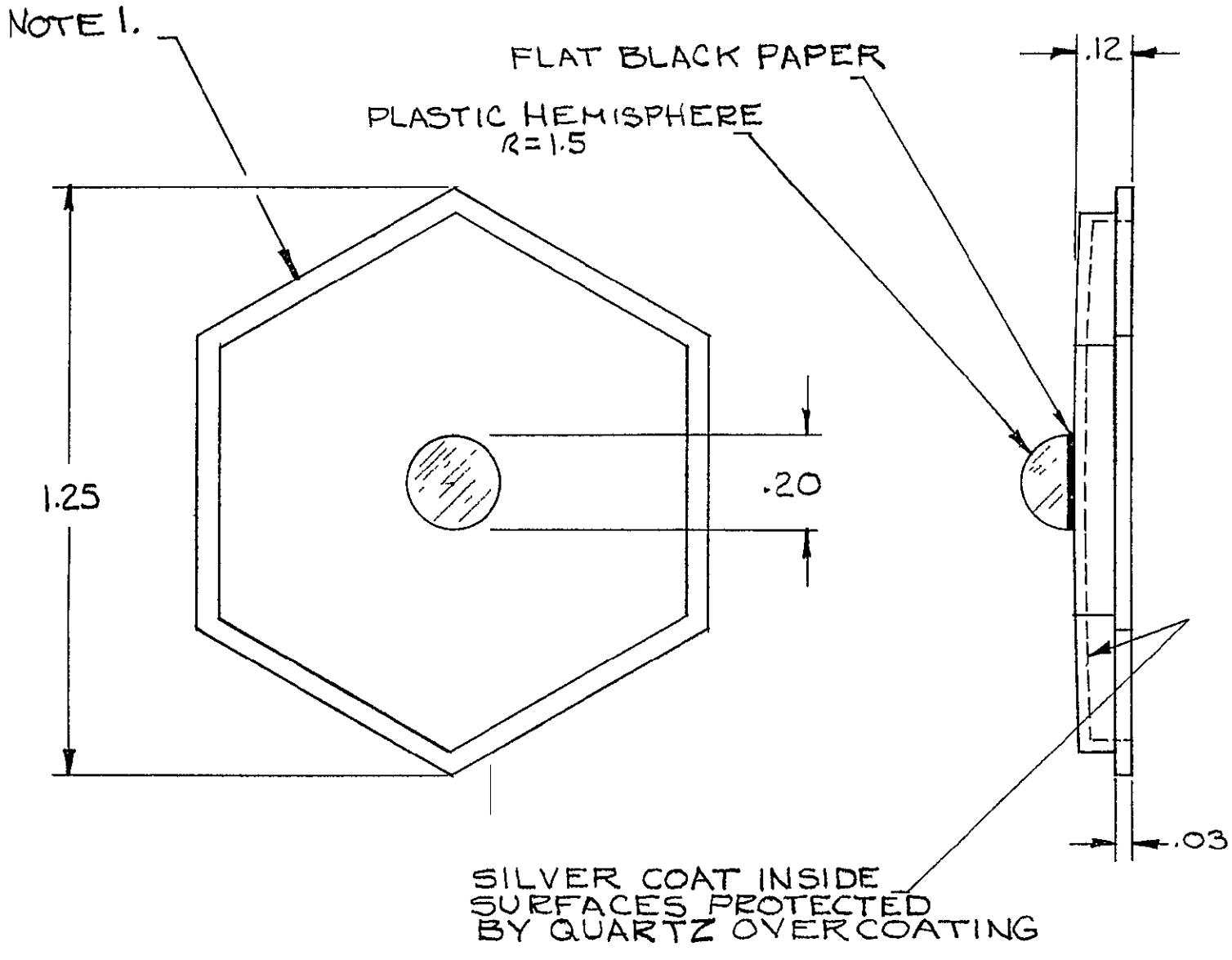

Figure 3.--Head Marker Detail

Operating Procedure For The Optical-Mechanical Subsystem

A nominal range, from mirror to eye, will be selected (any value from 28-40 inches). The negative lens manual position knob will be turned so as to position the negative lens correctly for the selected nominal range. This will be done either by

1) Setting up an artificial pupil target at the desired nominal range and adjusting the negative lens position, with the system tracking the pupil, until the scan diameter (as read out from the electronics unit) has the correct value.

or,

2) Positioning the negative lens correctly (by means of a calibrated dial associated with the negative lens position control knob) according to a precalculated table of values.

The iris diaphragm defining the common illumination and collection system aperture must then be set to a value corresponding to F/60 at the nominal range. The optical-mechanical subsystem is then ready for operation.

The system will have a number of modes of operation. They are shown in Figure 4. Initially, the moving mirror system will execute a raster motion which will cause the 1-inch diameter beam of Oculometer illumination to be scanned over the 12-inch x 12-inch region of eye space. If the beam intercepts the head marker, a large optical signal will be reflected back to the Oculometer. This will be picked up by the image dissector tube, and, when detected in the electronics system, cause the scanning mirror motion to be stopped and replaced by a marker tracking motion. While the head marker is being tracked by the moving mirrors and the image dissector, focus information will be generated so that the system will also be tracking in the z axis (focus tracking). After sharp focus has been achieved, the moving mirror will deploy the 1-inch instantaneous field of view to the eye. An electronic search will then be made for the pupil and corneal reflection, leading finally to a normal track mode (Mode 8 in Figure 4).

On a definite loss of track indication, the electronics system will initiate a predetermined search procedure which will result in regaining normal track as soon as possible.

1. Normal marker search
2. Marker pupil search
3. Market pupil track/corneal search
4. Marker pupil track/corneal track/focus track (using corneal reflection)
5. Deploy to eye
6. Pupil search
7. Pupil track/corneal search/focus track (using pupil)
8. Pupil track/corneal track/focus track (using corneal reflection).

LOSS OF TRACK SEQUENCE (ON PUPIL AND CORNEAL LOSS)

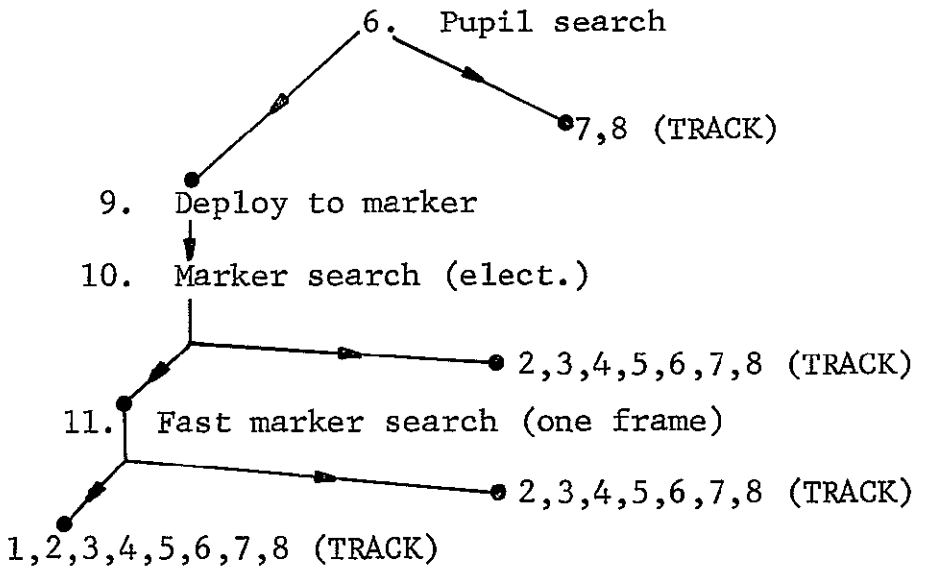

Figure 4.- Modes Of Operation

OPTICAL-MECHANICAL SUBSYSTEM PERFORMANCE SUMMARY

The ouput radiation level of the Oculometer that is directed at the eye will be that of a 1.5 watt/cm^2/steradian source having an angular diameter of 1/60 radian.

The radiation collected from the eye pupil will generate 5.5×10^4 signal electrons per second at the image dissector with a pupil having unity apparent reflection factor. This will give a total pupil tracking rms noise level equivalent to 0.24 degree of eye motion. The pupil radiation directed to the auxiliary sensor will generate 3×10^6 electrons/s - yielding a pupil search time of less than 10 ms.

The moving mirror system will execute a frame of raster search (for the head marker) in 340 ms at the continuous motor rating. At the peak rating of the motor, the frame time is 187 ms. The peak rating will be used for one frame only in a fast marker search mode, if necessary, after a blink; that is, if the eye is not immediately reacquired by an electronic search. In the track mode the mirror performance exceeds the maximum velocity and acceleration characteristics of head motion by about two orders of magnitude.

The autofocus system consists of an out-of-focus sensor and a motor driven focussing lens. The out-of-focus sensing system will have unity signal/noise ratio, over 0.01 s for a 0.4-mil diameter geometric blur circle. In practice, focussing to a blur circle of 5 mils will be all that is required because the system is diffraction limited at this value. The dynamic response of the motor driven focussing lens system will follow head velocities and accelerations well in excess of the maximum possible head motions.

The auto focussing system will maintain sharp focus for all axial head motions within ±6 inches of the nominal range. The magnification (eye space - photocathode) will have its nominal value (0.75 inch) when the eye is exactly at the nominal range. As the eye moves about within ±6 inches of the nominal range the magnification will change. In the worst case the magnification change will be:

Nominal range 28 inches:

eye 22 inches from the moving mirror: M = 0.898
eye 28 inches from the moving mirror: M = 0.750
eye 34 inches from the moving mirror: M = 0.644

Other system parameters change with magnification, as indicated below:

Nominal Range	28 in.		
Actual range to eye	22 in.	28 in.	34 in.
Scanning aperture diameter at eye (mils)	5.8	7	8.2
f/number	50	60	70
Instantaneous eye space coverage	0.835 in.	1.00 in.	1.16 in.

The magnification can be set to the nominal value (0.75 in.), for any value of the nominal range from 28 to 40 inches, by manually changing the negative lens position.

OPTICAL-MECHANICAL SUBSYSTEM - COMPONENT DESCRIPTION

The Optical Mechanical Subsystem has been divided into eight sections in order to describe the function each performs in the overall system.

Optical System

The optical consists basically of two similar subsystems· collection optics and illumination optics (see Drawings F2100-3109, F2100-3111 and F2100-3112). The collection and illumination systems join at the system beam splitter (part No. 1 in Figure 2).

The collection system, itself, splits into two parts at a beam splitter (part No. 6) which shares the available radiation between an image dissector (main sensor and used for accurate tracking) and a scanning photomultiplier (auxiliary sensor, used primarily for rapid search).

The common telephoto system design (for illumination and collection optics) images the eye space onto a 0.75-inch region within the Oculometer. For the collection system this region is a photocathode.

For the illuminator system it is the central portion of an aspheric collection lens (part No. 26 and Figure 2), which is itself illuminated by rays diverging from a 0.06-inch diameter region of a fiber optics faceplate. This aspheric lens images the 0.06-inch fiber optics faceplate onto the iris diaphragm of the system (part No. 40) for the median position of the positive lens in the telephoto combination. A sufficiently large image of the fiber optics is formed at the iris so that the actual clear aperture is fully illuminated for all settings of the telephoto lens system.

Focussing.--The collection optical system images eye space on the image dissector tube to provide a constant magnification for different longitudinal eye positions. This is effected by shifting the negative element manually to an indicated position. Automatic focussing is then obtained by movement of the positive lens unit. Preset negative lens positions are provided for eye locations of 28 to 40 inches from the scan mirror. Additional head motion of ±6 inches is accommodated by the automatic focussing movement of the positive lens.

Lens position data.--Positional data of the lenses to provide a magnification of 0.75 over an equivalent path of 18.94 inches from the scan mirror to the detectors is given in Table I for four longitudinal eye positions.

Summary of lens data.-- Radii, thickness, and material data for the lenses and prisms are given in Table II.

Antireflection coatings are specified for prisms and lenses with maximum transmittance at 0.825 microns (see relevant drawings). No reflective coatings are required for the prisms. For maximum reflectivity, silver is specified for mirrors with a quartz protective overlay.

Image quality.--The optical system must be diffraction limited to have adequate resolution. It is also required that the image be essentially distortionless so that an accurate determination of eyeball angular position can be made.

The Oculometer optical system utilizes a relatively high f/ number, with which diffraction limited quality is, usually, easily obtained. However, in the, present case, a telephoto lens system is to be used in which the individual elements will be operating at much lower f/numbers. For this reason the telephoto lens will consist of three elements (instead of two as in a simple system) so that adequate quality can be achieved. Table III gives the spot

Table I

LENS POSITIONAL DATA AS A FUNCTION OF EYE POSITION

Distance of Eye to Scan Mirror (inches)	Change in Position of Positive Lens Unit (inches toward Detector)	Change in Position of Negative Lens Unit (inches toward Detector)
40	0	0
36	0.681	0.784
32	1.346	1.573
28	1.987	2.367

Table II

LENS DESCRIPTION

Element	Radii (inches)	Thickness (inches)	Clear Aperture (inches)	Material
1	6.8105 -69.219	0.200	1.16 1.16	SK5 (589 613)
2	5.3914 26.666	0.200	1.15 1.13	SK5 (589 613)
3	-61.003 1.3744	0.150	0.40 0.38	SF11 (785 258)
4(Porro Prism)	Plane	3.000	0.56 0.66	SK1—(610 567)

diameter containing 90% of the energy for four eye space longitudinal positions. Also given is the percent distortion at the edge of the field. Values at other points are readily determined from the cubic power variation of distortion with field. At full field, distortion is within 0.17% for all positions. Energy distributions on-axis and at full field, based on ray tracing, show the spot diameter to be within 0.003-inch for a bandwidth (half power) of ±5 millimicrons.

Tolerances.--Table IV gives the construction tolerances for the optical system.

System transmission factors.--The transmission factor of the various optical systems is estimated from the following (minimum) individual transmission factors:

Illumination System Transmission Factor.

Broad Banding Blocking Filter	0.9
Narrow Band Filter Transmission	0.7
Ultraviolet Rejection Filter	0.90
Fiber Optics	0.40
Silicon Detector Reflector	0.95
14 High Transmission Surfaces	0.86
Mixer	0.95
Beam Splitter	0.45
Total Transmission Factor	0.079

Main Collection System Transmission Factor

10 High Transmission Surfaces	0.90
Moving Mirror	0.95
Beam Splitter	0.45
Rotating Aperture	0.75
Auxiliary Sensor Beam Splitter	0.75
Narrow Band Filter	0.70
Total Transmission Factor	0.152

Auxiliary Sensor Collection System - This will be the same as for the main collection system except that the auxiliary sensor beam splitter will contribute a factor of 0.25. This gives a total transmission factor of 0.051.

Table III

IMAGE QUALITY (RAY TRACE ANALYSES)

Eye Position (inches)	Distortion Edge Field Point (%)	Spot Dia. at Eye 90% of Energy (on-axis)	Spot Dia. at Eye 90% of Energy (full field)
40.0	0.17	0.0025	0.0029
36.0	0.17	0.0026	0.0032
32.0	0.16	0.0029	0.0037
28.0	0.14	0.0037	0.0040

Table IV

TOLERANCES (COLLECTION OPTICS)

1. All lenses: Decentration ±0.004 inch

2. All lenses: Thickness ±0.004 inch

3. Radii of Curvature:

   Surface (1) ±0.007 inch
   (2) ±0.3 inch
   (3) ±0.005 inch
   (4) ±0.1 inch
   (5) ±0.3 inch
   (6) ±0.001 inch

4. Surface Regularity:

   Reflective Surfaces: 1/4 ring
   Refractive Surfaces: 1/2 ring

5. Surface Quality:

   All Surfaces: 60:40 *

6. Surface Angles:

   All Surfaces: ±2 minutes of arc

For the illumination optics, all tolerances relaxed by 10 times.

* See MIL-O-13830A: the first number refers to scratch defects, the other to dig (i.e., pits) defects.

The xenon lamp will deliver an effective source brightness of 0.2 W/cm^2/steradian/Å (see Section-Optical System Measurements). The system bandwidth is 100 Å so that the source radiance is 20 W/cm^2/steradian. The illumination system transmission factor is 0.079 so that the apparent source will be 1.58 W/cm^2/steradian (adjustment to the nominal operating level of 1.5 W/cm/steradian will be made by the focussing adjustment of the arc lamp into the fiber optics, and by adjustment of the electrical power supplied to the lamp).

For the purpose of this calculation, assume a pupil reflectivity of one. The main photocathode signal (W_{pc}) due to this pupil will be (at F/60):

$$W_{pc} = 1.1 \times 10^{-12} \text{ watts}$$

The image dissector tube will have an S25 surface having a specified sensitivity of 8 mA/watt at 0.825 μ. Thus the photocathode current, with the aperture fully covering the pupil will be:

$$1.1 \times 10^{-12} \times 8 \times 10^{-3} = 8.8 \times 10^{-15} \text{ A}$$
$$= 8.8 \times 10^{-15} \text{ coulomb/s}$$

$$\frac{}{1.6 \times 10^{-19} \text{ coulomb/electron}}$$
$$= 5.5 \times 10^{4} \text{ electrons/s}$$

From the calculation on pupil tracking signal noise ratio, given in Reference 2 p. 76 the rms noise level, over a 20 ms averaging time, will be,

$$(x_n^2 + y_n^2)^{1/2} \left(\frac{N_1}{N_2}\right)^{1/2} \frac{D_2}{D_1} \text{ inches.}$$

where x_n, y_n are the noise levels given in Reference 2, N_1 is the number of electrons per millisecond collected in the present case, N_2 the number collected per millisecond in the case of reference 2, D_2 is the aperture diameter (in mils) in the case of reference 2 and D1 is the aperture diameter in the present case.

i.e., rms noise level is

$$(.47^2 + .63^2)^{1/2} \left(\frac{55}{600}\right)^{1/2} \frac{20}{7} \approx 0.72 \times 10^{-3} \text{ inches}$$

or about 0.24 degree of eye motion.

The auxiliary sensor will utilize a 0.1-inch scanning aperture (referred to the eye). Thus, its pupil signal level will (allowing for the lower collection transmission factor) be 3×10^6 electrons/s.

To analyze the pupil acquisition time that this signal level will provide, we may assume that 100 electrons will reliably indicate an acquisition. In order to find a minimum diameter pupil, the raster lines should be 1.5 mm apart - i.e., a frame of about 15 lines is required. A 1.5 mm pupil transition will occupy about 1/15 line so that the minimum frame time is given by T;

$$\frac{T_x \; W}{N} \times R = S$$

where

T = the minimum frame time in seconds

N = number of line scans per frame

W = fraction of a line width subtended by a minimum diameter (1.5 mm) pupil

R = signal level rate in electrons/s

S = detection level threshold in electrons/s

that is

$$\frac{T}{15} \left(\frac{1}{15}\right) \times 3 \times 10^6 = 100$$

i.e.,

T = 6.8 milliseconds

Moving Mirror System

The 1-inch diameter instantaneous field of view of the system will be deployed over the required 12-inch x 10-inch eye space by means of a two axis moving mirror system. Approximately ±15 degrees of mirror motion is required (at the minimum range) to cover this field.

The dynamic performance of the mirror system is defined by the inertial load and the motor torque. The inertia in the horizontal axis is composed of the following components:

TQ 18-7 Aeroflex Motor. Rotor Inertia 6.7×10^{-4} oz/in./s^2

SSH 17-A-1 Clifton Resolver: Rotor Inertia 1.98×10^{-4} oz/in./s^2

Mirror about 1×10^{-3} oz/in./s^2

Total inertia $< 2 \times 10^{-3}$ oz/in./s^2

Continuous Torque Rating of Motor = 6 oz/in.

Frictional Torque < 1 oz/in.

Therefore, the angular acceleration of the mirror about the horizontal axis, at the continuous motor rating, is 2.5×10^3 rad/s^2.

The inertia in the vertical axis is composed, principally, of:

TA 18-7 Aeroflex Motor, 1.4 inch of Axis 2×10^{-2} oz/in./s^2

SSH 17-A-1 Resolver, Plus Balance Weight, 2×10^{-2} oz/in./s^2

TQ 25-2 Aeroflex Motor: Shaft Inertia 4×10^{-3} oz/in./s^2

SSH 17-A-1 Resolver: Shaft Inertia 1.98×10^{-4} oz/in./s^2

Total Inertia = 5×10^{-2} oz/in./s^2

Continuous Torque Rating of Motor = 25/oz/in.

Therefore, the angular acceleration of the motor about the vertical axis, at the continuous motor rating, is 500 rad/s^2.

The angular velocity at which the back EMF generated by the motor will reduce torque by 50% (with a constant voltage source) is 100 rad/s for the horizontal axis and 30 rad/s in the vertical axis.

Performance in the head marker search mode.--In the head marker search mode the mirror will be made to execute a raster motion in order to sweep the 1-inch instantaneous field of view over the 12-inch x 12-inch region of eye space.

The minimum time to execute a raster line is defined by the angular mirror motion (θ) required (6/22 radians at the worst case minimum range) and the angular acceleration (α) available. In the horizontal axis (elevation motion of the raster) the minimum frame time (T_{FE}) is given,

$$T_{FE} = 2\sqrt{\frac{\theta}{\alpha}} = 2\sqrt{\frac{6/22}{2.5 \times 10^{3}}} \approx 2.1 \times 10^{-2} \text{ s}^2$$

In the vertical axis,

$$T_{FE} = 2\sqrt{\frac{\theta}{\alpha}} = 2\sqrt{\frac{12/22}{5 \times 10^{2}}} \approx 5.6 \times 10^{-2} \text{ s}^2$$

In order to completely cover the required region, at the maximum range (34 inches), each raster line must subtend 1 3/4 radian. Thus,

$\frac{12}{22} \times 34 \approx 19$ lines are required.

Complete coverage is not required, however, since the scanning photomultiplier can search for part of the head marker. Twelve lines will, therefore, be sufficient. Thus the frame time is given by,

$$T_F = 12 \times 2.1 \times 10^{-2} \text{ s}$$
$$= 340 \text{ ms}$$

At the peak torque rating (20 oz/in.) of the horizontal axis motor (which can be employed for at least 30 seconds) the frame time is reduced to,

$$T_F = \sqrt{6/20}\ 340 = 187 \text{ ms}$$

Performance in the track mode.--In the track mode the maximum transient eye motion that will occur is:

a) Saccade: 800 degrees/s of eye velocity or 4.5 in./s
6,000 degrees/s^2 of eye acceleration or 34 in./s^2

b) Head Motion: From Figure 13, maximum velocity is 70 in./s
maximum acceleration is 700 in./s^2

In the worst case, minimum range, condition the peak eye motion condition becomes (in terms of mirror angle),

$$\text{velocity } \frac{70}{2 \times 22} = 1.6 \text{ rad/s}$$

$$\text{acceleration } \frac{700}{2 \times 22} = 16 \text{ rad/s}^2$$

These figures are well below the limiting performance figures of the horizontal and vertical drive systems (500 rad/s^2, 30 rad/s and 1,500 rad/s^2, 100 rad/s).

Step mode.--The time to execute a step change of position of 2 inches)typical displacement from eye to head marker) will be about 10 ms at the continuous motor rating.

AUTOFOCUS SYSTEM

The defining aperture of the collection optical system will be a clear F/60 circle with a 90-degree opaque wedge, as shown in Figure 5. This aperture will rotate at about 4000 rpm.

The magnitude and sign of any out-of-focus condition will be determined by sensing the effect of this unsymmetrical rotating aperture on the corneal reflection image.

For the purpose of explanation, assume that the corneal reflection is a point source and - apart from out-of-focus blur - is imaged as a point. Under these conditions, the image of the corneal reflection in the general out-of-focus condition is a sharp image of the defining aperture (Figure 6). Note that the size of the image is proportional to the degree of out-of-focus and that the orientation of the image relative to the orientation of the defining aperture depends upon the sign of the out-of-focus condition. In the normal operation of the Oculometer, the corneal

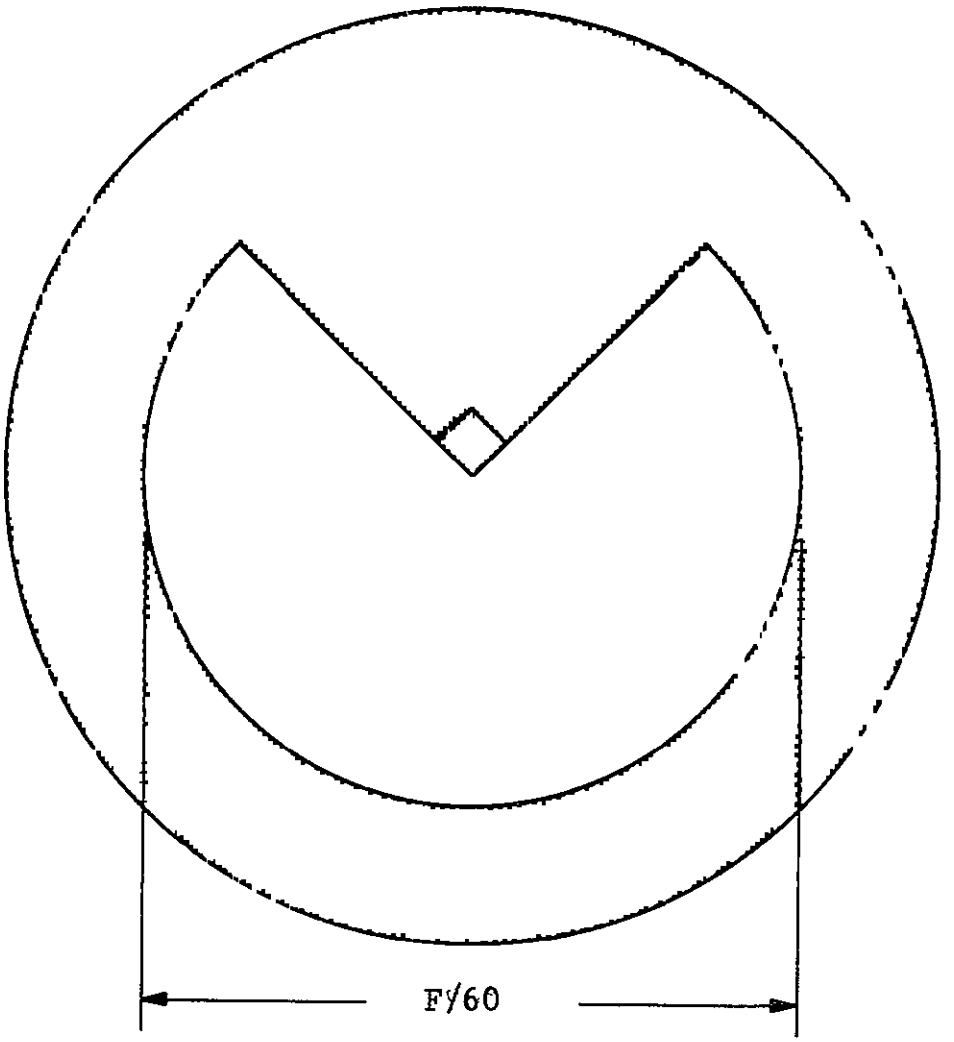

Figure 5.--Collection Aperture

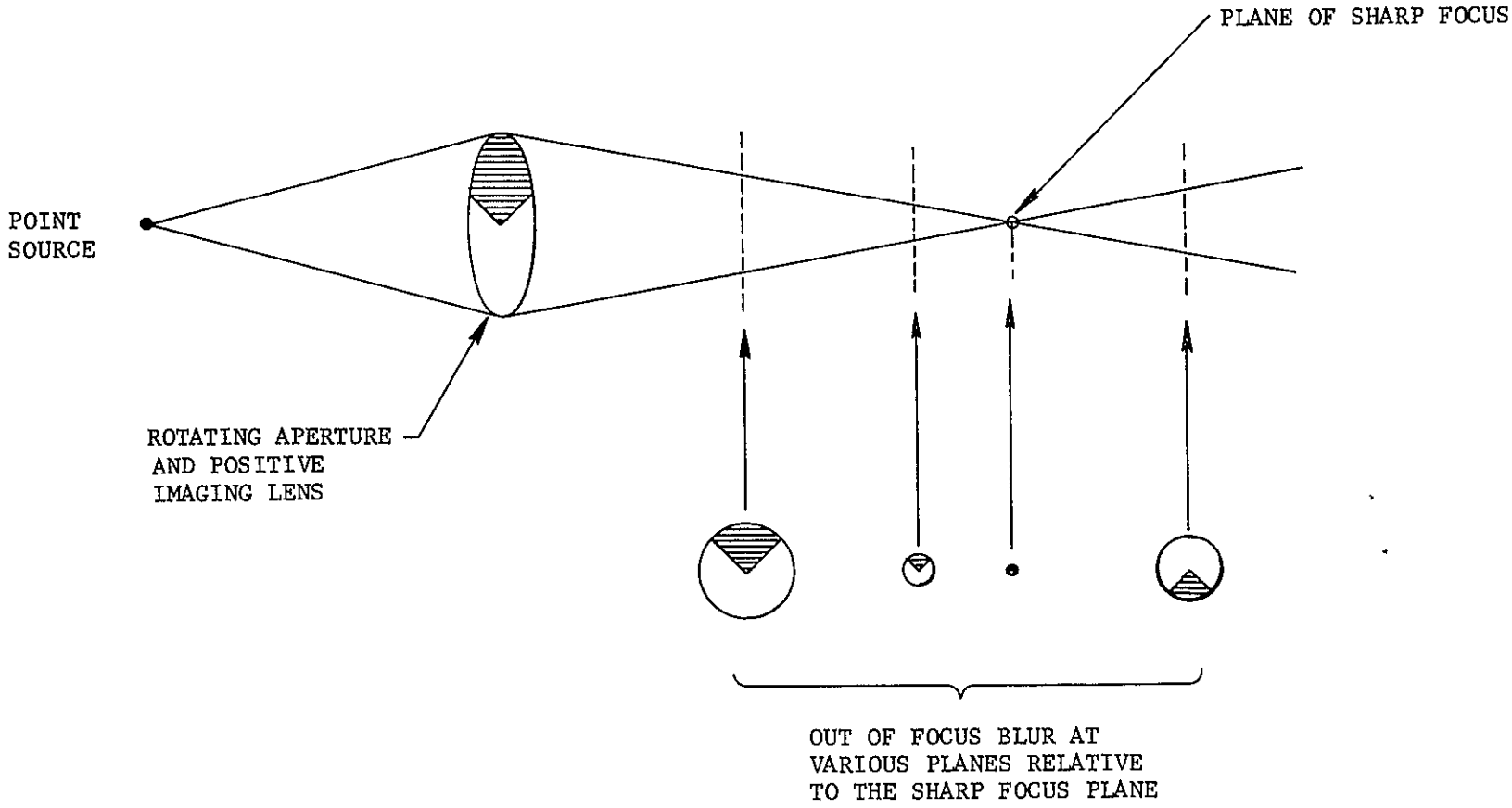

Figure 6.--Out-Of-Focus Effect Of Rotating Aperture

reflection image is scanned around the image dissector aperture in a circular scan of diameter equal to the diameter of the aperture (Figure 7). It is clear that, in the ideal case, the image dissector output will have a sinusoidal modulation impressed upon it. The magnitude of this modulation will vary with the out-of-focus condition as shown in Figure 8. Note that the phase of the sinusoid changes abruptly as this (ideal) system goes through the exact focus condition.

In actual practice the corneal reflection is not an ideal point and the optical system is not perfect due to diffraction and geometrical blur. The net effect is that the corneal image in the sharp focus condition will be a finite blur diameter instead of an ideal point. The effect of this blur can be most easily seen by defining an effective image dissector aperture profile as the convolution of the actual aperture with the sharp focus image of the corneal reflection (see Figure 9). Applying this aperture to the situation given in Figure 7 it can be seen (Figure 10) that one band of the aperture contributes a positive modulation (as in the ideal case of Figure 7) but a more peripheral band contributes a negative modulation component of lower intensity. The net effect is the same as in Figure 7 but the modulation level is lower (Figure 10).

As a result of the finite slope of the edges of the effective aperture profile, the relationship between modulation level and degree of out-of-focus will be not as in Figure 8 but rather as in Figure 11. This modulation will be at approximately 100 Hz (the circular scan frequency ± the asymmetrical aperture rotation frequency).

The immediate effect of this modulation will be to cause the corneal scan to be slightly displaced. Thus, in an out-of-focus condition, the corneal tracking system will perform a circular scan, at about 66 Hz, around the nominal position of the corneal reflection. The magnitude of this 'scan wander' will be proportional to the out-of-focus condition and the direction of the 'scan wander' will define the sign of the out-of-focus condition.

This sinusoidal modulation, synchronized with the motion of the rotating unsymmetrical collection aperture, will be recovered from the tracking loops by demodulation by a reference sinusoid generated by a tachometer attached to the rotating aperture.

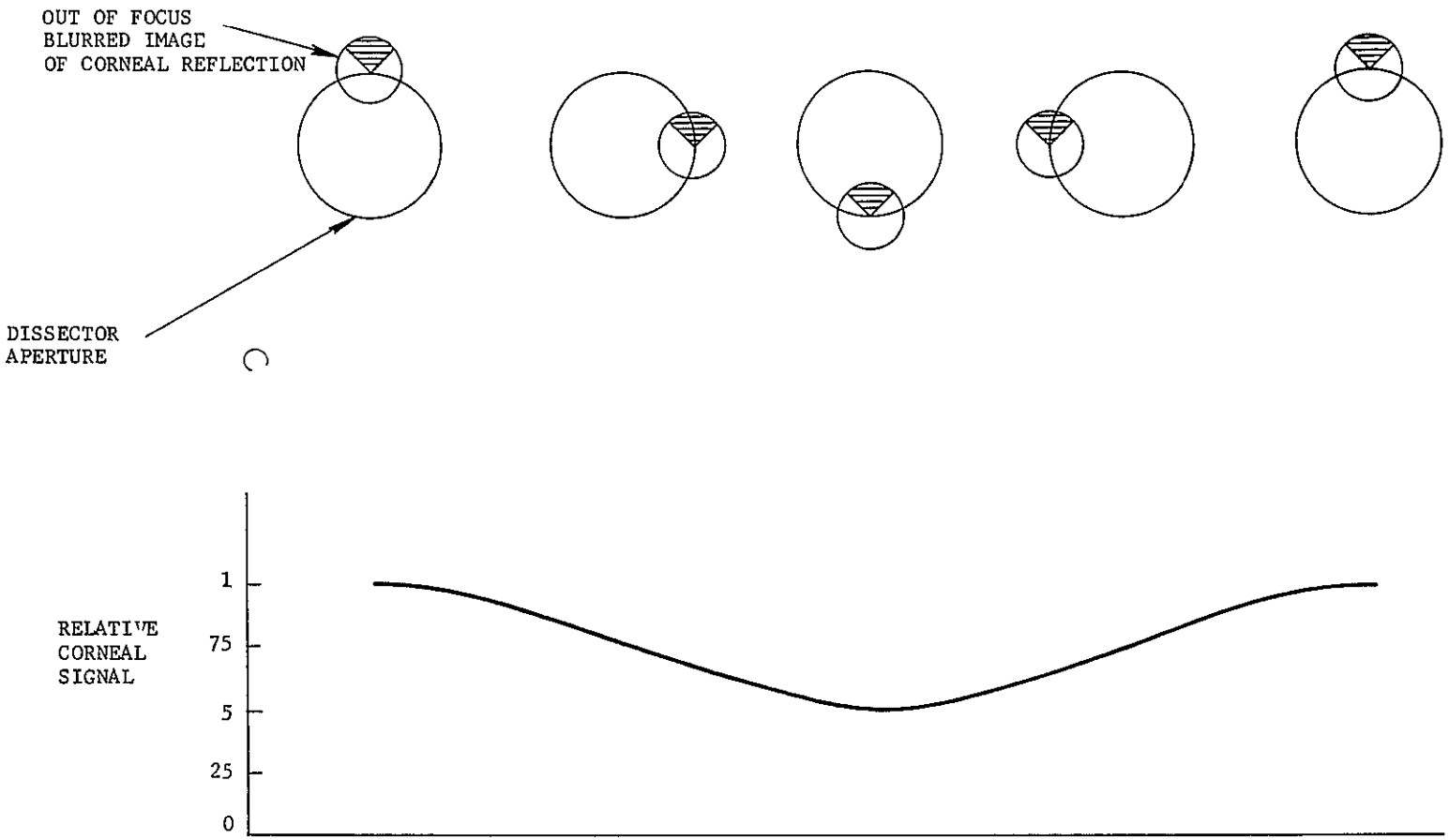

Figure 7.--Modulation Produced By Out-Of-Focus Condition

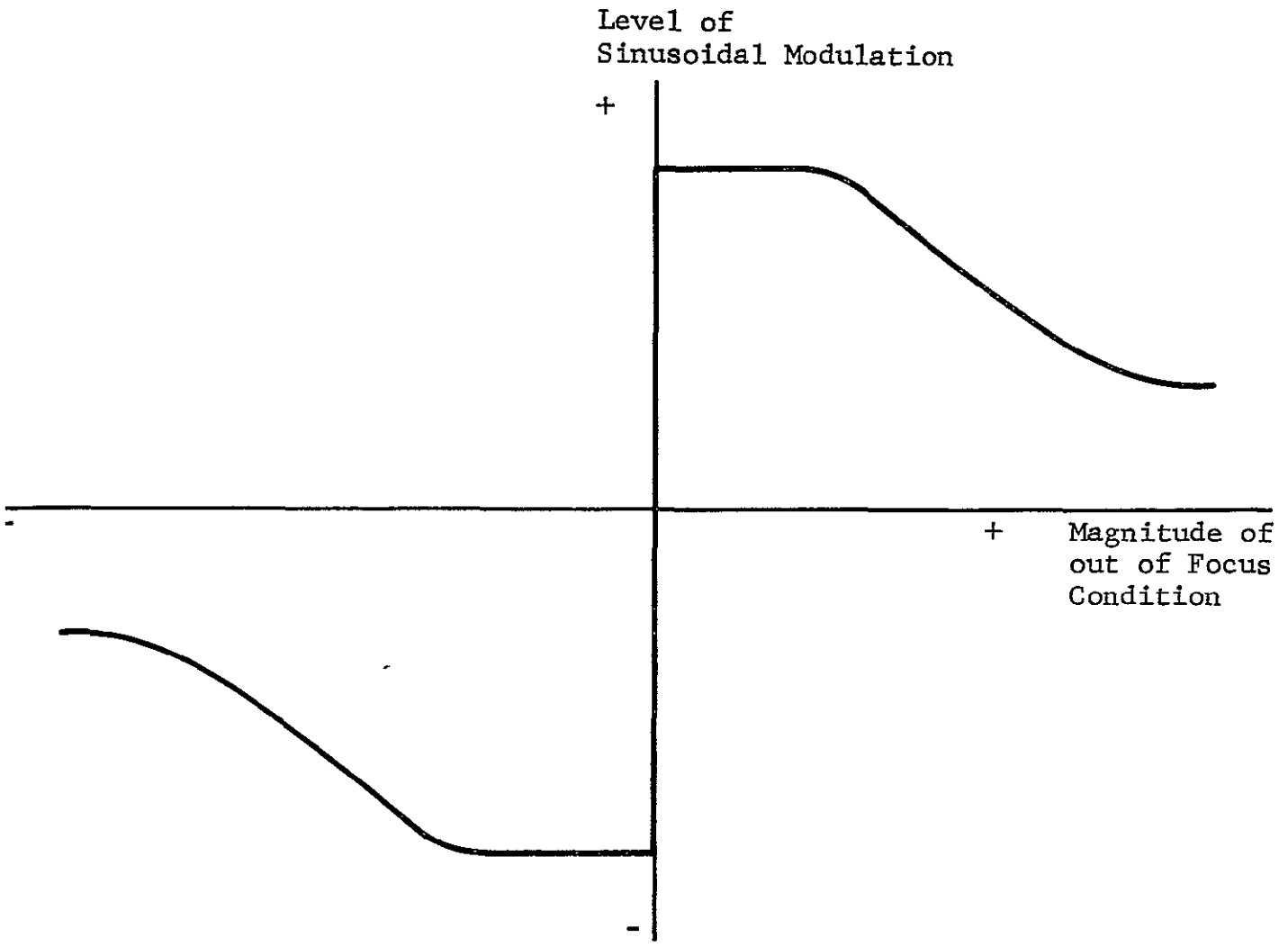

Figure 8.--Ideal Out-Of-Focus Signal As A Function Of Out-Of-Focus Condition

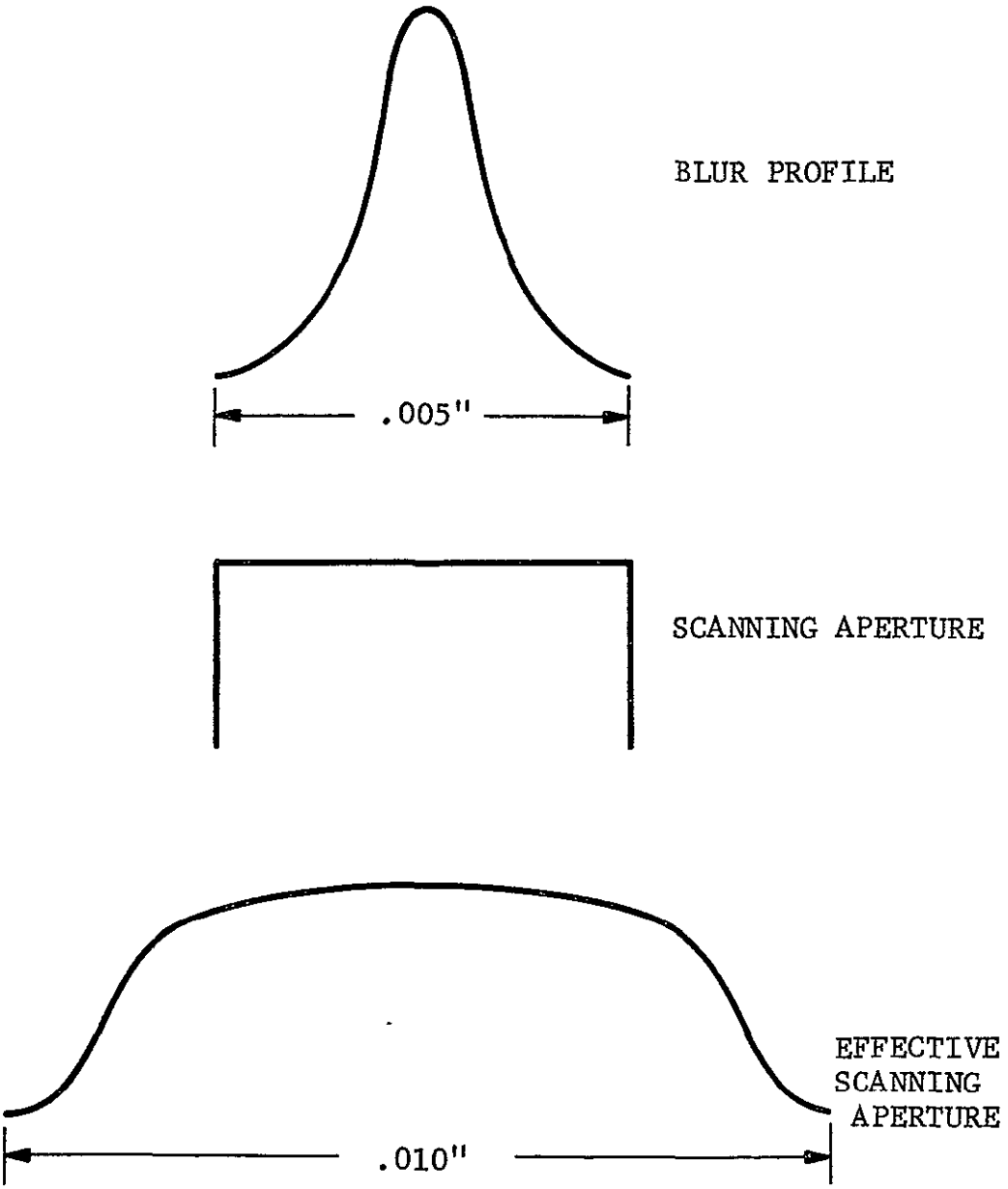

Figure 9.--Effective Scanning Aperture Profile

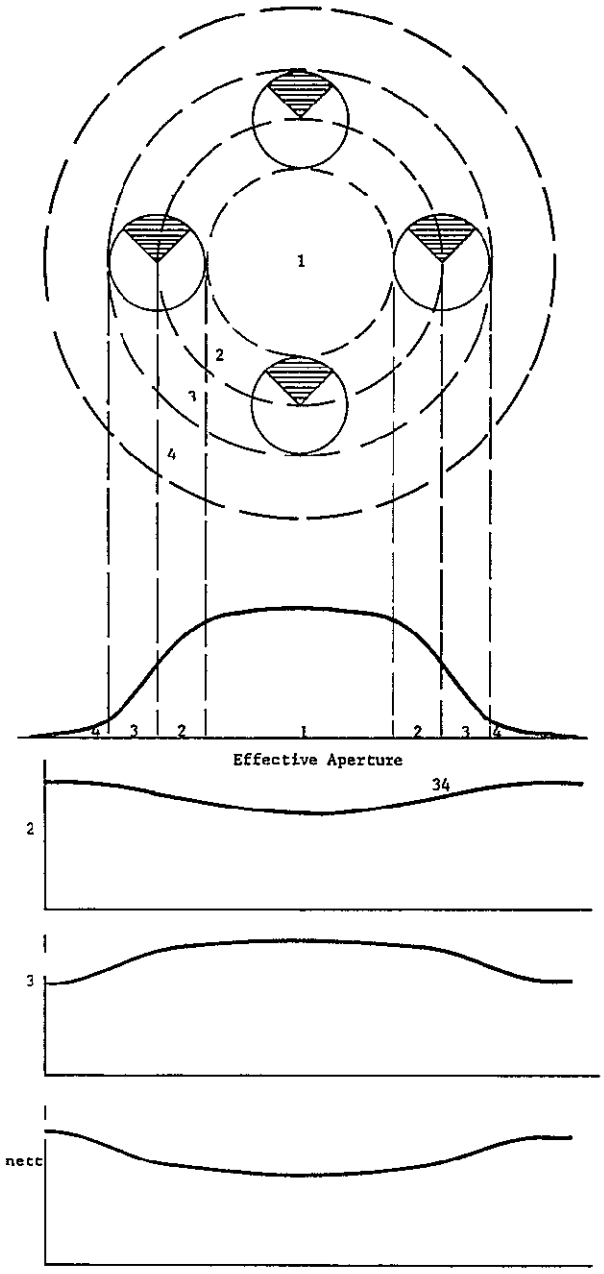

Figure 10.-- Effective Out-Of-Focus Modulation

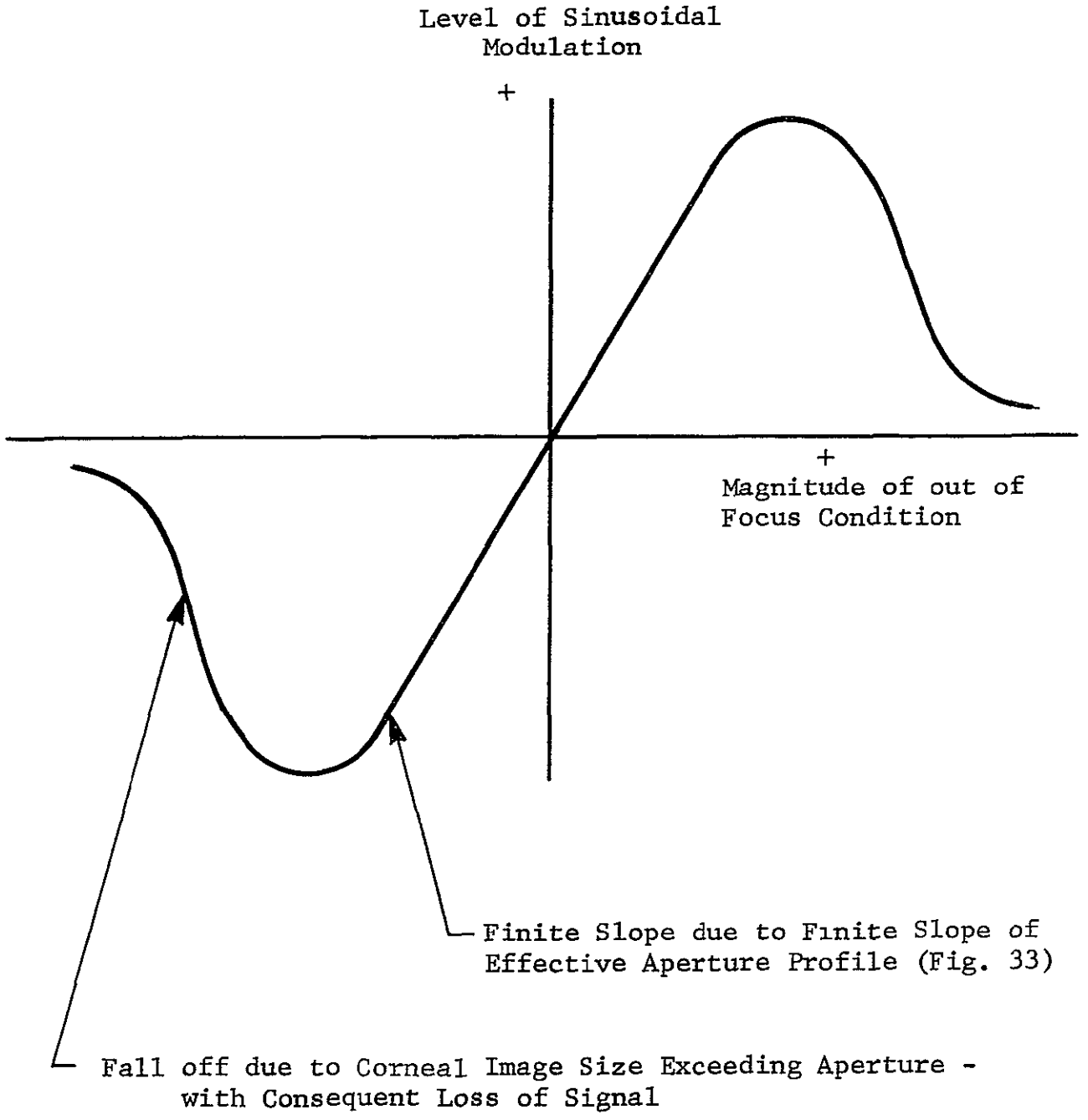

Figure 11.--Out-Of-Focus Signal Level

The out-of-focus error signal thereby derived to drive the autofocus motor, which in turn will control the axial portion of the positive lens in the telephoto lens system.

Due principally to diffraction, as well as geometrical blur, (and also the finite size of the corneal reflection) it is estimated that the slope of the effective aperture (Figure 10) will correspond to a 0-100% change in the profile over a range of 0.010 inch. Let the out-of-focus blur diameter be β (Figure 12). The peak-peak magnitude of the two competing sinusoids (shown in Figure 10) will then be:

$$+\frac{I_o}{2}\left(1+\frac{\beta/4}{0.010}\right) \text{ and } -\frac{I_o}{2}\left(1-\frac{\beta/4}{0.010}\right)$$

Thus the effective sinusoid will be,

$$\frac{I_o\,\beta}{0.04}$$

As shown in Reference 2, pages 70 and 71 the corneal signal consists of about 3×10^6 photoelectrons per second. This indicates that the threshold resolution of this out-of-focus sensor system will be given by β_n

$$10^6\ T\ \beta_n/0.04 = \sqrt{10^6 T}$$

where T is the averaging time employed, in seconds, i.e.,

$$\beta_n = \frac{0.04}{10^3\sqrt{T}} = \frac{0.04}{\sqrt{T}} \text{ mils}$$

Thus for $T = 0.01$ s

$\beta_n = 0.4$ mils

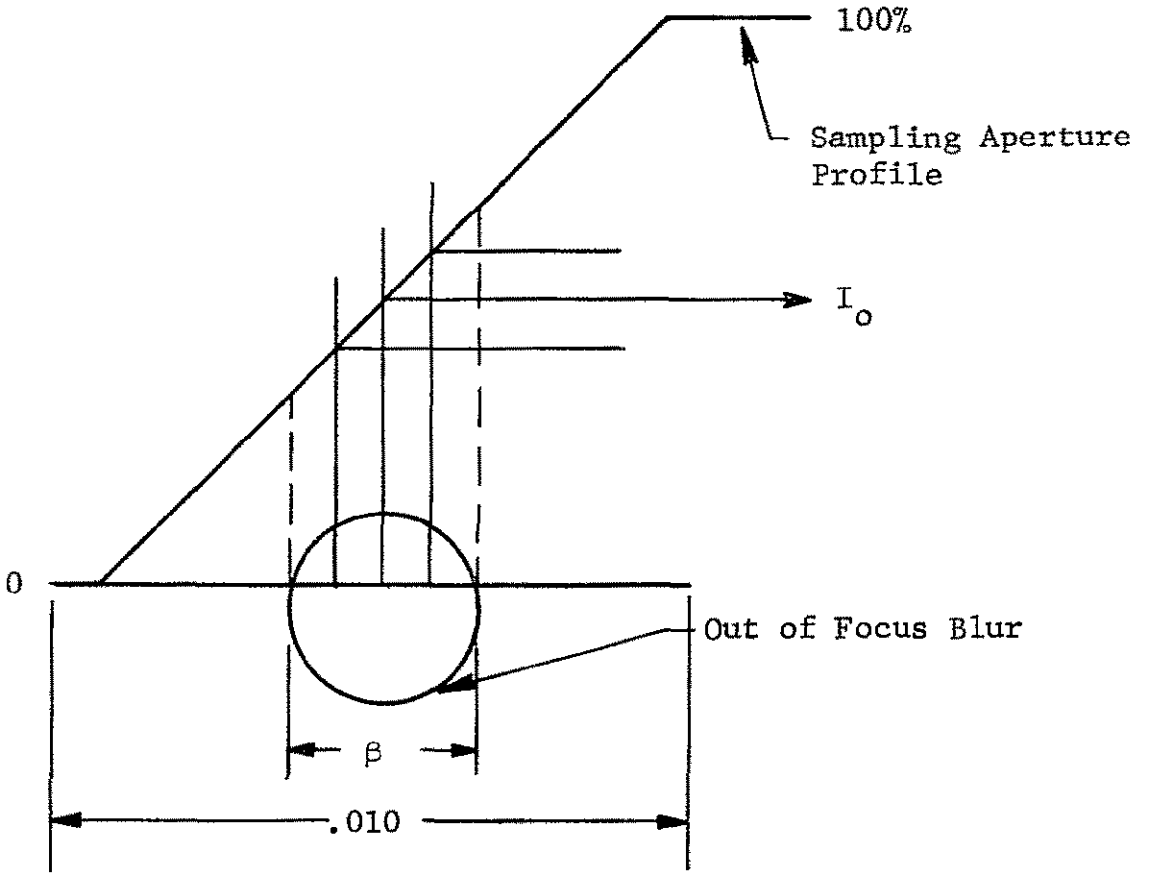

Figure 12.--Sampling Out-Of-Focus Blur

This indicates that there will be ample sensitivity for the focus system since it is important to focus the system only to about 5 mils - the diffraction blur limit on resolution. (It may be noted that the diffraction pattern produced by the unsymmetrical collection aperture will not have any asymmetricity that would, of itself, yield an apparent out-of-focus signal. Any modulation of the corneal video signal by the diffraction pattern will be at the second harmonic of the circular scan frequency.)

Dynamic design of the autofocus system.--In order to determine the maximum motions associated with voluntary displacements of the head, a series of photographs were taken of a subject wearing a bright head marker, and using a strobe lamp for illumination. By measuring the relative displacement of each of the multiple images of the marker thereby formed, it is possible to determine the actual time history of the motion. The results are shown in Figure 13 for both front-rear, and lateral motion of the head of the maximum possible intensity. The peak acceleration of the head was 700 inches-s^2 and the maximum velocity 70 inch-s. These maximum figures will be used in the analysis of the moving mirror and autofocus systems.

The axial position of the positive lens in the telephoto combination is controlled by a motor driven screw. The motor (Inland T-0709) has a peak torque capacity of 6.6 oz-in. and a rotor inertia of 1.1 x 10-4 oz-in-s^2. The mass of the positive lens, and carriage, is about 1.5 lb. The rotating screw driving the shaft is 3.75 inches long and 0.25 inch in diameter. It will have a mass of about 1.5 oz. Its inertia will be about 3 x 10^{-5} oz-in.-s^2. It has a pitch of 0.1 inch (i.e., 10 turns per inch of travel).

Let x be the lens displacement, M the mass of the lens and carriage, p the pitch of the screw, and θ the angle of rotation of the screw. Then:

$$\theta/2\pi p = x$$

Let T be the torque applied to the screw and F the force transmitted by the screw. Then (by conservation of energy),

$$F_p = 2\pi T$$

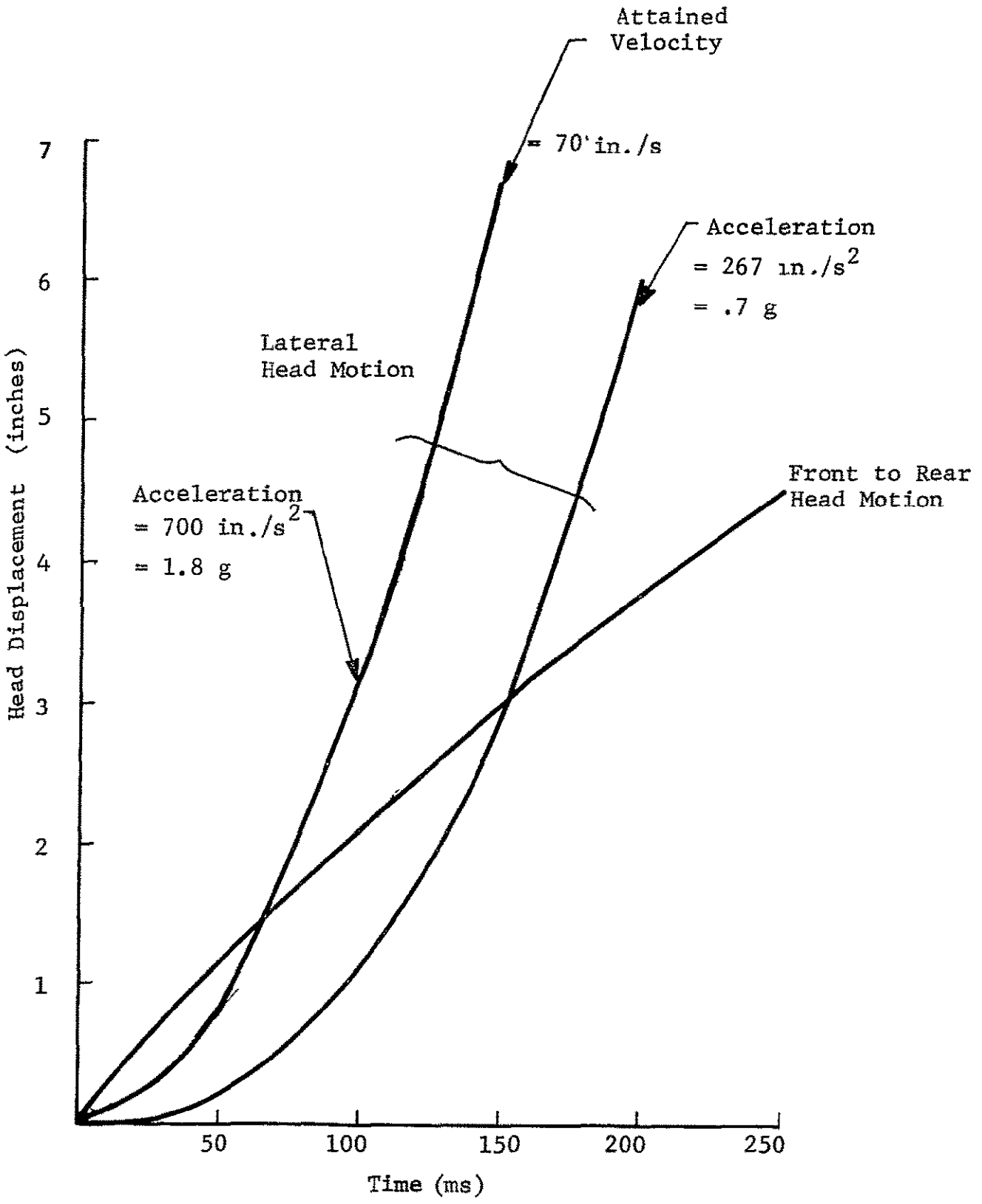

Figure 13.--Measured Head Positions For Maximum Voluntary Motions

The inertia force of the lens plus carriage is,

$$M\ddot{x} = M_p \frac{\ddot{\theta}}{2\pi}$$

The corresponding torque is given by,

$$T = p/2\pi\ (\ddot{Mx}) = \frac{pM\ p\ddot{\theta}}{2\pi\ 2\pi} = \frac{Mp^2\ \ddot{\theta}}{4\pi^2}$$

Thus the lens and carriage can be considered to have a moment of inertia of,

$$\frac{M_p^2}{4\pi^2}$$

In the present case,

Reflected inertia of lens + carriage $= \frac{16 \times 1.5 \times 10^{-2}}{4\pi^2 \times 384} \approx 1.6 \times 10^{-5}$ oz-in.-s2

Thus the total inertia at the motor is about 1.6×10^{-4} oz-in.-s^2.

The peak torque of the motor is 6.6 oz-in. Allowing for friction, the peak available torque will be about 5.5 oz-in. Thus in response to a maximum input command, the motor will accelerate at,

$$\frac{5.5}{1.6}\ 10^4 = 3.44 \times 10^4\ \text{rad/s}^2$$

In terms of lens displacement this is equivalent to:

$$\frac{3.44 \times 10^4 \times 0.1}{2\pi} = 548\ \text{in./s}^2$$

The viscous damping of the motor is 5×10^{-3} oz-in./rad/s (zero source impedance). Thus the rate of rotation at which the available torque is reduced to one half, is

$$\dot{\theta} = \frac{5.5}{5 \times 10^{-3}} = 1.1 \times 10^{3} \text{ rad/s}$$

This corresponds to a lens velocity of,

$$\dot{x} = p/2\pi(\dot{\theta}) = \frac{0.1}{2\pi} \times 1.1 \times 10^{3} = 17.6 \text{ in./s}$$

The lens motion characteristics can be derived from the head motion characteristics (Figure 13) by dividing the square of the optical magnification associated with the positive lens. Thus if u, v are the image and object distances for this lens:

$$1/u + 1/v = 1/f$$

$$du/u^2 = - dv/v^2$$

$$dv = -du\ v^2/u^2$$

In the worst case,

$$v/u \approx 5/35 = 1/7$$

$$\therefore dv \approx - du/50$$

Thus the focus lens drive system has a capability of following head accelerations up to 2500 in./s^2 and head velocities up to at least 900 in./s. From the data shown in Figure 13 it is clear that the focus servo drive system is adequate for all anticipated head motions.

Focus control system.--During normal use of the system a nominal range (moving mirror-eye) will be selected within 28-inches-42 inches. The negative lens position will then be set to the appropriate value by either of the two following methods:

1) An artificial pupil consisting of a white disc (0.2 inch in diameter) against a black background, will be set up at the desired nominal position of the eye. The system will be allowed to acquire and track this detail. The focus motor will, as part of this operation, automatically position on the positive lens for sharp focus. The negative lens position will then be adjusted manually until the indicated diameter of the pupil i.e., a pupil diameter signal derived from the electronics unit shows a diameter of 0.2 inch. The position of the positive lens at this point will be automatically read into the electronics system, thereby defining the nominal range.

2) The negative lens will be set manually to the correct position for the selected nominal range. The lens position control knob will activate a turns counter so that it can be set exactly to a precalculated value. The nominal range value in this case will be entered manually into the electronics system (computer).

In normal track the dynamic control of the lens position will be controlled by the following:

1) The out-of-focus signal derived by the electronics system from the effect in the rotating (unsymmetrical) aperture (a signal proportional to lens displacement).

2) The focus motor tachometer output (a signal proportional to angular rate).

3) The difference between the actual focus lens position-pick-off output and the pick-off output when tracking a pupil at the nominal range (a signal proportional to inches of lens displacement).

The control will be exerted in the form of a commanded motor torque.

Autofocus system operation.--Initially, the Oculometer system will search for, and then acquire, the head marker. The head marker (see Drawing No. F2100-3115) has sufficient detail (a 5 mm dark "pupil" set in the middle of the 1-inch active area of the marker) to permit track even with a maximum defocus condition (i.e., the actual range differing by 6 inches from the nominal range, which will give about 100 mils out-of-focus blur). In

the center of this dark "pupil" a bright "corneal reflection" will be formed by convex reflection off a 5 mm diameter hemisphere connected to the head marker reflector. This reflection will be used by the autofocus system which normally operates with the real (eye) corneal reflection to drive the system to sharp focus. The signal level from head marker "corneal reflection" will be about 10^7 electrons/s, when sharply focussed.

Because the auxiliary-sensor-tube scanning-aperture is 100 mils in diameter (at the eye) the head marker "corneal reflection" signal will not be appreciably reduced in the out-of-focus condition. With the main sensor the out-of-focus signal, however, will be about 10^5 electrons/s. This is sufficient to allow the main sensor to be used for tracking, and focus control, from initial acquisition (performed by the auxiliary sensor) to fine focus.

When fine focus has been achieved with the head marker, the moving mirror will be commanded to switch the instantaneous field of view to the eye. The auxiliary sensor will then search for the pupil. As soon as it is acquired, the main dissector will be used to track the pupil and corneal reflection. The time needed to switch from the marker to the eye will be about 10 ms. The worst case (unpredictable) axial displacement of the eye in this time will be about 0.07 inch, however, this will have a negligible effect on the focus condition. Thus, when first acquired, the eye will be within (at least) 1 inch (axially) of the sharp focus condition. (There is an inevitable uncertainty in the difference between the Oculometer-marker range and the Oculometer-eye range of about an inch.) The consequent out-of-focus blur (16 mils maximum diameter) is just about at the limit for detection of the corneal reflection in the worst case i.e., with the largest pupil diameter and thus brightest pupil. It may be necessary, therefore, to obtain preliminary focus drive information from the effect of the rotating aperture on the pupil tracking channels.

Image Dissector Aperture

At f/60 the diffraction blur is 5 mils at the eye (Figure 14). The image dissector aperture (referred to the eye) should not be appreciably smaller than this because, the video signal is then reduced without any corresponding increase in resolution and the tracking noise (normally independent of aperture diameter) increases.

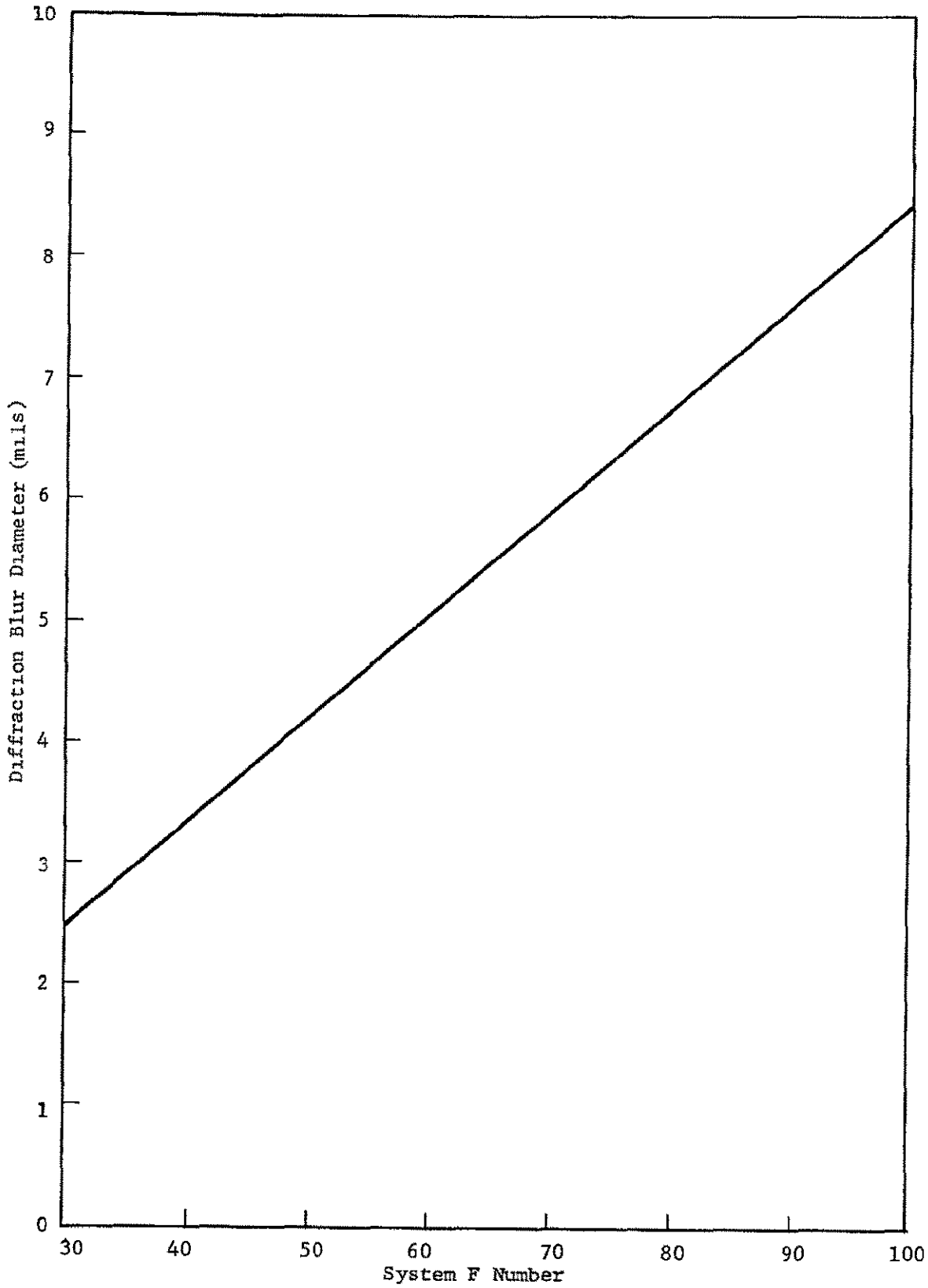

Figure 14.--Diffraction Blur Diameter Of A Function Of f/Number

In the operation of the automatic focus system, magnification changes will occur because only the positive lens moves with the ±6 inch head motion around the nominal range. Thus, the image dissector aperture should be slightly larger than the expected diffraction blur so that, in the extreme case of magnification change, it is not smaller than the blur.

Allowing for some margin, this shows that the optimum aperture diameter is 7 mils at the eye. Over the magnification range it will vary, at the eye, between 8.4 and 5.5 mils. Since the magnification between the photocathode and eye space is 4/3 the actual dissector aperture diameter is 3 x 7/4 = 5 mils.

Oculometer Source Intensity

The level of retinal irradiation (Reference 1, p. 41) that is conservatively rated as safe is 0.15 W/cm^2. Figure 16 in Reference 1 gives the maximum apparent source brightness as a function of pupil diameter consistent with this safety criterion (assuming, again conservatively, a 1.0 transmission factor of the eye). An apparent source brightness of 1.5 W/cm^2/steradian is within this limit for pupil diameters of 2-8 mm. However, at small pupil diameters the retinal level is well below the safety threshold. This raised the possibility of adjusting the illuminating intensity with pupil diameter (i.e., 15 W/cm^2/steradian at 2 mm) so as to derive the maximum possible signal at minimum pupil diameters. This approach has been rejected for the following reasons:

1) The xenon arc intensity cannot be adjusted over a wide range by varying the input electrical power. Stable operation of the arc requires that it be driven at, or near, its rated level.

2) There is insufficient energy available in a spectral peak in the xenon illumination system to provide a source radiance of 15 W/cm^2/steradian and yield, at the same time, maximum sunlight discrimination.

3) Alternative mechanical methods of adjusting source intensity are judged to be undesirable, in the present context, in relation to:

- complexity of mechanization,
- safety requirements,
- benefits to be gained through the use of an adjustable source.

Fail Safe Mechanism

In the event of a failure of the infrared filter (No. 22 in Figure 2) which immediately follows the xenon source in the illumination optics system, it is possible for the eye to receive a radiation level that is higher than specified as (very conservatively) safe for continuous illumination. Therefore, a mechanism has been added to the design to preclude this possibility.

The operation of this mechanism depends upon a silicon photodetector (No. 34 in Figure 2) which continuously monitors the instantaneous radiation level in the illumination path. Referring to the figure, we see that the radiation destined for the user's eye first reflects off a 'hot' mirror No. 31, so named because it reflects most of the infrared band used to illuminate the eye but passes most of the other wavelengths, which are then imaged onto the detector, through a second identical "hot mirror" (No. 33) which reduces the ambient IR reaching the detector by another factor of one-twentieth, making it more responsive to the appearance of unwanted radiation. Should the light level reaching the detector rise due either to subtle degradation or gross failure of the filter, the change in signal from the detector will, within microseconds actuate semiconductor circuitry shutting off the lamp. This event is followed within milliseconds by electromechanical latching circuitry which additionally disables the arc and starts a warning indicator. These latching circuits must be purposefully reset by manual means in order for the lamp to be reignited.

The sensitivity of the light detecting mechanism will easily enable the detection of cracks in the filter equal to one millionth of its area or a slow increase of 10% in light level due to filter degradation. It should also be noted that similar failure of the "hot" sampling mirror (No. 31 or 33) will also cause shut off of the arc.

Precautions have also been taken in the implementation of the associated circuitry. As previously mentioned, two separate means, semiconductor and electromechanical, are employed to disable the arc. The electromechanical latches are held on by permanent magnets making their operation independent of other circuitry.

Operation.--Upon rising signal level, the increased output from the silicon detector causes a comparator (LM201) to go from -0.6V to +10.6V virtually instantaneously ($\approx$10 μs) robbing the xenon lamp of current by discharging the capacitor bank in the arc supply and thereby causing the arc to extinguish. A few milliseconds later the relay closes into a latch mode disabling the arc supply control circuitry, preventing the capacitor bank from receiving a new charge. An audible warning is simultaneously sounded. To reignite the arc, a reset button must be pushed to unlatch the relay. The fail safe control circuit is shown in Drawing No. F2100-3108.and in Figure 15 .

This fail-safe circuit (Figure 15)is to be incorporated in the xenon arc power supply housing as bought from Eimac (see Figure 16). The meter, reset button and audible warning device will be mounted on the front panel of the supply along with the already present standard controls.

The Solitron SS-11 silicon detector is connected as a current source whose output is directly proportional to the radiation incident on its sensitive area. This arrangement gives excellent stability and speed of response. The output current, after passing through a meter, is compared to a preset reference current at the input of the LM201 op amp. Should the detector current exceed the reference current, the op amp rapidly (2 μs) changes between its bounds as set by the feedback diodes, going from -0.6V to +10V. This signal turns on the 2N2905 and 2N3940 transistors, the latter of which shorts the current destined for the xenon lamp at point A. This current originates from a capacitor bank (C1A to C1C in Figure 15 which is charged via a gated full wave bridge rectifier. The shorting does not take place at the lamp itself because then the shorting transistor would be subject to the 15 kV starting pulse at lamp ignition, causing it to punch through. Since the lamp requires a certain level of current to maintain the arc, extinction will begin during the approximately 10 μs turn on time of the 2N2940. Concurrently, the rising comparator output turns on the MPS3704 transistor actuating the Teledyne relay which closes in one millisecond simultaneously sounding a solid state pulsating

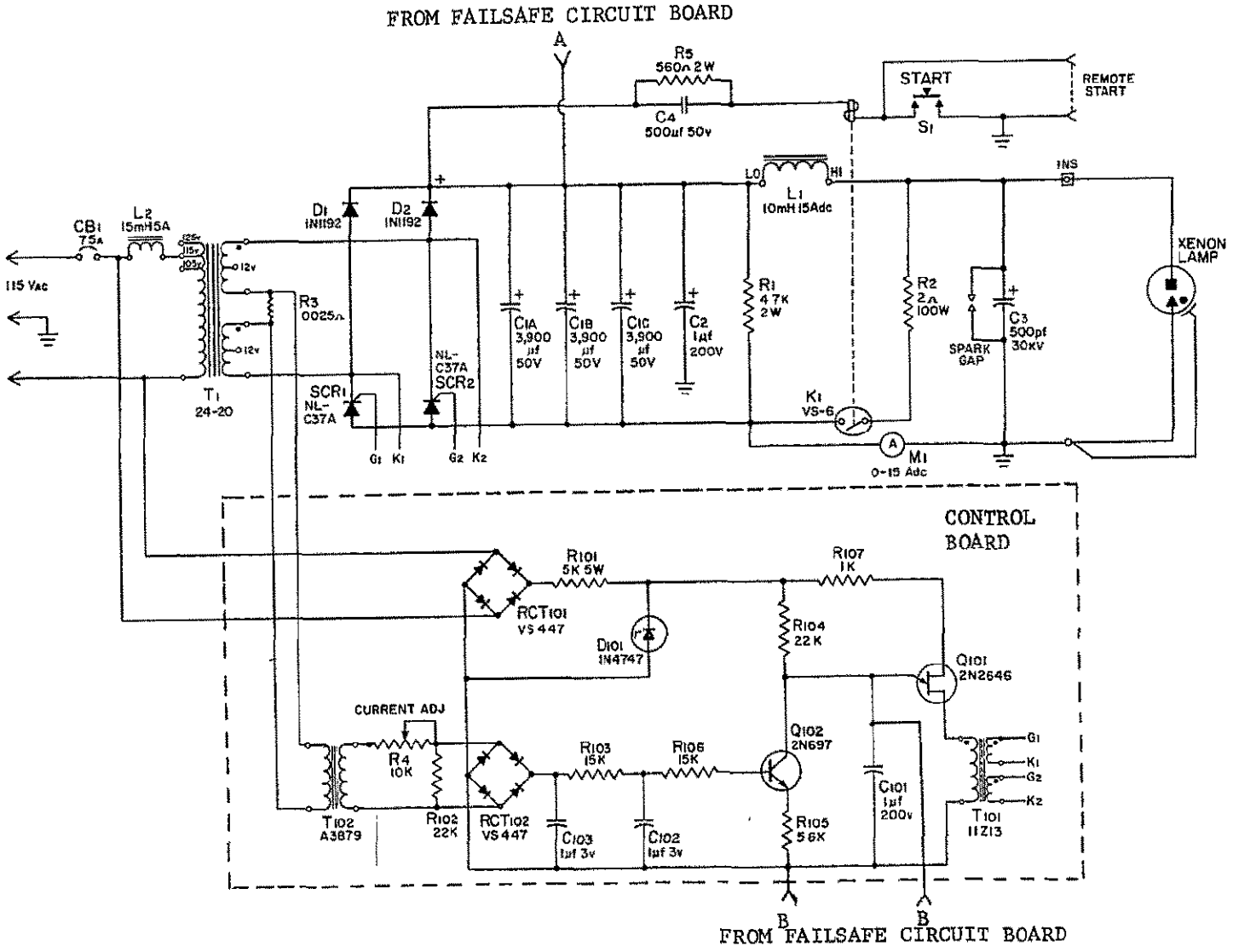

Figure 15.--Xenon Short Arc Lamp: Power Supply Schematic

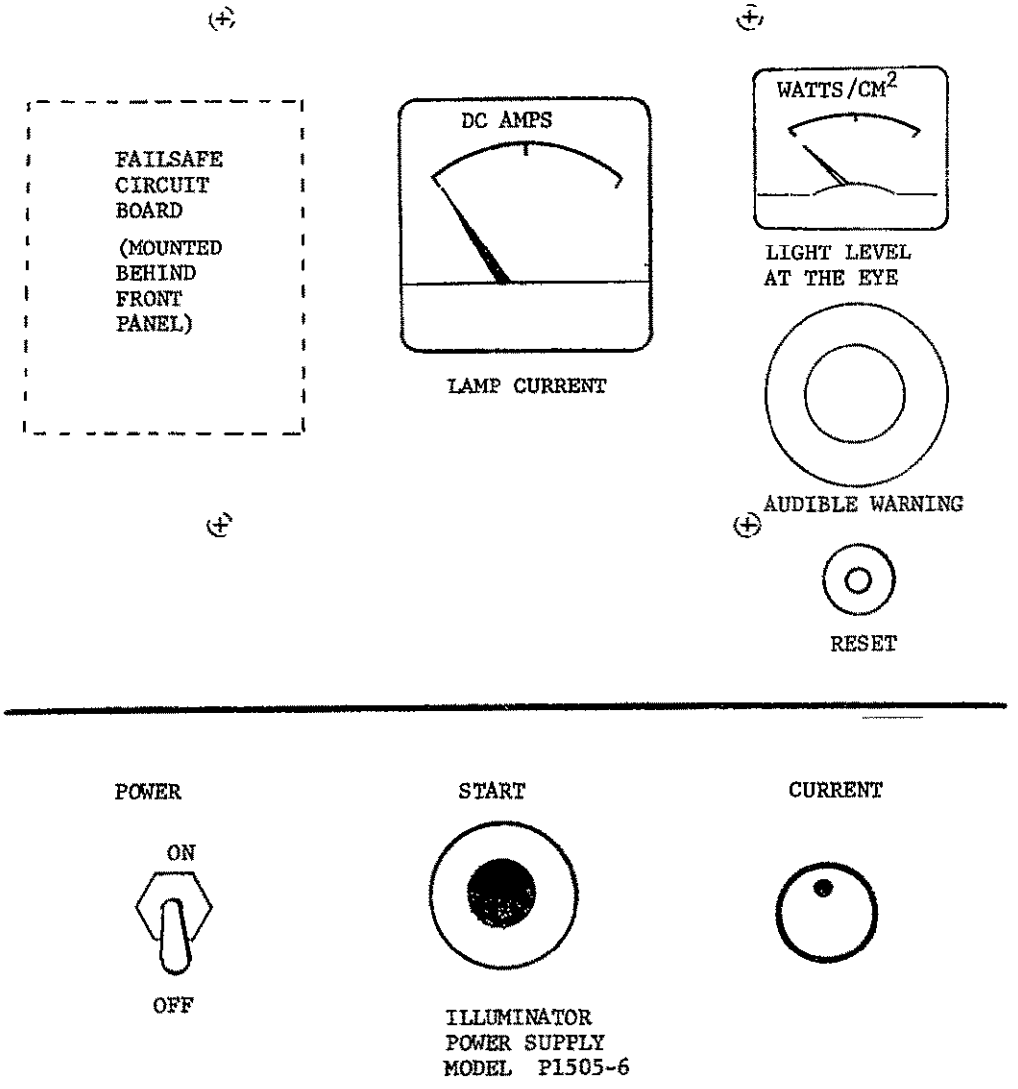

Figure 16.--Altered Xenon Power Supply Housing.

audio device and shorting a vital element on the xenon arc power supply control board (capacitor C101 in Figure 16). The disabling of C101 shuts down the unijunction relaxation oscillator (Q1) preventing turn on, via coupling transformer T101, of the SCR gates, SCR1 and SCR2, which control the entrance of charge to the lamp supplying capacitor banks mentioned above. The relay is of the latching variety and so must be manually reset by pushbutton in order to reignite the lamp. The latching action depends on the force of permanent magnets and thus is independent of circuit considerations.

Head Marker

The subject being monitored by the Oculometer will wear a passive head marker near to and at a defined displacement from his eye. The marker (see Figure 3) will consist of a piece of corner reflecting material with a 5 mm diameter hemisphere cemented to the center of its active area. The corner reflecting material is silver coated (to increase angular coverage) and the hemisphere is also silver coated to provide an intense pseudo "corneal reflection." The main area of the reflector that is obscured by the hemisphere will provide a pseudo black "pupil."

The signal intensity received back (on axis) from the corner reflecting material, relative to that received from a magnesium oxide screen, was measured and is shown in Figure 17 as a function of the angle of incidence of the radiation onto the reflector. The number of signal electrons that will be collected, per second, by the auxiliary sensor from the head mark signal, is also shown in Figure 17. At the fastest marker search frame time of 187 ms, the marker would be seen, by the system, for about 1 ms. It is clear from Figure 17 that either sensor would yield sufficient signal for reliable marker acquisition.

OPTICAL SIGNAL MEASUREMENTS

The basic function of the Oculometer is to electro-optically track both the pupil/iris boundary of the eye and also a corneal reflection formed by the eye. The eye is irradiated, by the Oculometer, with a source of near IR (virtually invisible)

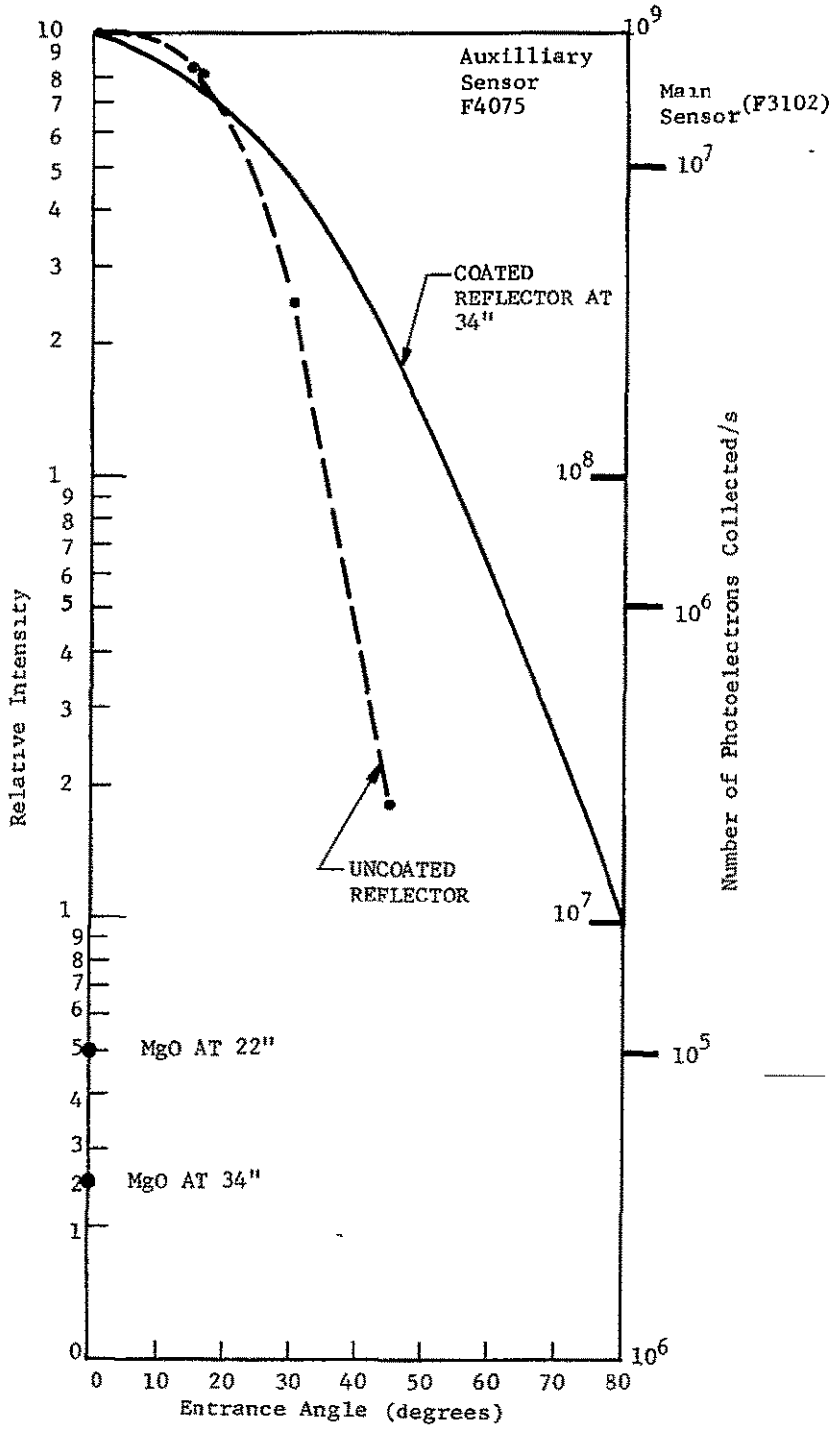

Figure 17.--10% Variation Due To Focus

radiation at a level such that a sufficiently intense image of the eye is formed at the photocathode of an image dissector tube. The image dissector acquires and tracks the pupil iris boundary and the corneal reflection detail in the eye image existing at the photocathode.

A conventional eye illumination system would show the eye detail as in Figure 18. The "bright pupil" illumination technique used in the Oculometer, however, shows the eye as in Figure 19. The bright pupil technique illuminates the pupil iris boundary by irradiating a small part of the retina and allowing the scattered radiation coming back out of the eye from the retina to back-light the pupil. The scattered radiation that is intercepted by the pupil is refracted back out of the eye along the same path, but in the opposite direction, as the rays that came into the eye from the source of illuminating radiation. The rays leaving the eye, therefore, tend to be focussed back onto the source. Through the use of a beam splitter, as shown in Figure 20, the emergent radiation can be separated from the incident radiation. A small collection aperture placed at the position of the virtual image of the source (as seen in the beam splitter) then collects all the rays scattered back from the retina through the pupil, and transmitted through the beam splitter. By using a very small, very bright source a correspondingly small collection aperture can be used and still generate a sufficiently intense bright pupil image at the photocathode. When the collection aperture is small, it accepts very little radiation from the sclera and iris yet receives all the available radiation from the retina via the pupil. By placing a suitable lens at this small aperture, an image of the eye can be formed at a plane behind the lens. This image will show the pupil as bright (because all the available retinal rays coming through the pupil are picked up) but will show the surrounding regions of the eye as relatively dark because the small aperture accepts very little scattered radiation from this other detail. This bright pupil has been used successfully in the proximate and remote Oculometers.

The technique has been investigated experimentally (Reference pp. 60-66) and analyzed theoretically (Reference pp. 46-63). The latter analysis has indicated the need for additional experimental work in order to formulate an optimum design. The principal parameters of the bright pupil system are:

a) the angular size of the illumination aperture (i.e., the effective source).

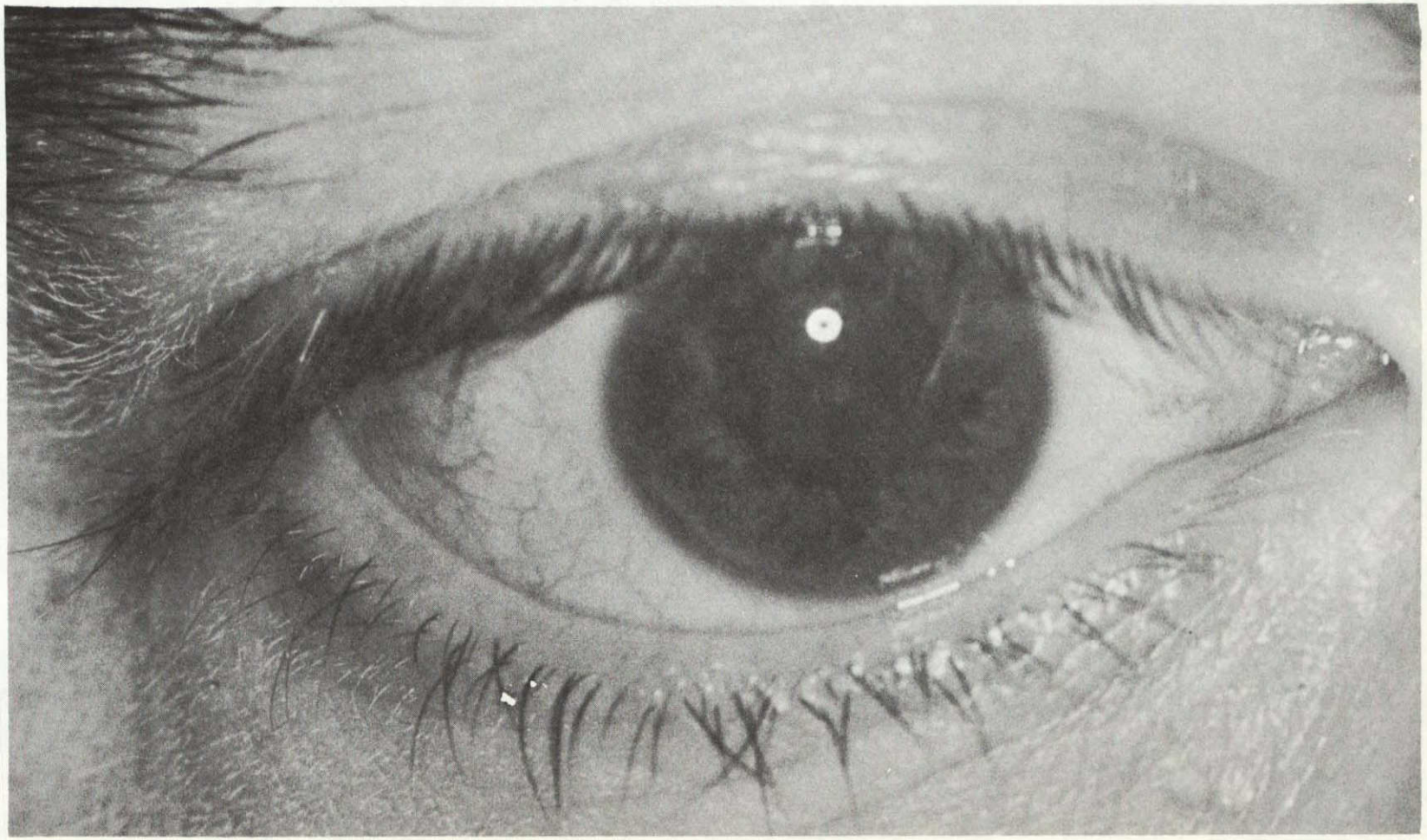

Figure 18.--Conventional Pupil/Iris Illumination Technique

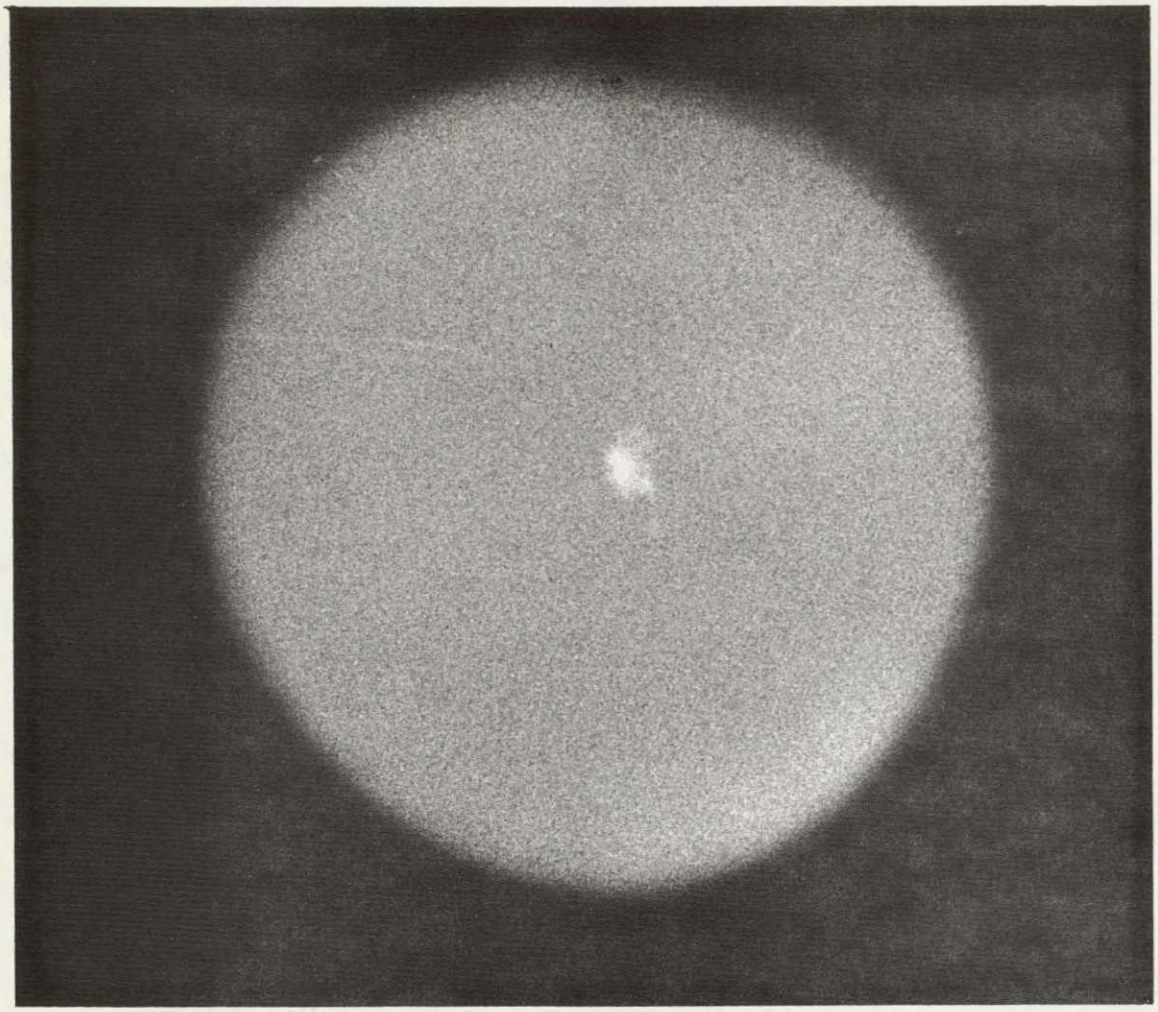

Figure 19.--Bright-Pupil Illumination Technique

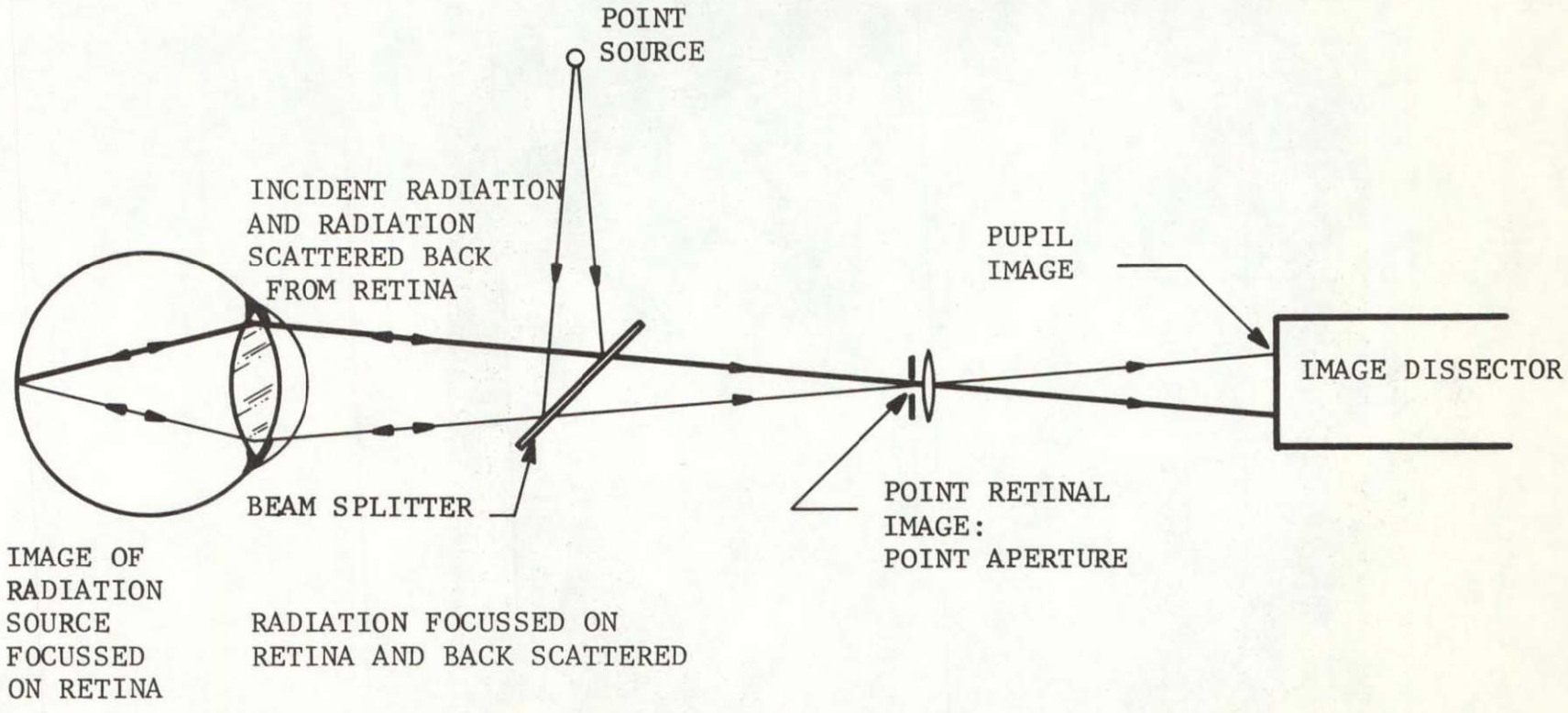

Figure 20.--Bright-Pupil Optical System

b) the angular size of the collection aperture.

c) the alignment of the collection aperture with the virtual image of the illumination aperture (as seen in the beam splitter).

d) the irradiance of the illuminating source.

The relevant parameters of the eye are:

a) the effective reflectivity of the retina (K_r) and the transmission factor of the eye (τ).

b) the diameter (d) of the eye pupil.

c) the state of accommodation of the eye.

The important performance parameters of the bright pupil technique are:

a) the apparent pupil reflectivity* i.e., the ratio of the intensity of the actual pupil image to the image intensity that would have resulted if a perfect white diffusing screen had been substituted for the eye).

b) the contrast between the bright pupil and the (relatively) dark iris.

c) the absolute intensity of the pupil image.

d) the signal/noise ratio in tracking the pupil/iris boundary with a given photosensitive surface (this can be derived from the absolute pupil signal (Item c) and the pupil/iris contrast ratio (Item b).

Analysis.--A general expression for the apparent pupil reflectivity (ρ) was derived on page 56 of Reference 1. It can be expressed in the form:

---

* The apparent reflectivity of the pupil is the reflectivity of a perfectly diffusing eye surface that would have the same radiance as that observed with the eye pupil when similarly illuminated. Note that the apparent reflectivity of the pupil is often greater than unity.

$$\rho = \left(\frac{K_r \tau^2 (d/a)^2 F^2}{1 + F^2/F_\beta^2} \right) + CF^2 \qquad (1)$$

where

K_r is the reflectivity of the retina

τ is the transmission factor of the eye

d is the pupil diameter

a is the anterior focal length of the eye

F is the Oculometer system f/number (the reciprocal of the angular size of the collection aperture as it appears to the eye: normally the illumination aperture is of the same angular size as the collection aperture).

F_β is the reciprocal of the effective angular size of the blur circle caused by accommodation error (it is a measure of the state of accommodation of eye).

It is shown in Appendix A that,

$$F_\beta \approx \frac{0.71\ 10^3}{\delta D\ d} \qquad (2)$$

where δD is the refractive error of the eye (in dioptres) and d is the diameter of the pupil (in mm).

Assume, for the moment, that in Equation (1), C = 0. Then,

$$\frac{1}{\rho} = \frac{a^2}{K_r \tau^2} \left(\frac{1}{F^2 d^2} + \frac{1}{F_\beta^2 d^2} \right)$$

Substituting for F_β from Equation (2),

$$\frac{1}{\rho} = \frac{a^2}{K_r r^2} \left(\frac{1}{F^2 d^2} + \frac{2(\delta D)^2}{10^6} \right)$$

Thus, if C is in fact zero, a graph of $1/\rho$ against $(1/F^2 d^2)$ should be a straight line.

Measurements

The apparent reflectivity of the human eye pupil was measured for various values of F (Oculometer f/number) and d (pupil diameter). The experimental arrangement is as shown in Figures 21 and 22.

A Tektronix Scope hood was used to position the head so that the subject's right eye was positioned within the field of view of the system.

A tungsten ribbon filament lamp fully illuminated the illumination aperture from which radiation was directed to the eye via a beam splitter. Wratten 87 or 87C, and Corning filters were used to select the desired near IR band of radiation. A collection aperture (of equal size to the illumination aperture) was accurately located at the virtual image of the illumination aperture (as seen in the beam splitter). A lens at the collection aperture formed an image of the eye in front of the camera lens. This image was recorded on high speed IR film with the Pentax S.L.R. camera. A Varo infrared image converter was used to view the image through the camera view finder. Visible radiation of variable intensity (filtered to remove IR components) caused the eye pupil to assume various diameters. The Oculometer f/number (F) was varied by adjusting the common diameter of the illumination and collection apertures.

A series of photographs of the eye were taken in this experimental arrangement. Photographs were also taken of Fiberfrax material placed in the eye space. Fiberfrax ceramic fiber paper 970 JH has a reflectivity of 0.9 at the wavelengths employed. Densitometer readings of these photographs were taken, and these readings converted to an absolute intensity by means of a calibration curve for the film. The calibration curve was constructed from data obtained by exposing the film to a fixed intensity source from 0.01 to 1 s and then measuring the density of the developed film with the densitometer.

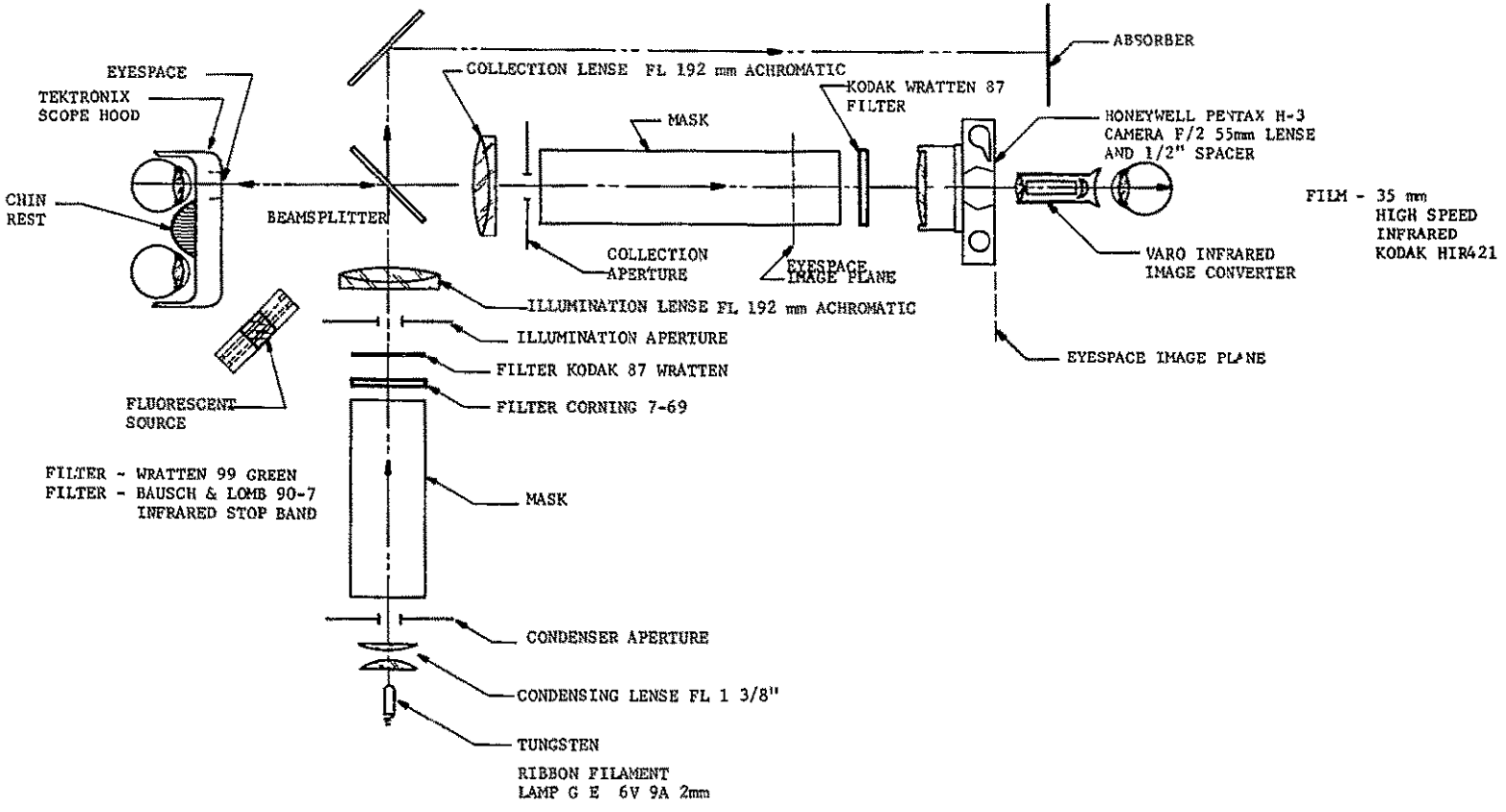

Figure 21.--Experimental Arrangement For Pupil Reflectivity Tests

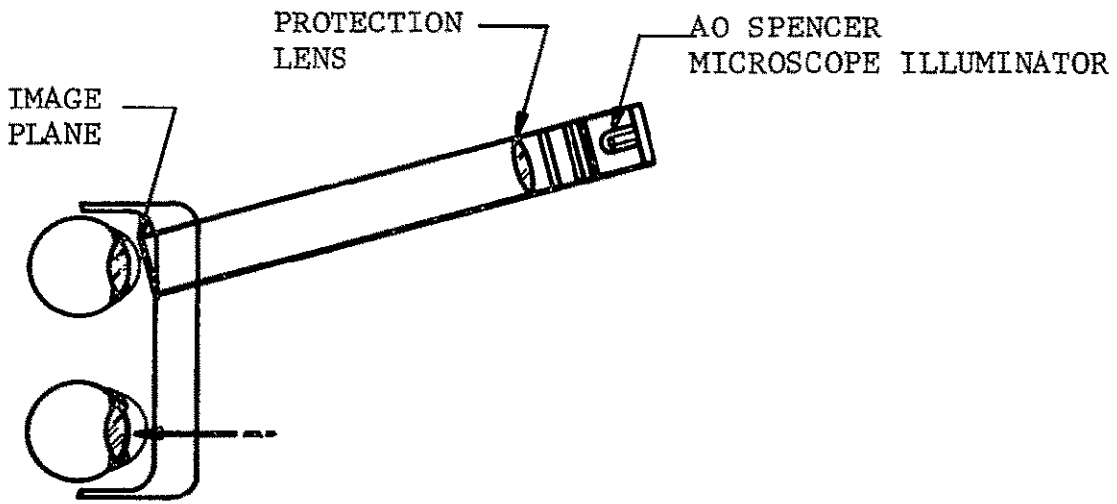

Figure 22.--Modification Of Figure 19 To Produce Minimum Pupil Diameter

The intensity of the "bright" pupil image is conveniently specified as an apparent reflectivity. That is,

$$\text{Apparent Pupil Reflectivity} = \frac{0.9 \text{ pupil image intensity}}{\text{Fiberfrax image intensity}}$$

The measured apparent reflectivity for various pupil diameters and f/numbers is shown in Figure 23. Smooth curves have been drawn through the data points in Figure 23. These curves were then used to plot $1/\rho$ as a function of $(1/F^2\ d^2)$, as shown in Figure 24.

It can be seen from Figure 24 that a good straight line approximation can be made for this data. It is,

$$1/\rho = 0.15 + \frac{0.755\ 10^4}{F^2\ d^2}$$

$$= 7.55 \times 10^3\ (\frac{1}{F^2\ d^2} + 1.99 \times 10^{-5})$$

This result shows:

1) that the assumption that $C = 0$ is valid, at least for the purpose of calculating ρ.

2) the value of $a^2/K_r\ \tau^2$ is given by,

$$a^2/K_r\ \tau^2 = 7.55 \times 10^3 \text{ i.e.,}$$
$$K_r\ \tau^2 = \frac{20^2}{7.55}\ 10^{-3} = 5.3\%$$

3) the value of δD is given by,

$$\frac{2(\delta D)^2}{10^6} = 1.99 \times 10^{-5} \text{ i.e.,}$$

$$D = 3.16 \text{ dioptres}$$

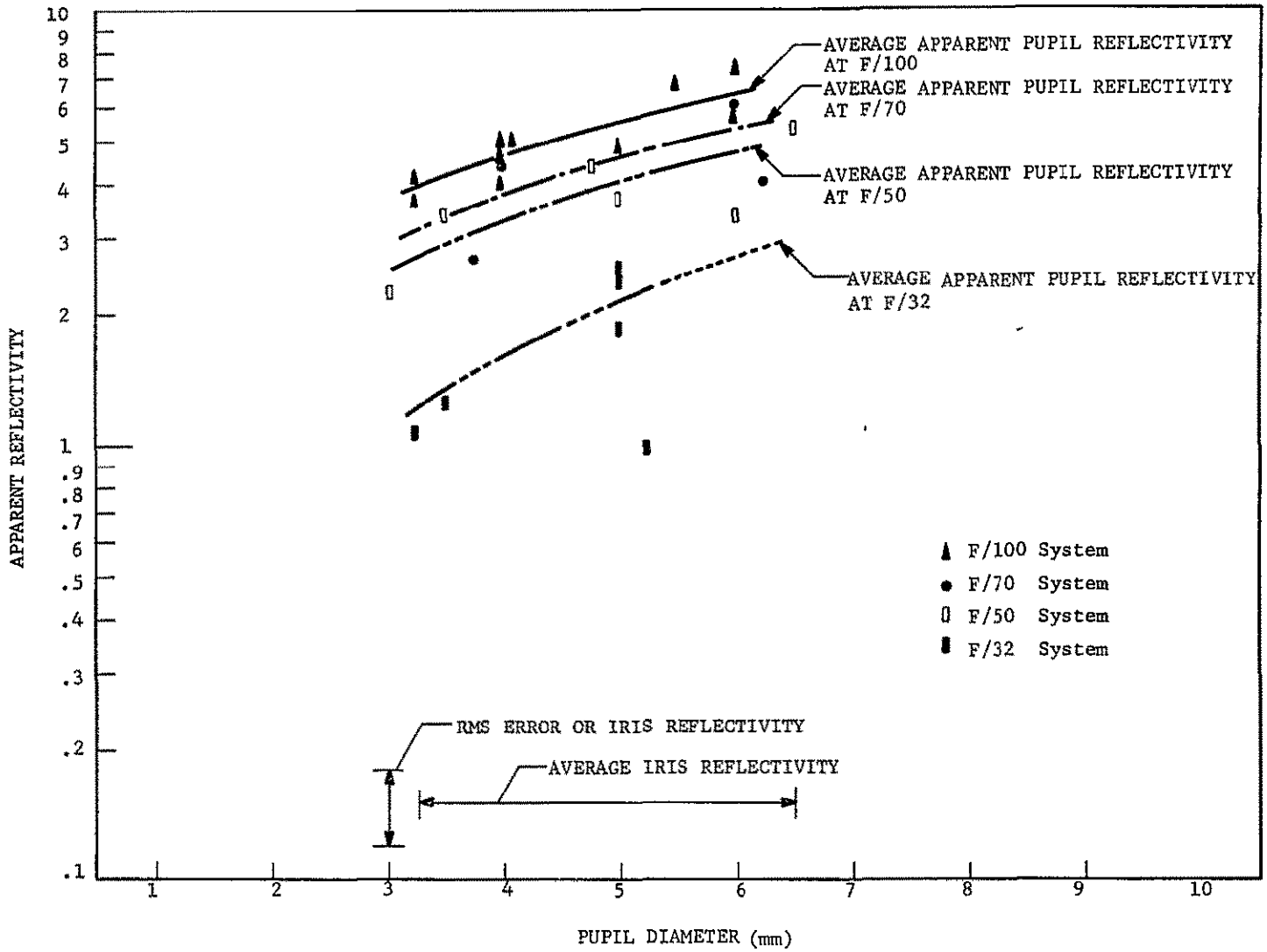

Figure 23.--Pupil Reflectivity

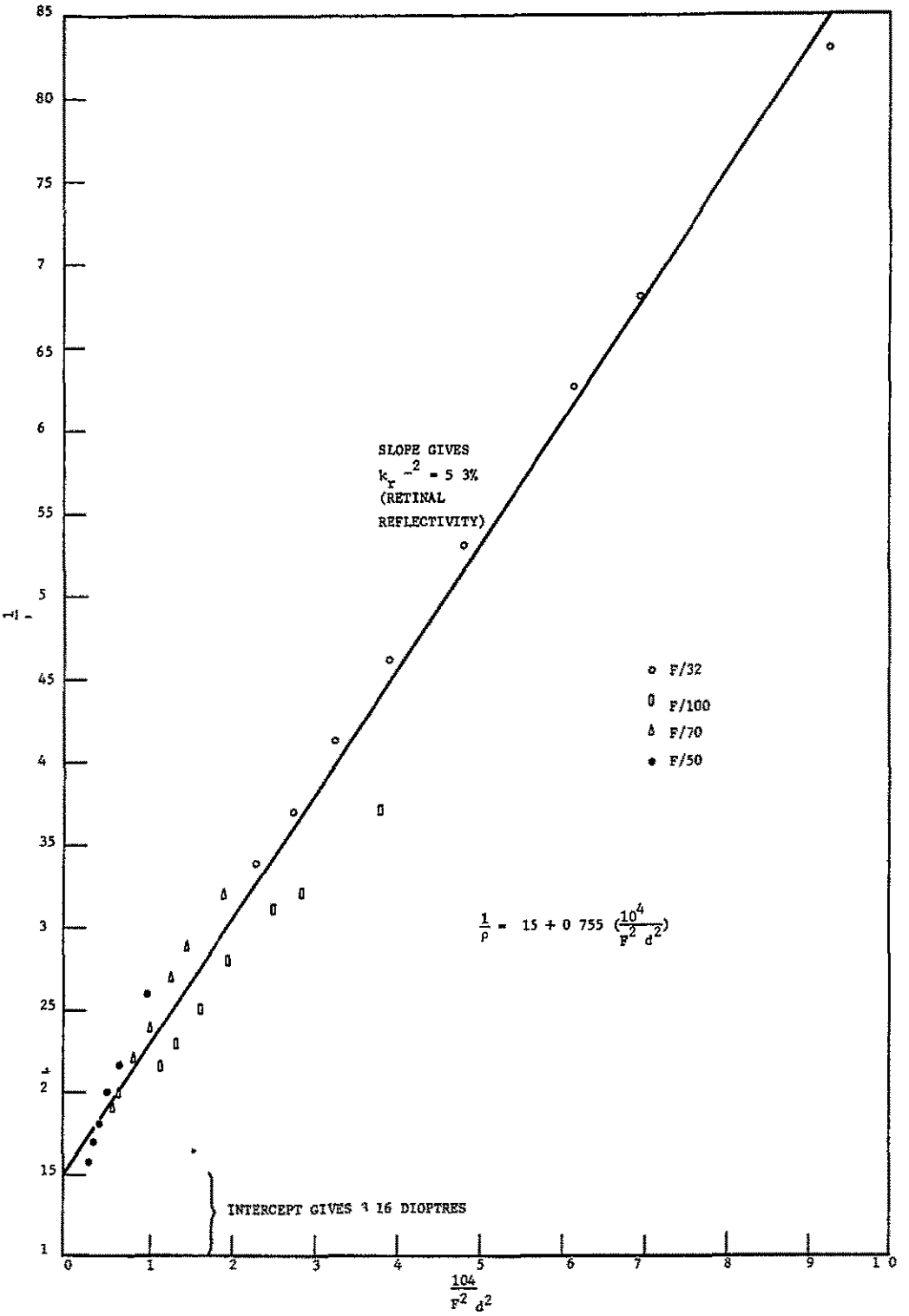

Figure 24.--Generalized Pupil Reflectivity

The variations of apparent pupil reflectivity of various subjects were measured, (Figure 25). There appeared to be some correlation between apparent pupil reflectivity and iris reflectivity. In prior work (with 16 subjects, Reference 2) a similar variation of pupil reflectivity was observed. The range of these (prior) variations is indicated on Figure 25. It can be concluded that pupil reflectivity, over the population, will be greater than 50% and less than 150% of the mean reflectivity.

Variation of pupil signal with direction.--The experimental arrangement was as shown in Figure 26. Measurements of apparent pupil reflectivity as a function of fixation direction were made using the previously described photographic technique, and also subjective estimates were made with the Varo image converter.

Taking the pupil signal intensity as 1.0 on the visual axis, the pupil signal, in general, increases to 1.42 at ±17 degrees off the visual axis for an F/100 illumination and collection aperture size, and decreases to unity again at ±30 degrees (see Figure 27).

An exception to this result was noted when the fixation direction was such as to cause the Oculometer source to be imaged on, or near, the optic nerve (blind spot). Subjective observations with the Varo (at F/50) indicated rapid signal fluctuations near the optic nerve (see Figure 27). Also the magnitude of these spatial variations on the retina was found to depend on the system f/number (that is, the reciprocal of the size of the bright image on the retina, see Figure 28).

The results of this investigation into pupil signal intensity versus fixation direction suggested the existence of rapid spatial variations of retinal reflectivity around the optic disc. Accordingly, an investigation was then made into the form of the retinal image formed at the collection aperture. The experimental arrangement is shown in Figure 29. The subject was instructed to fixate onto the plane of the collection aperture and to look in a direction so that the illuminating source was projected onto his blind spot (optic disc). The camera (Figure 29) was focussed onto the plane of the collection aperture and a photograph taken of the retinal image formed at the collection aperture. Other photographs were taken with the subject looking at various angles away from the original (blind spot) direction. Densitometer analyses of the photographs yielded the results shown in Figures 30 and 31.

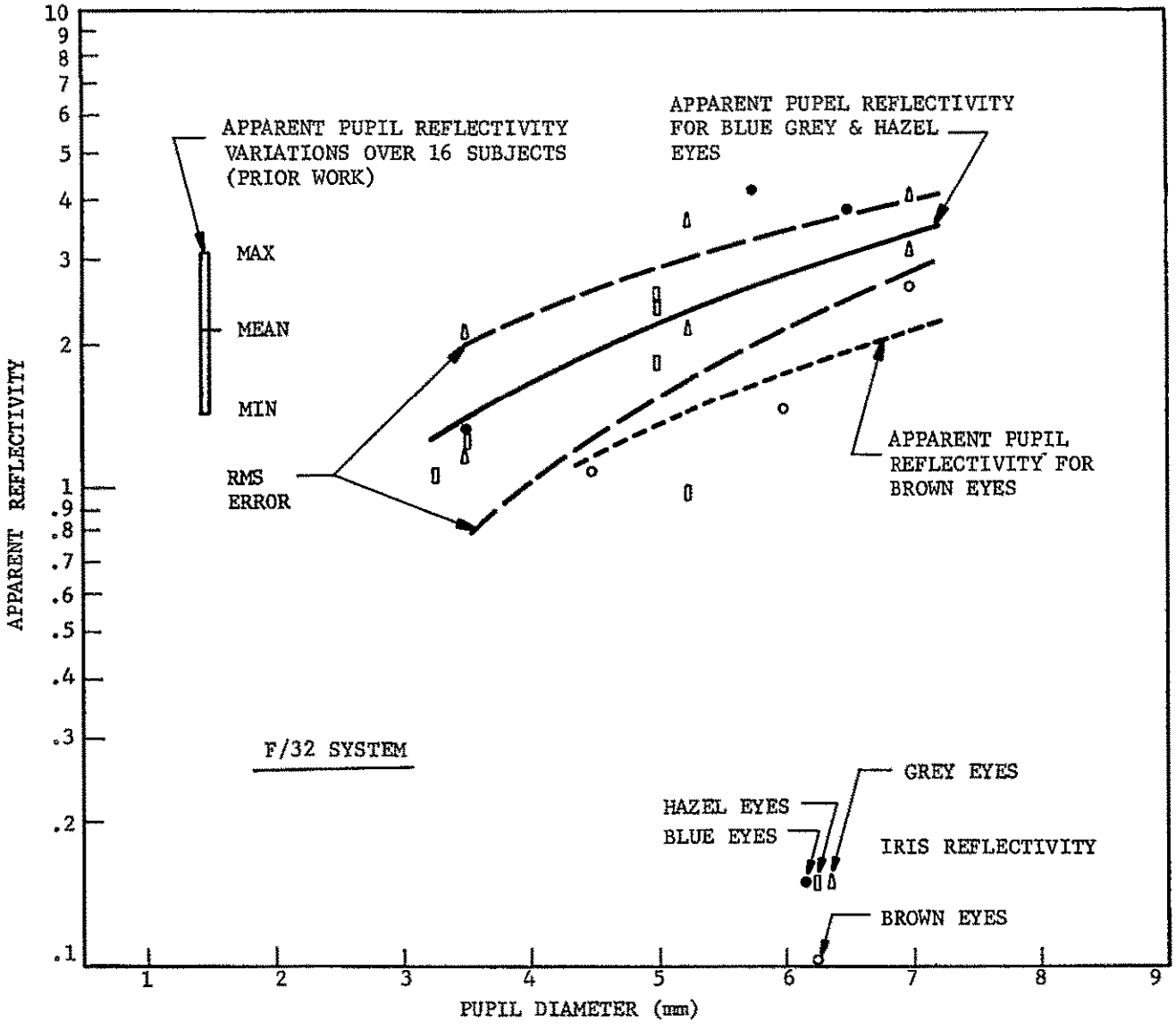

Figure 25.--Pupil Reflectivity At F/32

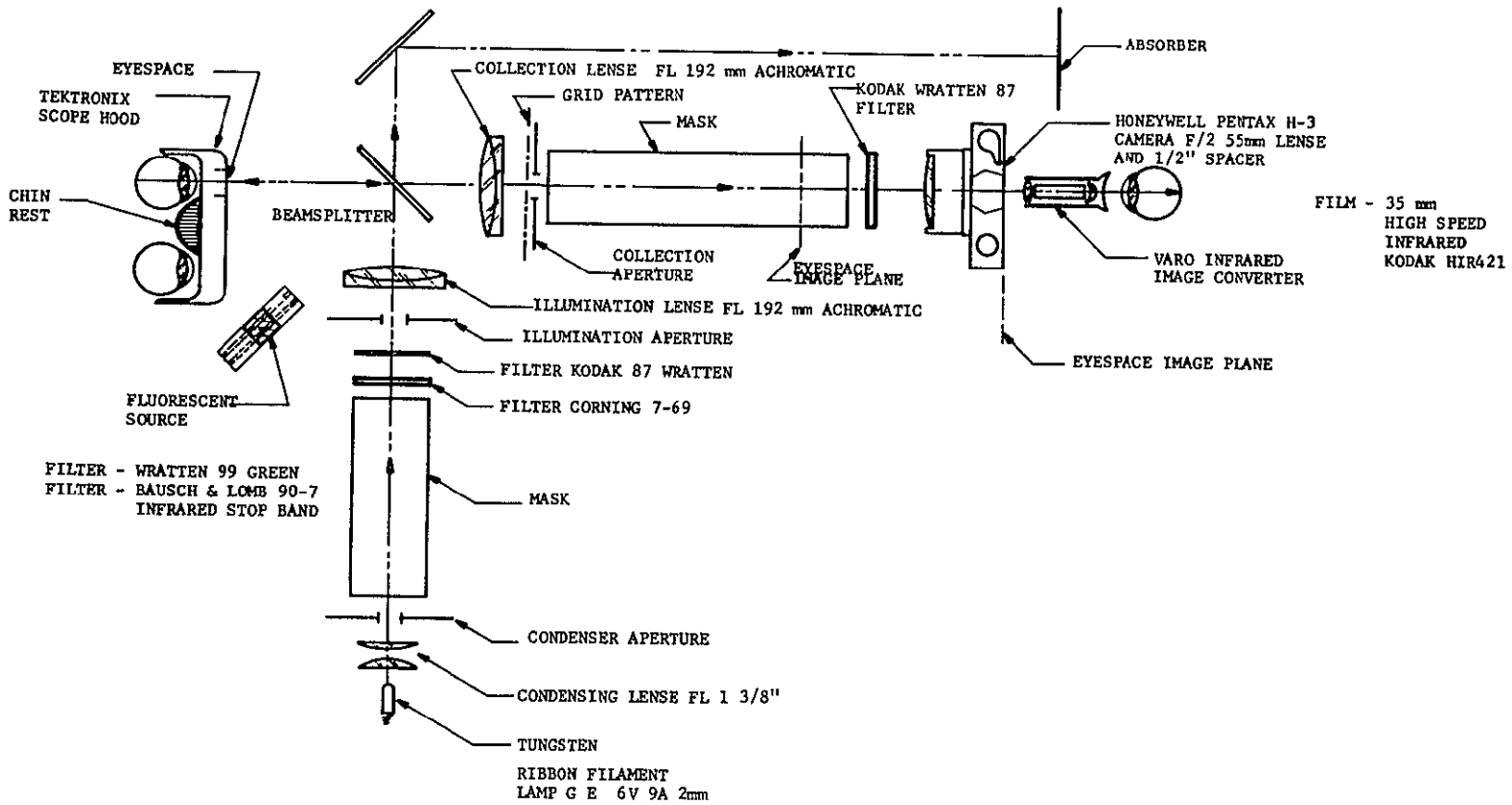

Figure 26.--Experimental Arrangement For Pupil Reflectivity vs Direction Tests

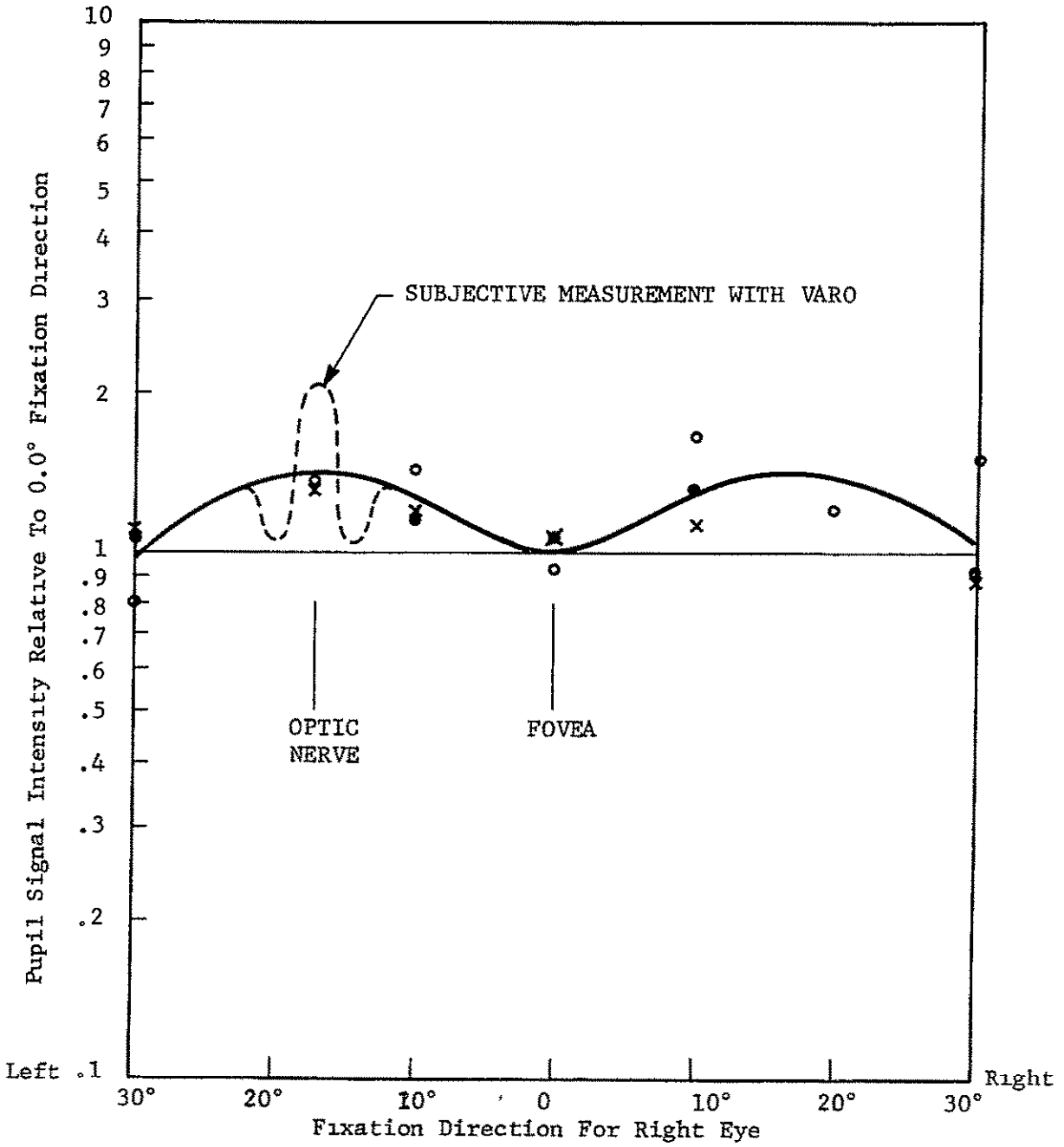

Figure 27.--Retinal Reflectivity Variations

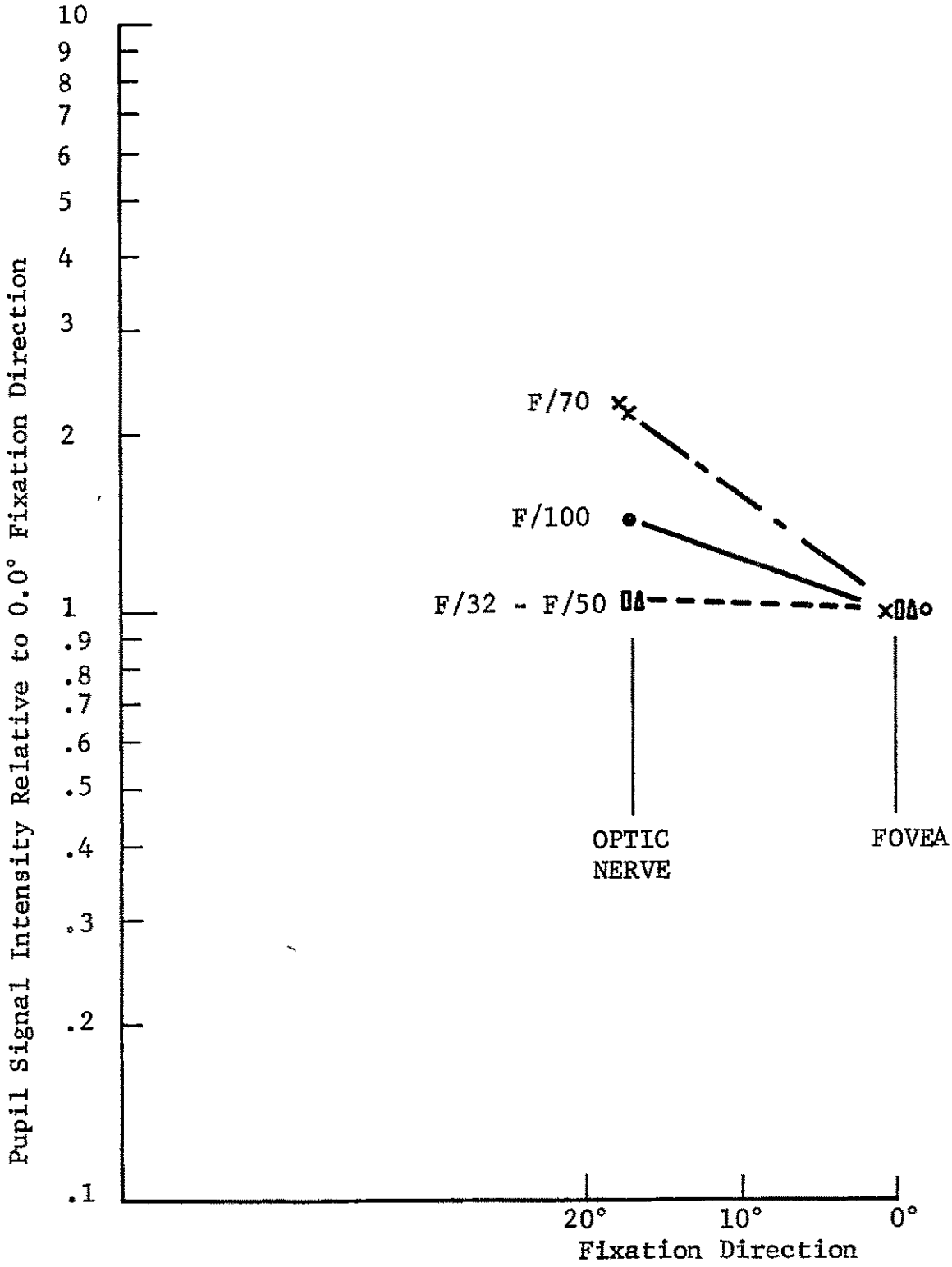

Figure 28.--Retinal Reflectivity Variations For Various Oculometer System F/Numbers

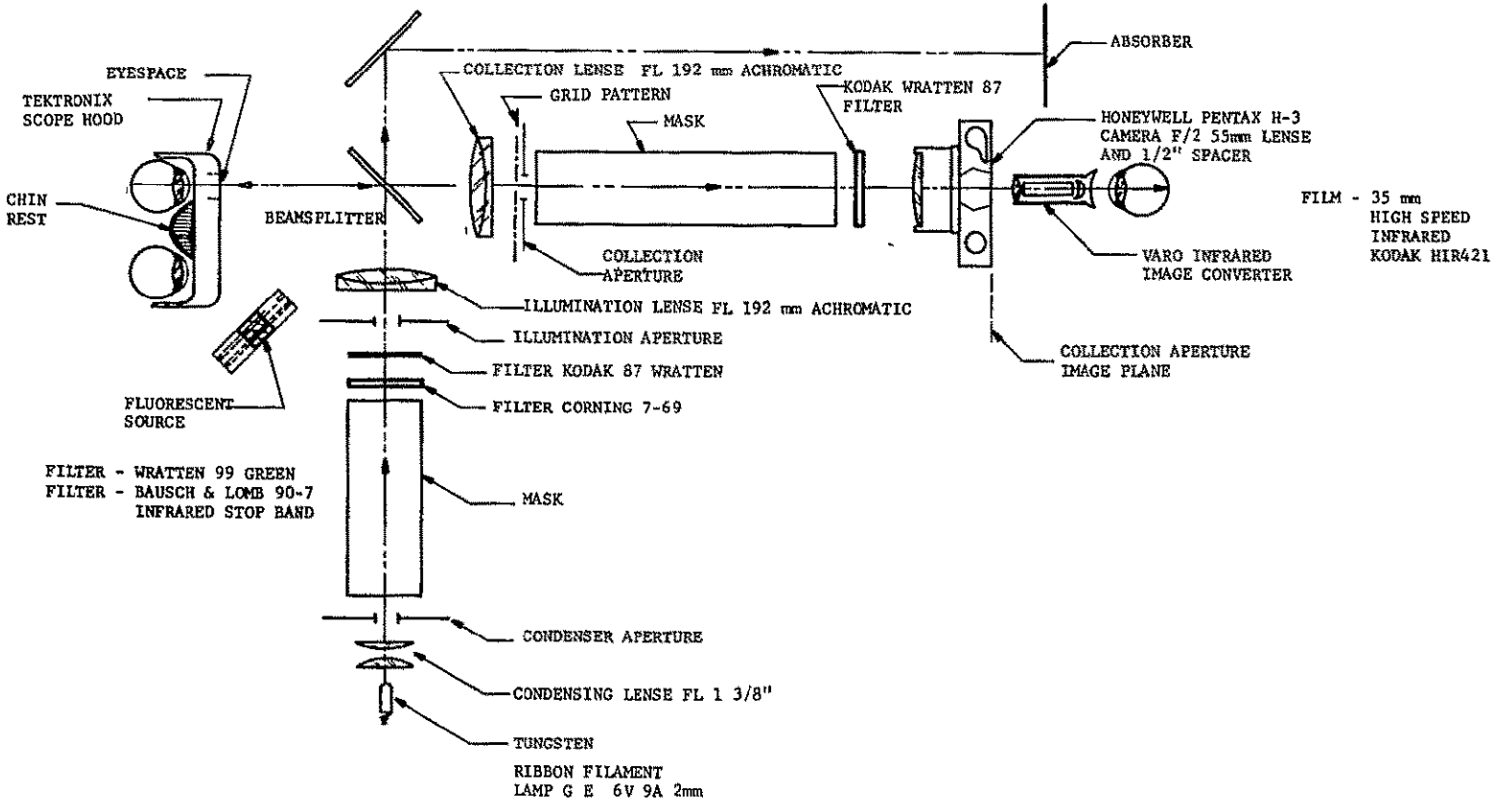

Figure 29.--Experimental Arrangement For Retinal Reflectivity Tests

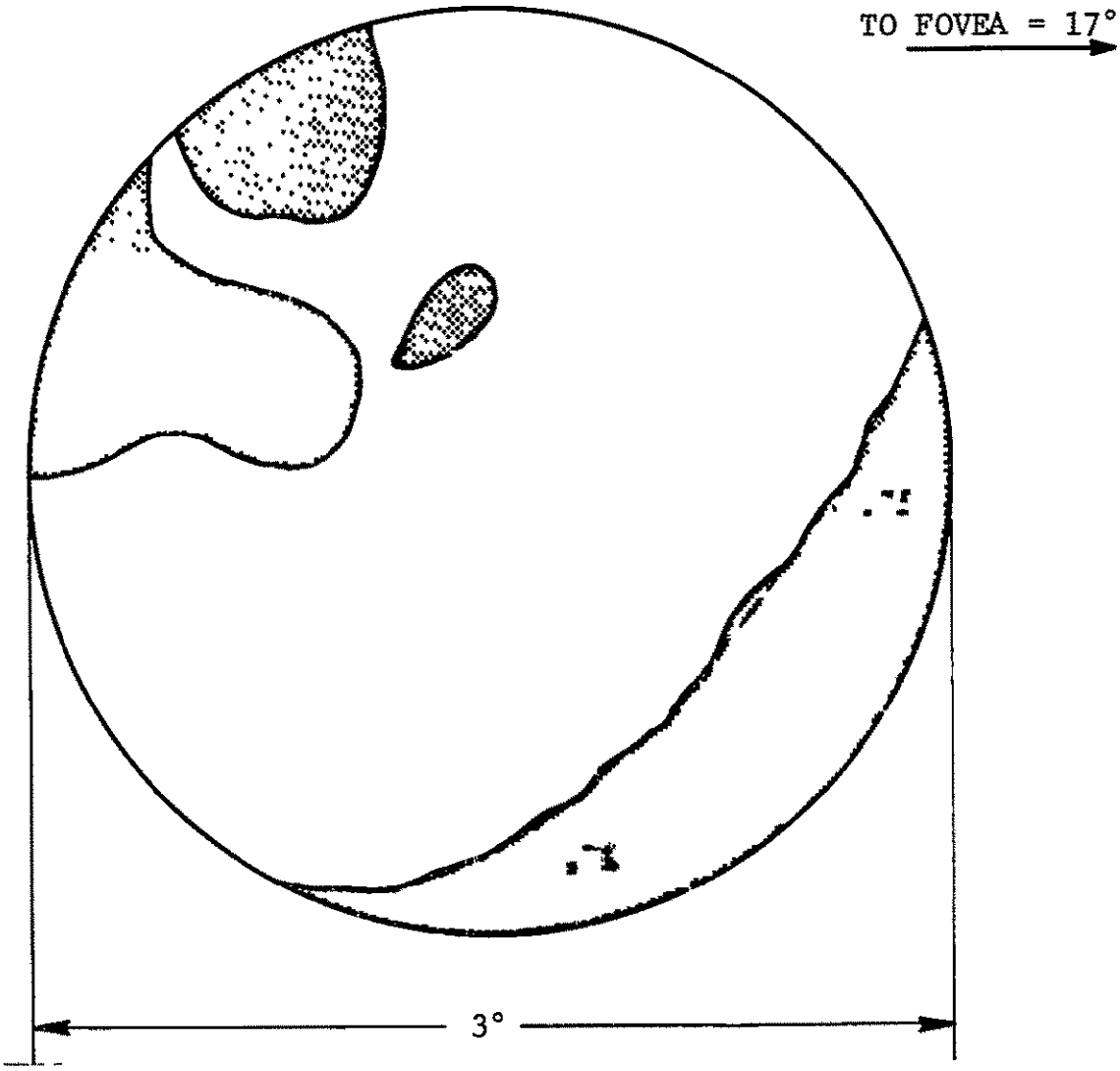

CONTOUR NUMBERS .58 - .90 CORRESPOND TO NEUTRAL DENSITY ON A NEGATIVE. LARGE NUMBERS INDICATE REGIONS OF HIGH REFLECTIVITY, SMALL NUMBERS LOW REFLECTIVITY.

Figure 30.--Retinal Reflectivity Contours

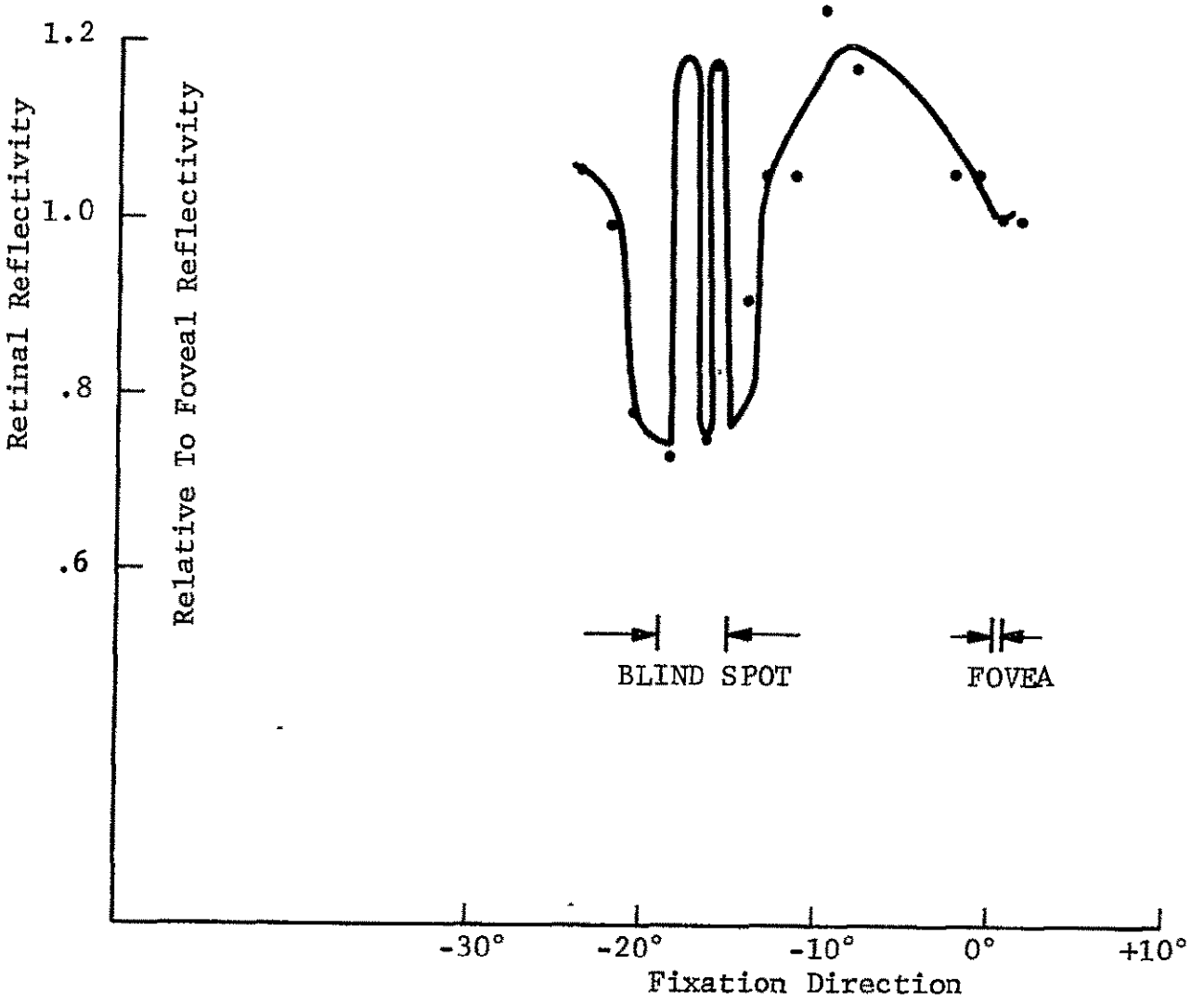

Figure 31.--Retinal Reflectivity

These results confirm the existence of rapid spatial variations of retinal reflectivity in the vicinity of the blind spot. The magnitude of the fluctuations is approximately 0.75 to 1.25 relative to a mean retinal reflectivity of 1.0. Detail (i.e., reflectivity variations) as small as 0.05° was observed.

Variation of pupil signal around the pupil iris boundary.--The pupil signal intensity was measured around the edges of the pupil in the photographs taken during the testing of pupil intensity variations with fixation direction. The illumination and collection apertures were coincident. Pupil uniformity was found to be better than the densitometer accuracy (5%).

Accommodation effects.--The effect of the state of accommodation of the subject on pupil signal intensity was investigated. In a concurrent Honeywell supported program (also reported here for completeness) an investigation was also made into techniques for measuring the state of accommodation of the subject.

In the first set of tests the signal intensity and distribution at the collection aperture were measured as a function of the state of accommodation of the subject. The experimental arrangement was as shown in Figure 32. The illumination aperture was set at f/100 and the collection aperture at f/16. The retinal image returned to the collection aperture was photographed while the subject accommodated at various ranges from infinity to the near point.

The photographs were analyzed to determine the intensity of the central region of the image formed at the collection aperture and also the half power width of the returned image. These measurements are shown, as a function of accommodation distance, in Figures 33 and 34. The collection aperture was located at 39 cms from the eye. It can be noted that the minimum image width (Figure 34) was observed when the subject accommodated for a range of 24 cms. This indicated a chromatic aberration of the eye of 1.6 dioptres between the visible and the IR band employed (about 0.8 μ). From Figure 28 in Reference 3 this chromatic aberration should be about 2.0 dioptres. In the previous analysis of the apparent pupil reflectivity function, a dioptric error of 3.16 was inferred. There are insufficient points near the peak of the curve in Figure 34 to enable the true maximum point to be determined accurately. Thus the value of the chromatic aberration, measured here, can be considered to be in reasonably good agreement with the accepted value.

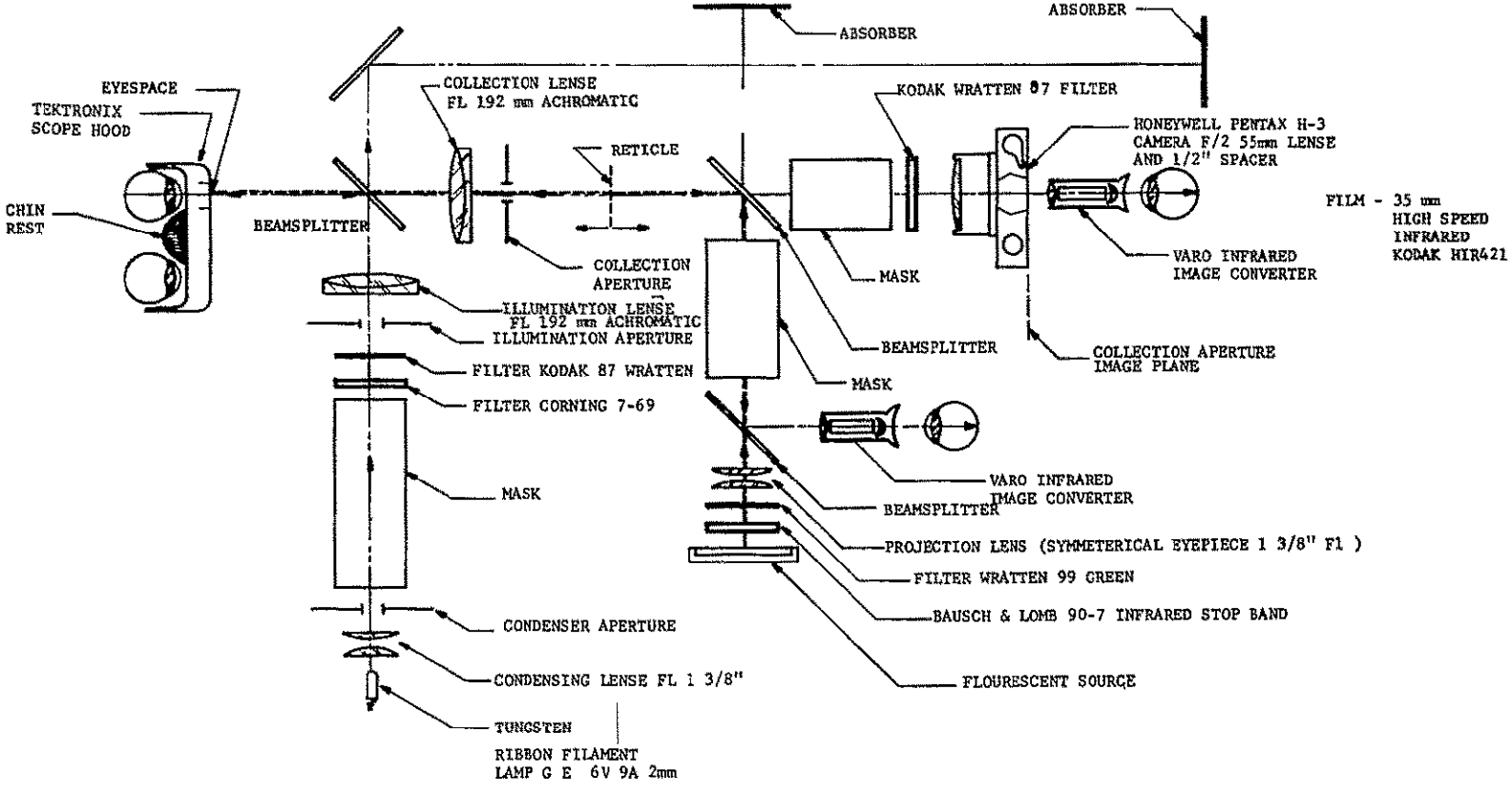

Figure 32.--Experimental Arrangement For Accommodation Tests

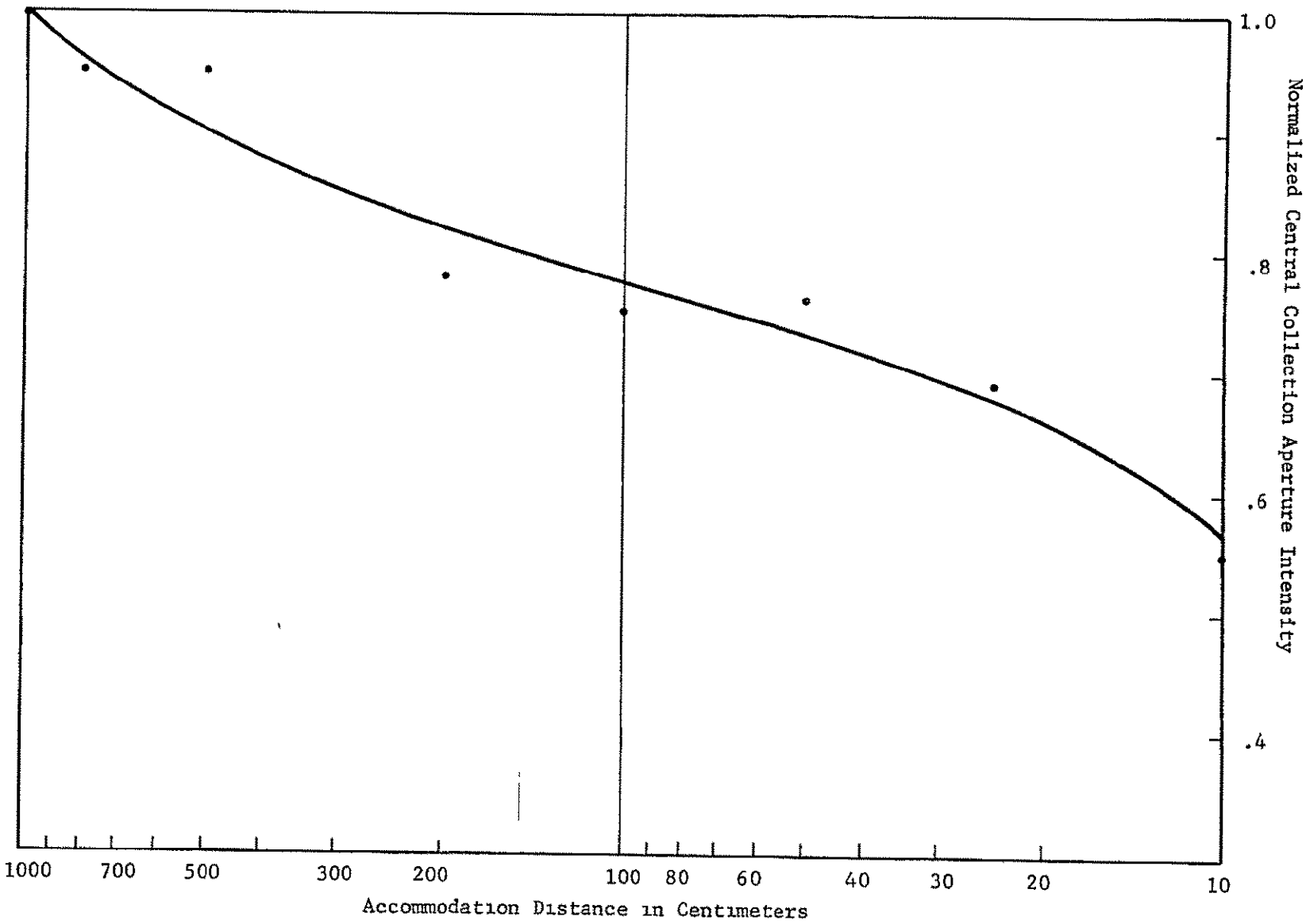

Figure 33.--Signal Intensity At Collection Aperture

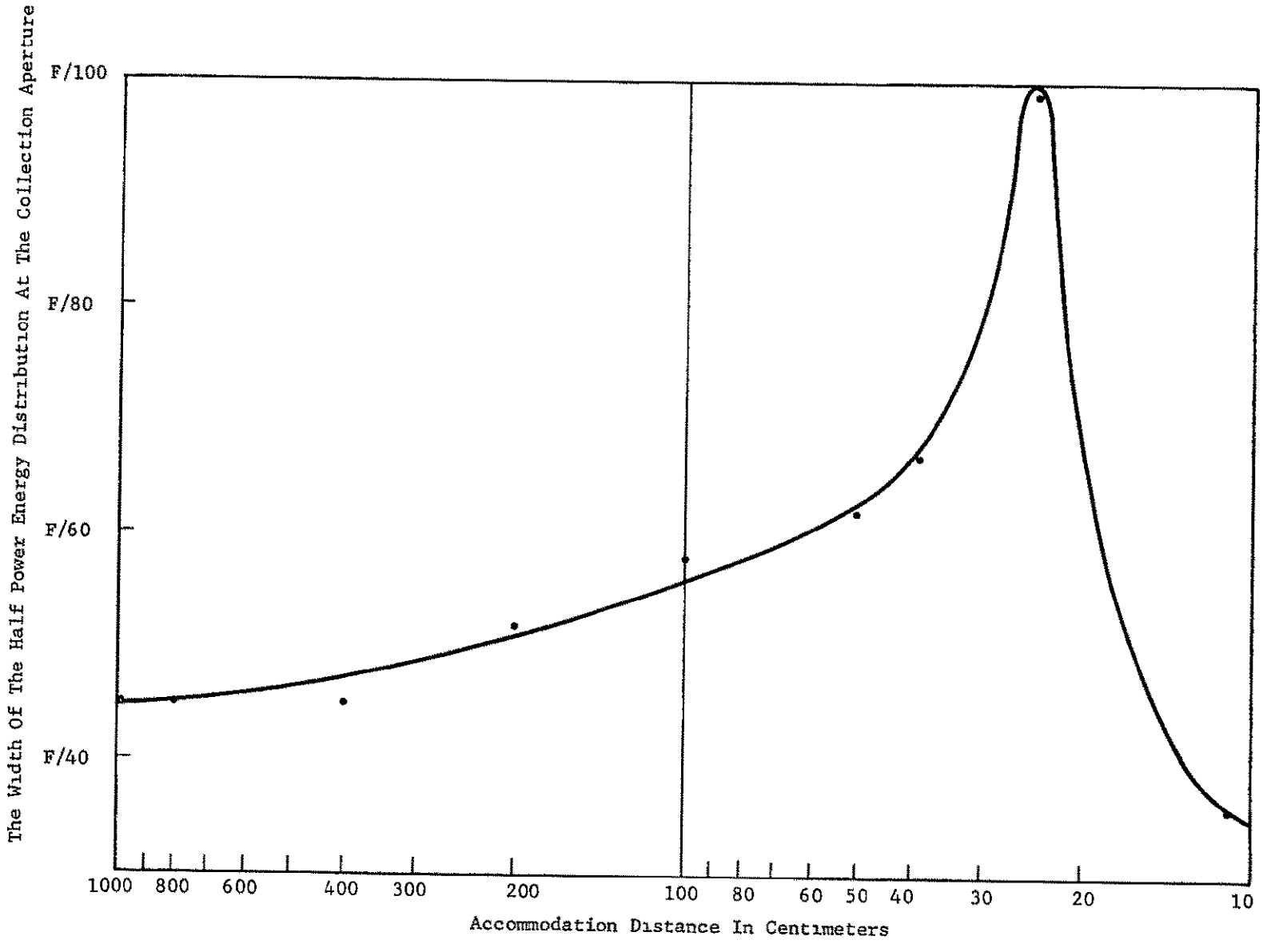

Figure 34.--Image Size At Collection Aperture

In the second set of experiments the pupil image was analyzed for various states of accommodation with the collection and illumination apertures slightly displaced. The experimental arrangement is shown in Figure 35. The pupil image was nonuniform when the eye was not accommodated (at 0.8 μ) for the collection aperture. Figures 36, 37 and 38 show microdensitometer traces of the pupil intensity for various states of accommodation. Figure 39 shows the measured percent variation (gradient) in the pupil image as a function of the state of accommodation of the eye.

Optimum f/Number Determination

The experimental results described in the previous section have established:

1) The functional relationship between nominal apparent pupil reflectivity, system f/number, and pupil diameter.

2) The variations of nominal apparent pupil reflectivity.

   a) over various subjects
   b) fixation direction
   c) state of accommodation

Specifically,

1) $1/\rho = 7.55 \times 10^{2} \left(\frac{1}{F^2 d^2} + 1.99 \times 10^{-5}\right)$

   (This equation leads to a value of 5.3% for the retinal reflection factor -Kr_7^2- and of 3.16 dioptres for the retinal blur effect.)

2a) ρ = 0.5 to 1.5 for various subjects (relative to a mean value of 1.0)

2b) ρ = 0.75 to 2.0 with fixation direction (relative to a mean value of 1.0)

2c) The returned energy at the collection aperture is a blurred version of the illumination aperture when an accommodation error exists.

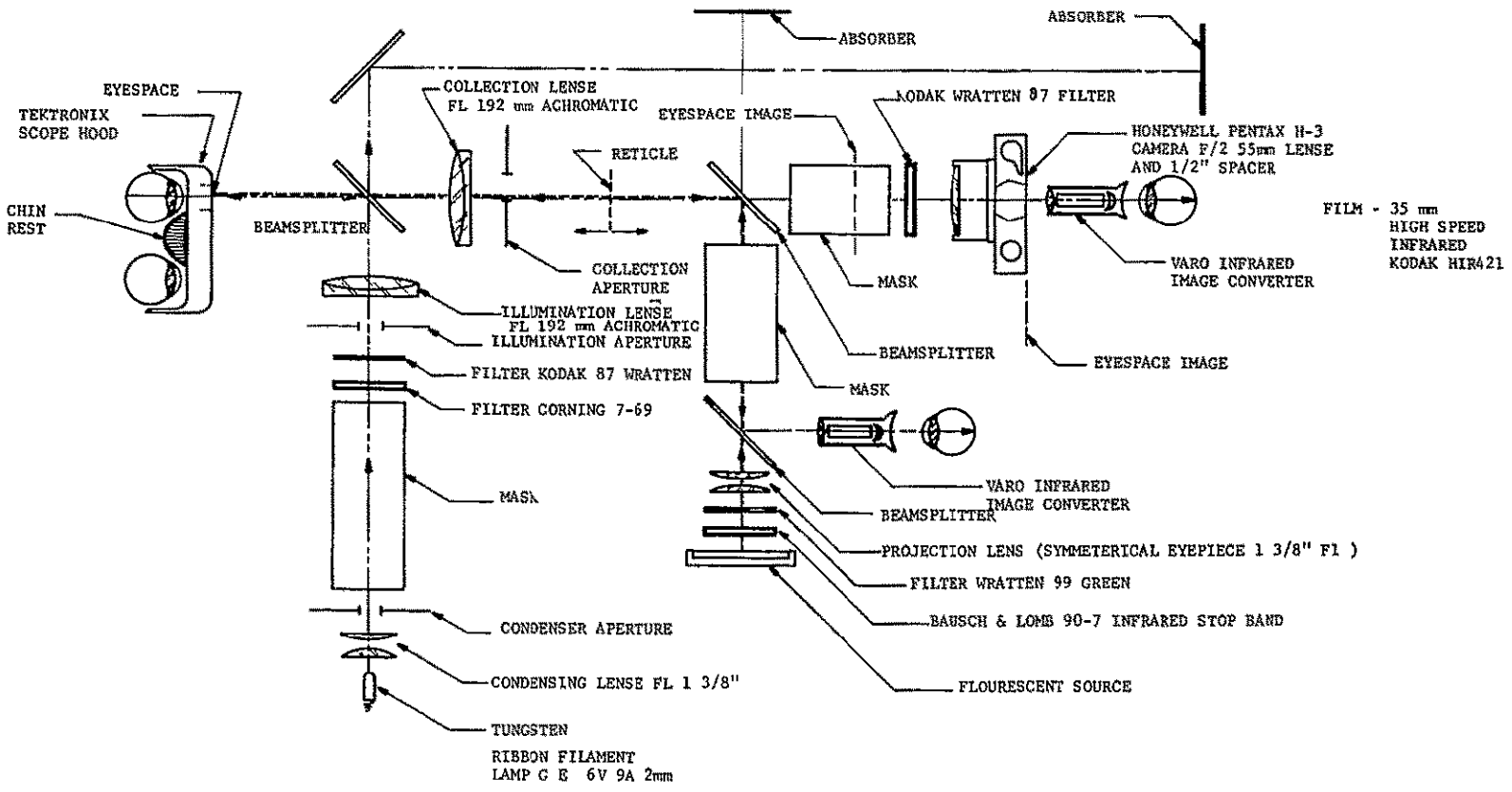

Figure 35.--Experimental Arrangement For Accommodation Sensing Tests

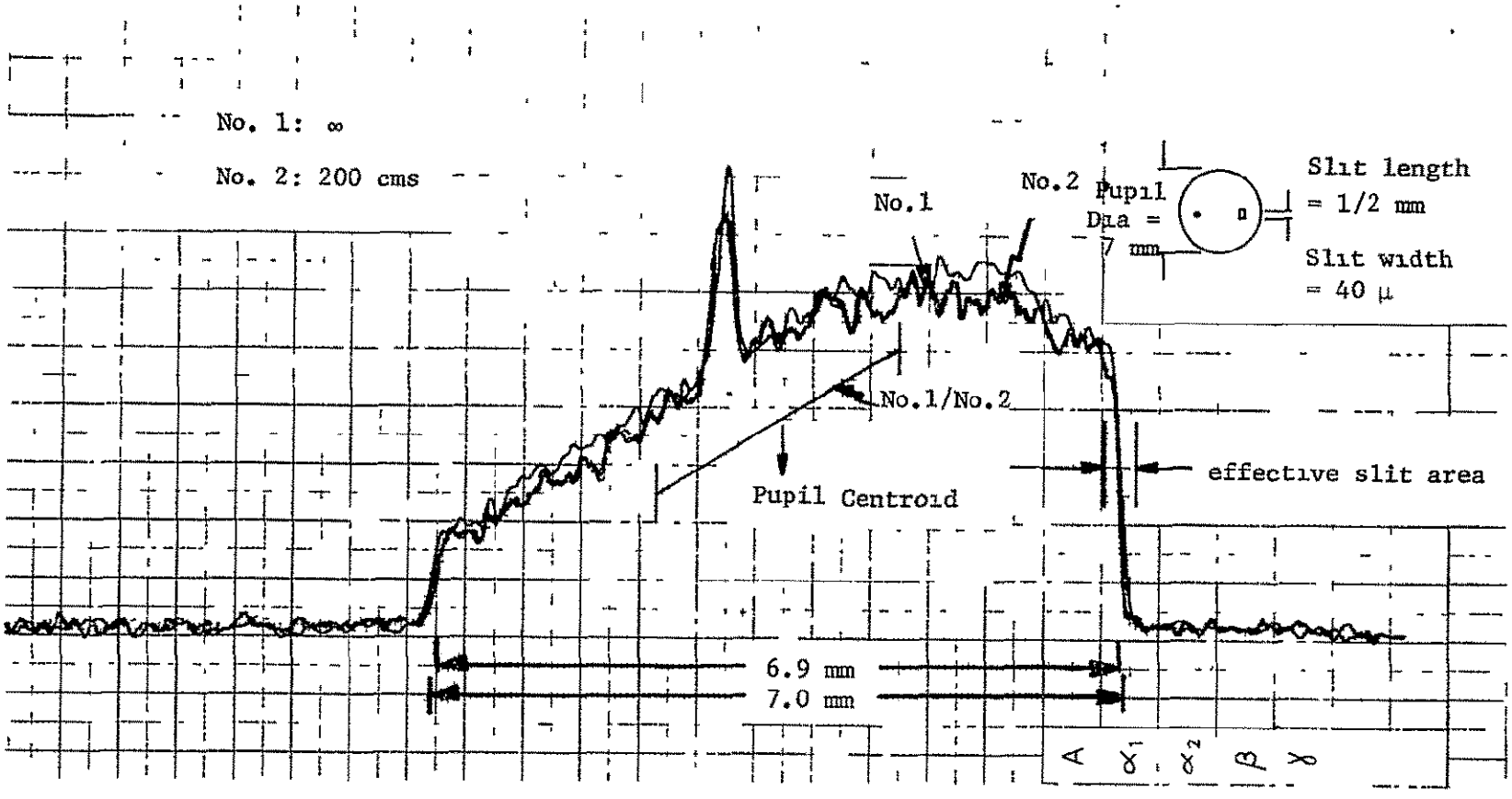

Figure 36.--Microdensitometer Traces Of Pupil Gradient, Accommodation At ∞ And 200 cms

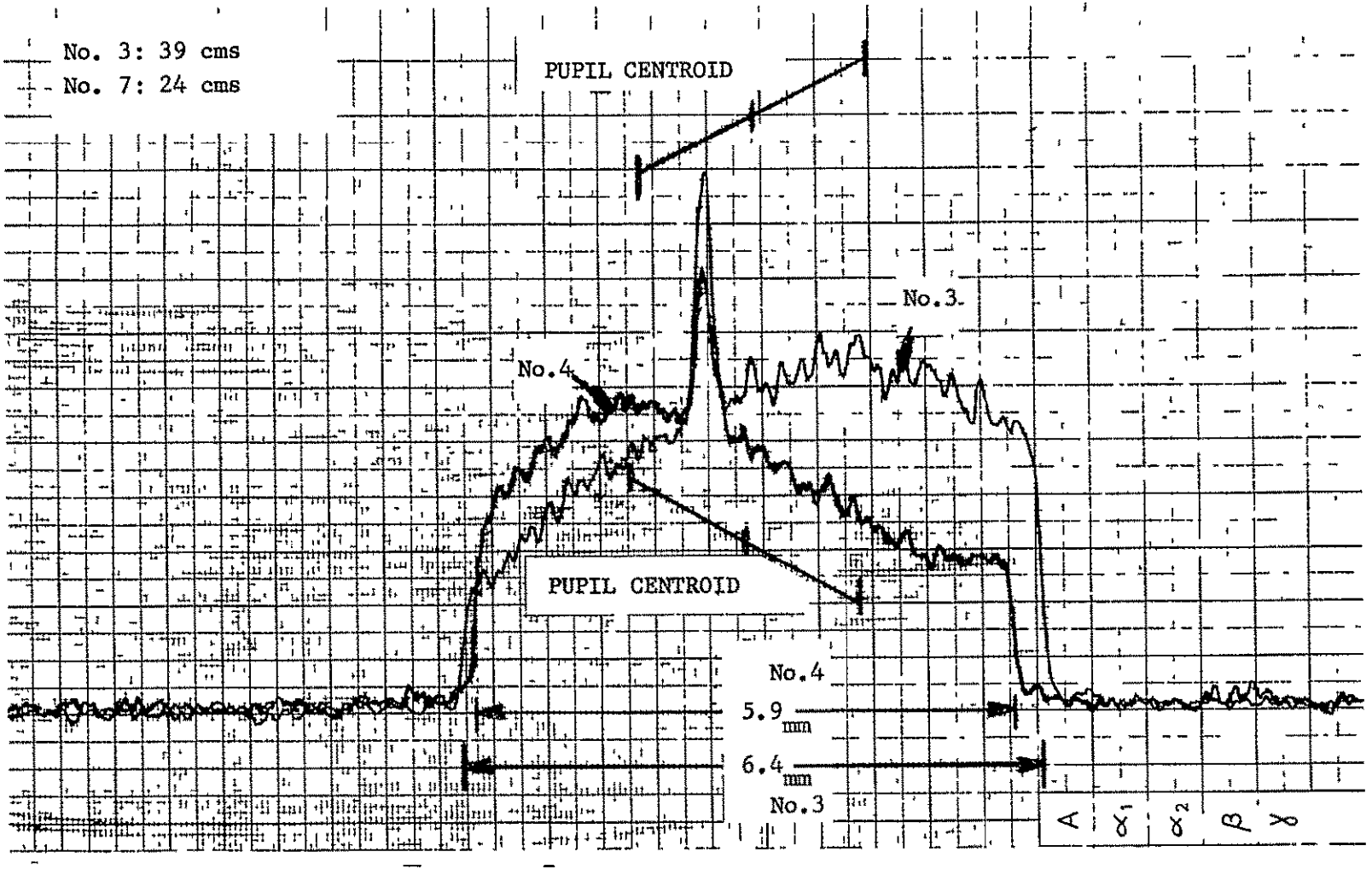

Figure 37.--Microdensitometer Trace Of Pupil Gradient Accommodation At 39 and 24 cms

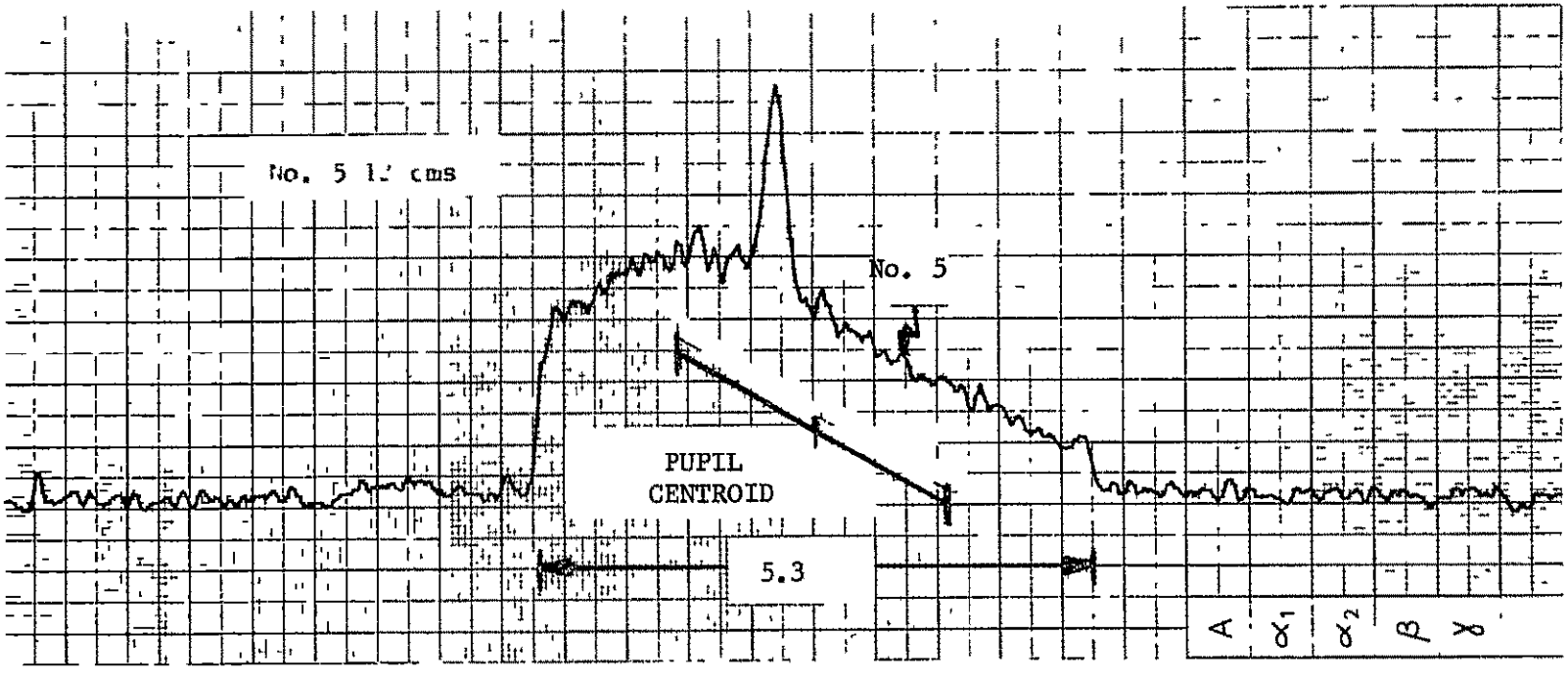

Figure 38.--Microdensitometer Trace Of Pupil Gradient, Accommodation At 12 cms

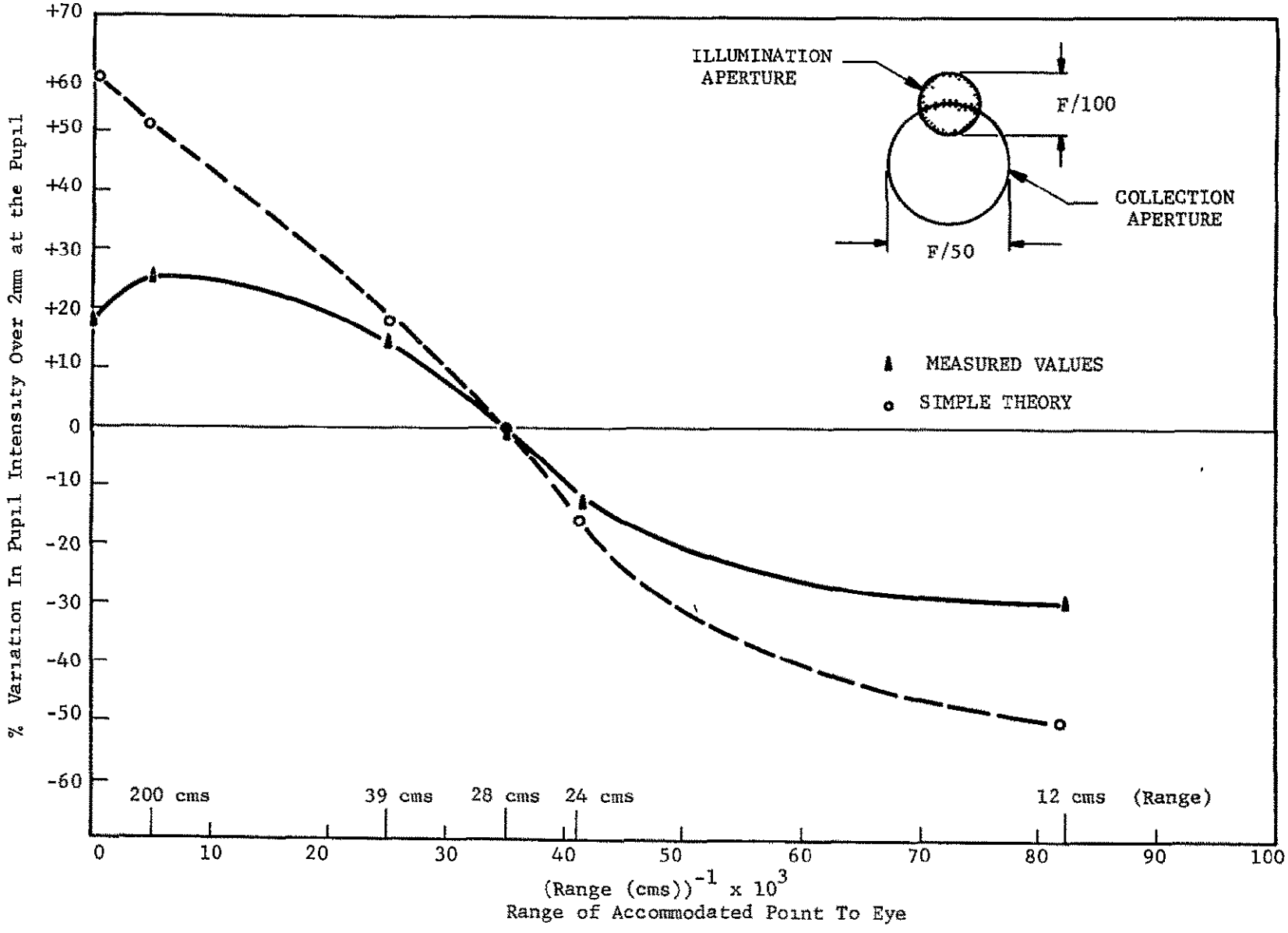

Figure 39.--Measured Pupil Gradient As A Function Of Accommodation

From this data a general expression for pupil reflectivity can be constructed·

$$1/\rho = \frac{7.55}{S} \times 10^3 \left(\frac{1}{F^2 d^2} + \frac{2}{10^6} \delta D^2\right)$$

where S is a factor expressing the variation in retinal reflectivity:

S = 0.8 to 1.6: frequently occurring variations

S = 0.5 to 2.0: less frequent (e.g., one σ of population sample, blind spot variations, etc.)

S = 0.4 to 3.0: theoretical maximum possible variations based on extremes of all variables.

and,

F is the Oculometer system f/number

d is the diameter of the eye pupil in millimeters

δD = is the accommodation error due to ametropia of the subject's eye, chromatic aberration, accommodation error etc.

The important performance parameter is the noise level in the pupil tracking system. Let P be the pupil signal intensity and I the iris signal intensity. The signal/shot noise in the tracking system will be proportional to $(S/N)_{REL}$.

where,

$$\left(\frac{S}{N}\right)_{REL} = \frac{P - I}{\sqrt{P + I}}$$

now,

$$P \alpha \frac{\rho}{F^4}$$

and,

$$I \alpha \frac{\rho_o}{F^4}$$

where ρ is the apparent pupil and ρ_o the iris reflectivity.

Therefore,

$$(S/N)_{REL} = \frac{\rho - \rho_o}{F^2\sqrt{\rho + \rho_o}}$$

For the case when $\rho = 1$, $\rho_o = 0$ and $F = 1$ (i.e., a perfect white diffusing pupil, perfectly black retina and an F/1 optical system then,

$$(S/N)_{REL} = 1$$

Thus, the value of $(S/N)_{REL}$, given above, can be considered as the ratio of the tracking noise (tracking error) with this ideal diffusing white pupil to the tracking noise error obtainable with the actual eye pupil.

The iris reflectivity observed in the present study ranged from 0.1 to 0.15 (see Figure 23). In previous work (see Reference 1, page 50), the range was found to be 0.15 to 0.3. As a worst case condition, the iris reflectivity will be assumed to be 0.3. (It is significant that some correlation was found between retinal reflectivity and iris reflectivity. Thus for a subject with low retinal reflectivity, the pupil/iris contrast may be better than assumed here because this iris reflectivity may also be low.)

The value of $(S/N)_{REL}$ has been calculated from the above formula for a wide range of conditions. A selection of the computed data is plotted in Figures 40, 41 and 42.

The ability of the image dissector to reliably acquire and accurately track the eye is limited by two factors:

a) the pupil/iris contrast - obviously this must be greater than one.

b) the system f/number - although the pupil/iris contrast improves with increasing f/number the absolute value of the pupil signal decreases with increasing f/number. The net effect is that pupil tracking signal noise eventually decreases as the f/number is increased (see Figures 40, 41 and 42). The deleterious effect of diffraction also increases with increasing f/number.)

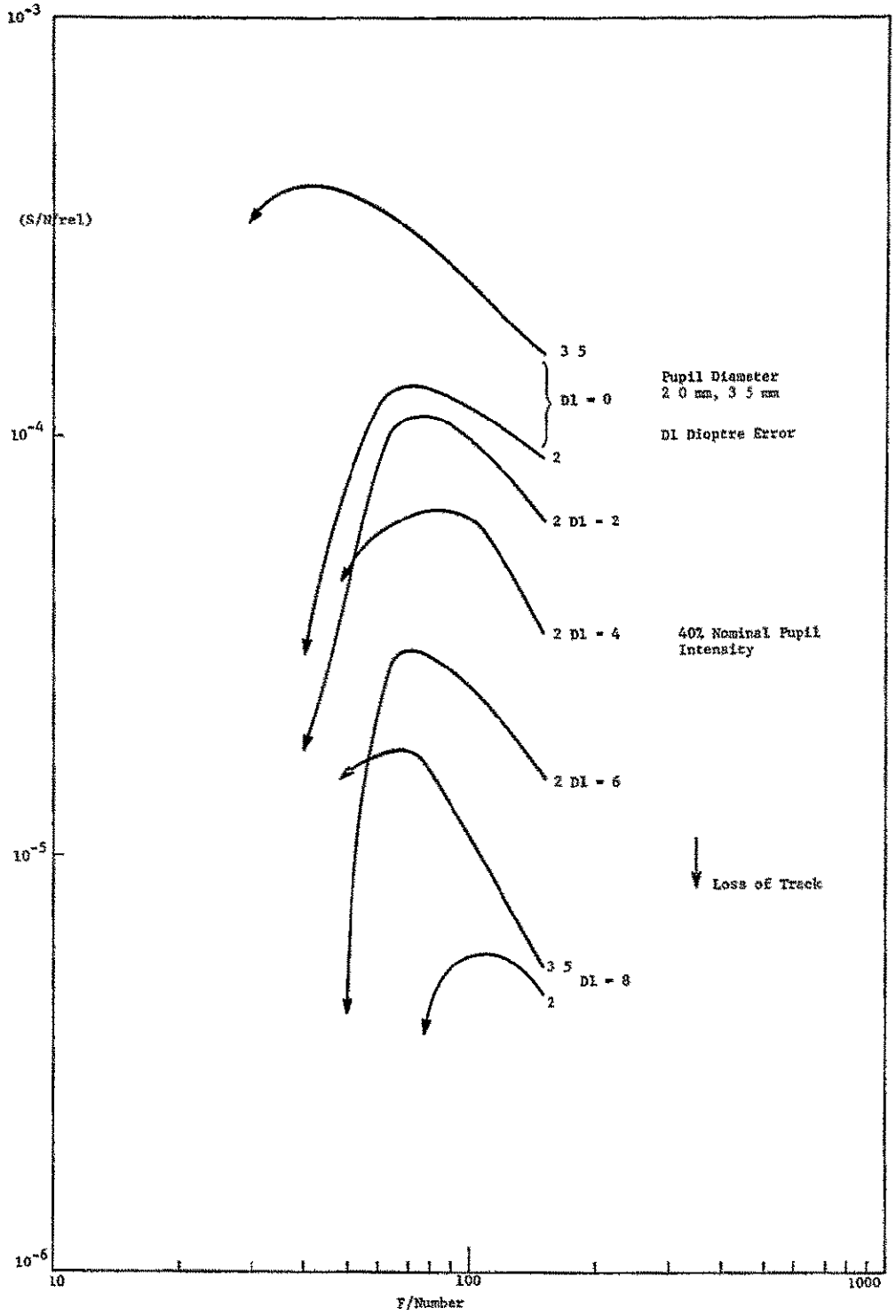

Figure 40.--Computed Data To Establish $(S/N)_{REL}$ Values

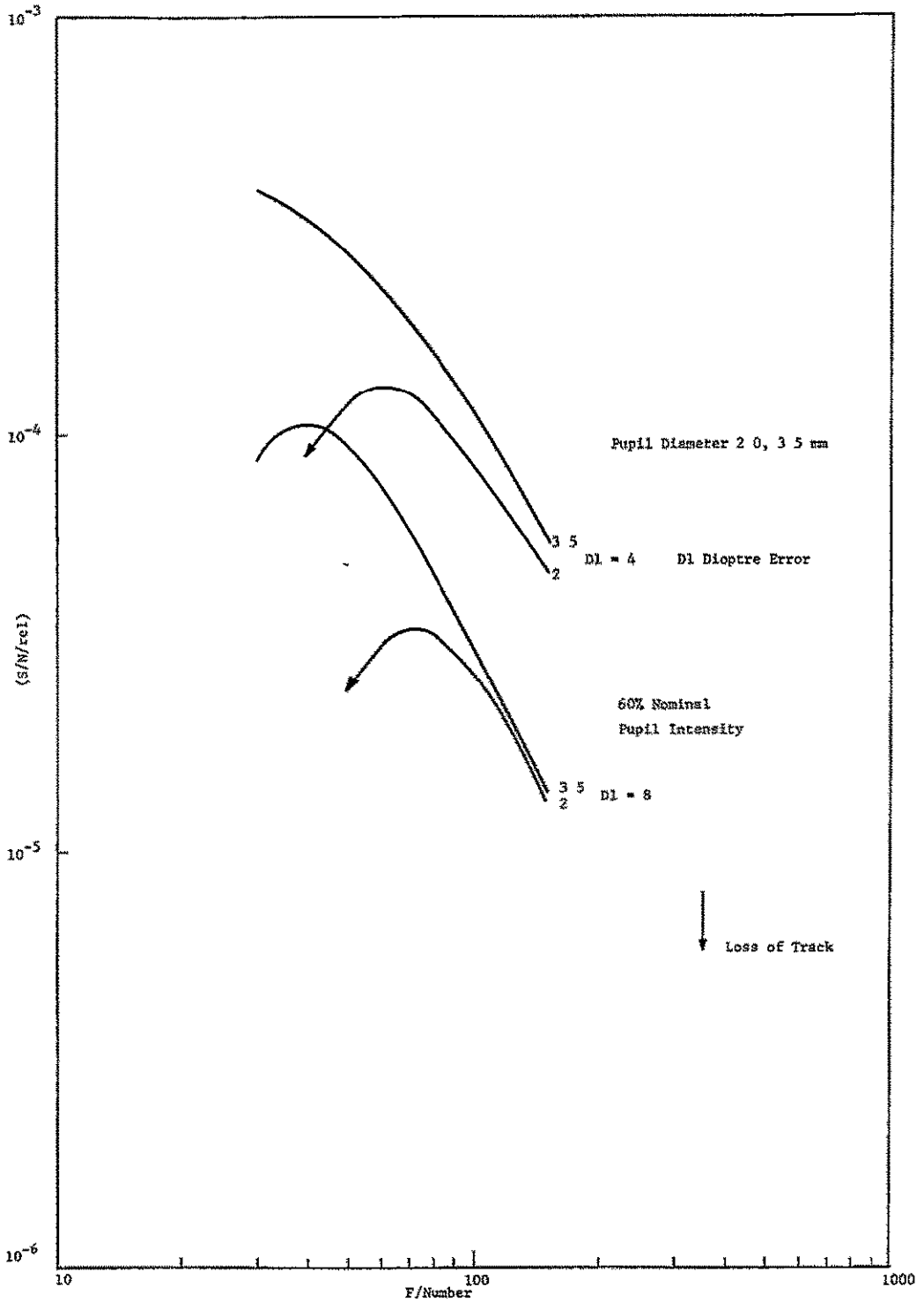

Figure 41.--Computed Data To Establish $(S/N)_{REL}$ Values

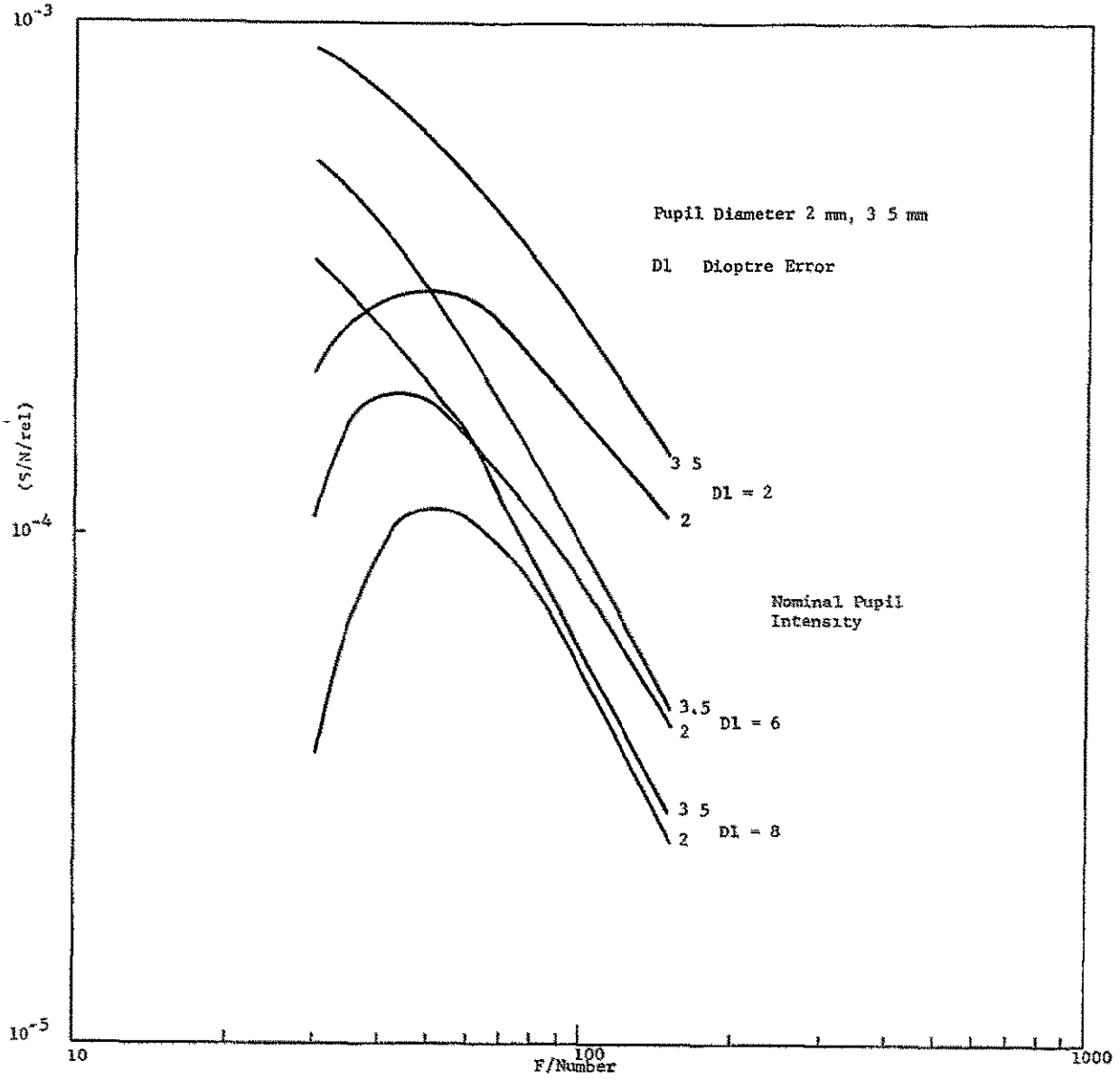

Figure 42.--Computed Data To Establish $(S/N)_{REL}$ Values

The worst case iris reflectivity is assumed to be 0.3. It may be assumed therefore that the pupil reflectivity must exceed 0.5 for reliable acquisition and accurate tracking. From consideration of absolute signal level, and also diffraction, it can be said that the f/number should not exceed 80. The condition expressing a minimum pupil reflectivity of 0.5 is,

$$2 = \frac{7.55}{S} \times 10^3 \left(\frac{1}{F^2 d^2} + \frac{2\,\delta D^2}{10^6}\right)$$

i.e.,

$$\frac{1}{F^2 d^2} + \frac{2\,\delta D^2}{10^6} = 2.65 \times 10^{-4}\ S$$

This relationship is plotted in Figure 43 for three values of S. Good system operation, as defined above, requires operation to the right of the curves. Thus,

a) The possible range of dioptre error is limited - particularly when S = 0.4. To cover 97% of the population with respect to ametropia in this case requires Fd = 180. For a worst case of 2 mm pupil diameter this cannot be achieved without exceeding F/80. However, it should be noted that S = 0.4 is probably unrealistic because the variation in pupil reflectivities over the population has been ascribed to retinal reflection variations. Some of the variation is undoubtedly due to ametropia. Taking S = 0.7, the 97% range of ametropia can be covered at F/50 with a 2 mm (worst case) pupil. Assuming accommodation at infinity, the Oculometer at one meter and a 2 mm pupil diameter, it can be seen from Figure 41 that an F/60 system is satisfactory.

b) From these considerations it is considered that F/60 is the optimum value of the system f/number. It should permit operation under all conditions except a combination of extremely (and probably unrealistically) low retinal reflectivity with accommodation error (or ametropia).

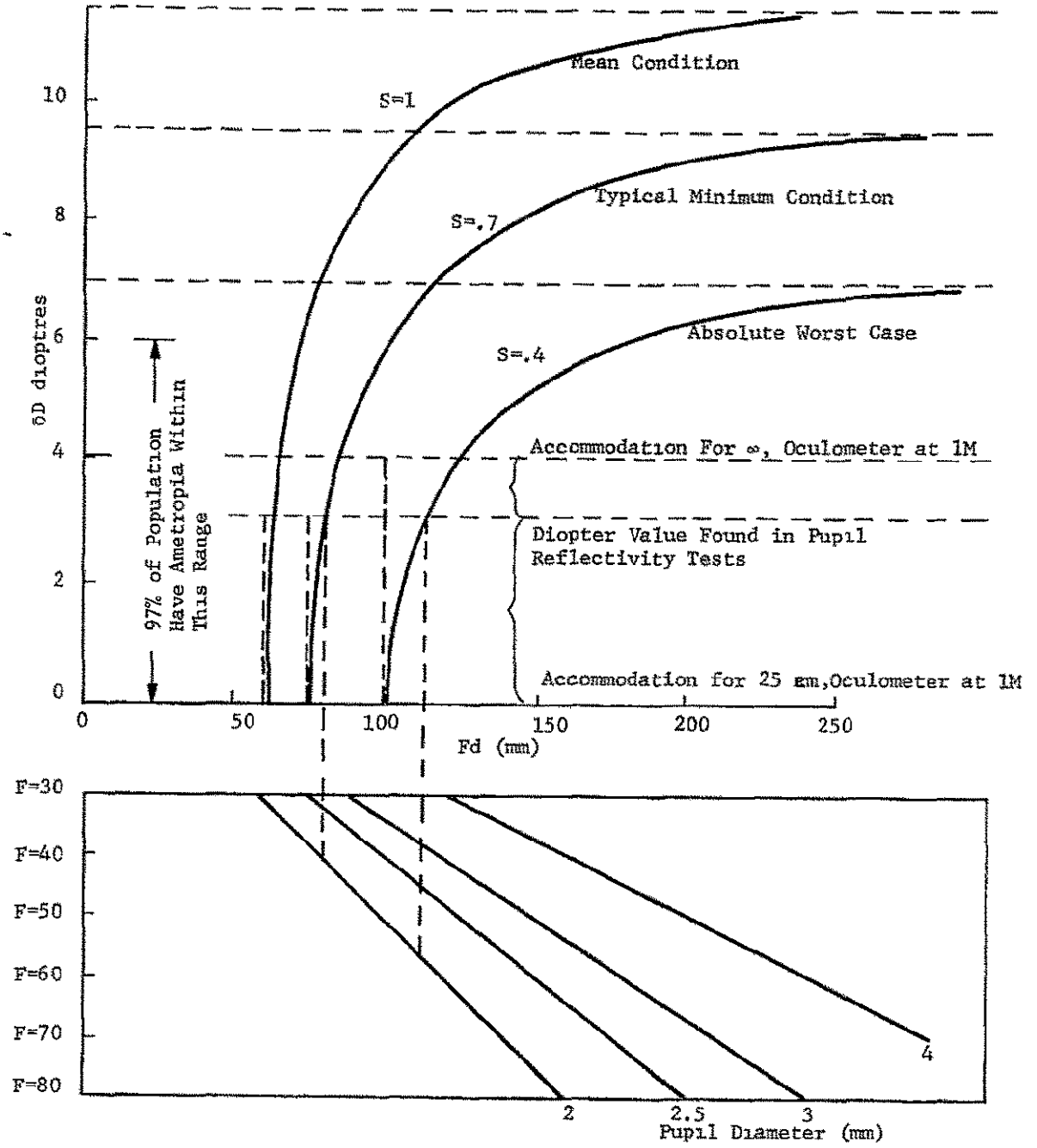

Figure 43.--Operating Contours

XENON SHORT ARC STUDY

Under this study two lamps were evaluated: the Varian Lamp and the PEK Lamp.

Varian Lamp

The Varian short arc lamp (X6163S) utilizes an internal elliptical reflector (parabolic is also available) to collect and direct the radiation from the arc (Figure 44).

The arc is imaged (in the particular lamp tested) at a point 3 5/8 inches from the sapphire window. There are two important parameters of this primary image of the arc:

1) the energy density (watts/cm^2) at the arc image.

2) the divergency (steradians) of the rays from the image.

Experiments have revealed that two distinct sets of rays can be distinguished in the arc image:

1) highly collimated rays.

2) divergent rays.

The distribution of these rays is shown in Figure 45. A screen placed at the image plane (3 5/8 inches from the sapphire window of the lamp) shows a central hot spot in the image. As the screen is moved away from the lamp the light distribution on the screen corresponds to the ray pattern as shown in Figure 45.

If the central, collimated rays coming from the arc image are collected and the peripheral divergent rays obscured (by means of 1.5-inch diameter aperture placed 26 inches from the lamp, the arc image (due to the collimated rays only) can be investigated. The particular arc image due to the collimated rays can be re-created by placing a lens at the aperture (26 inches from the lamp), see Figure 46. This experiment shows that the arc image due to the collimated rays has a central cold spot (with side arms which are an image of the electrode supporting arms). In contrast, the arc image due to all rays has a central hot spot.

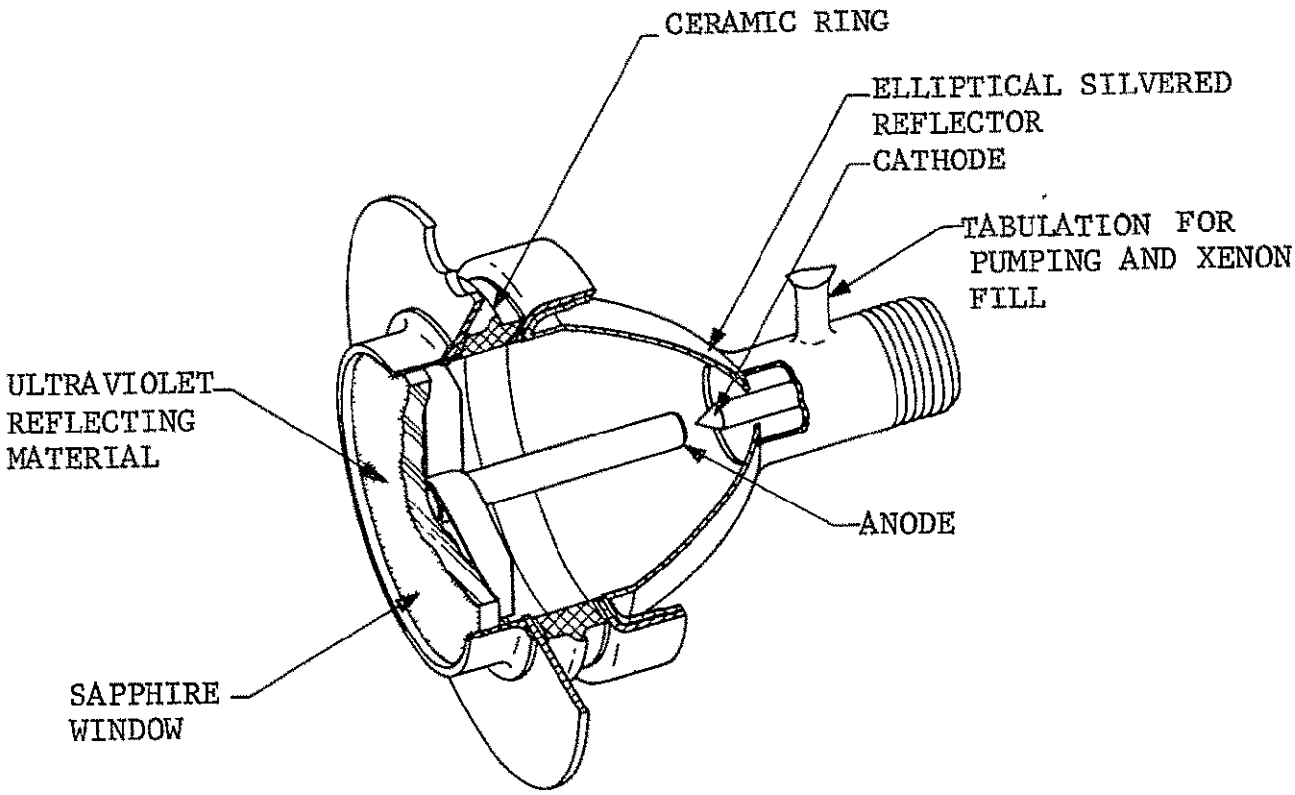

Figure 44.--Varian Xenon Short Arc Lamp

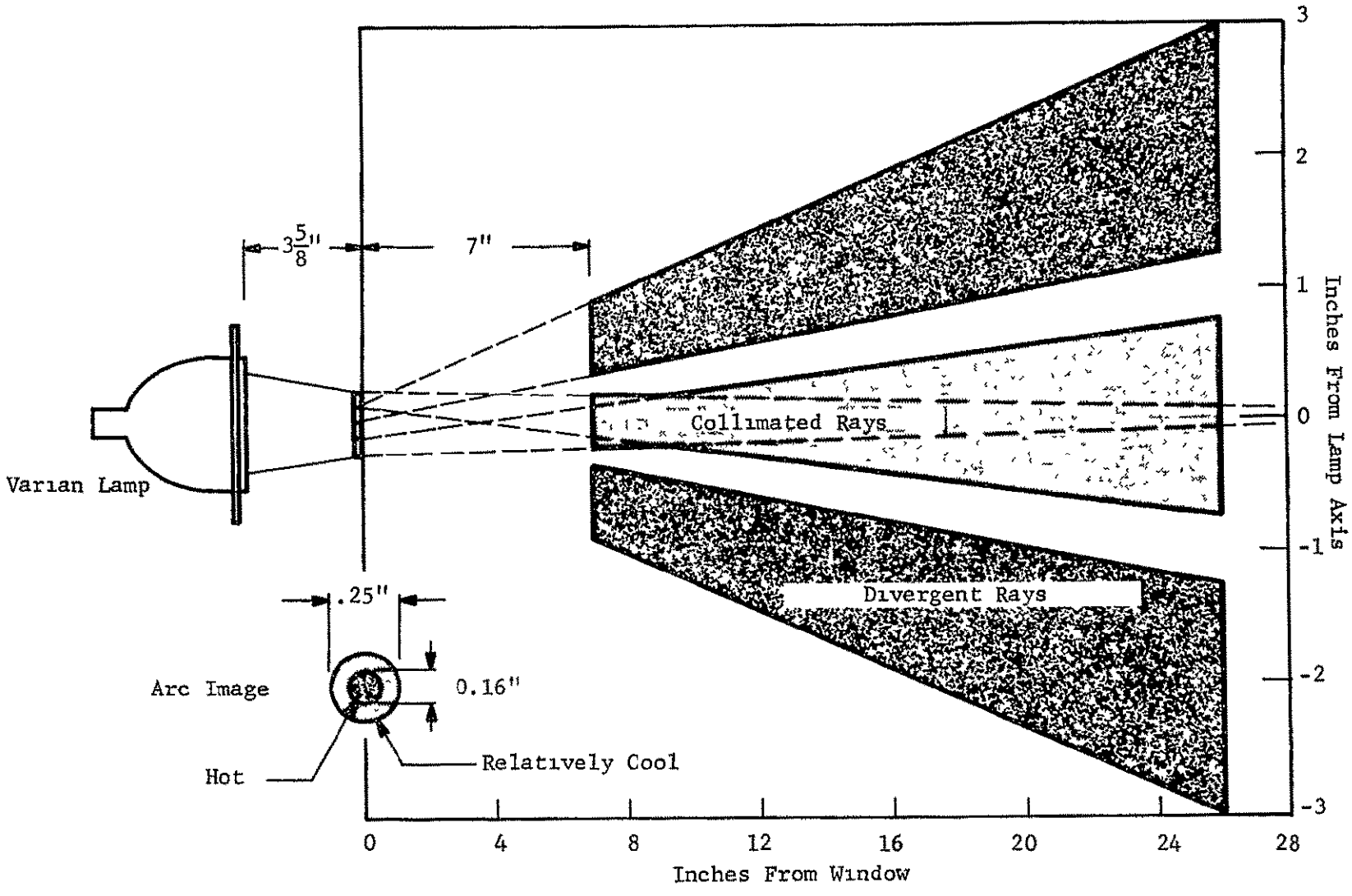

Figure 45.--Xenon Short Arc Ray Distribution

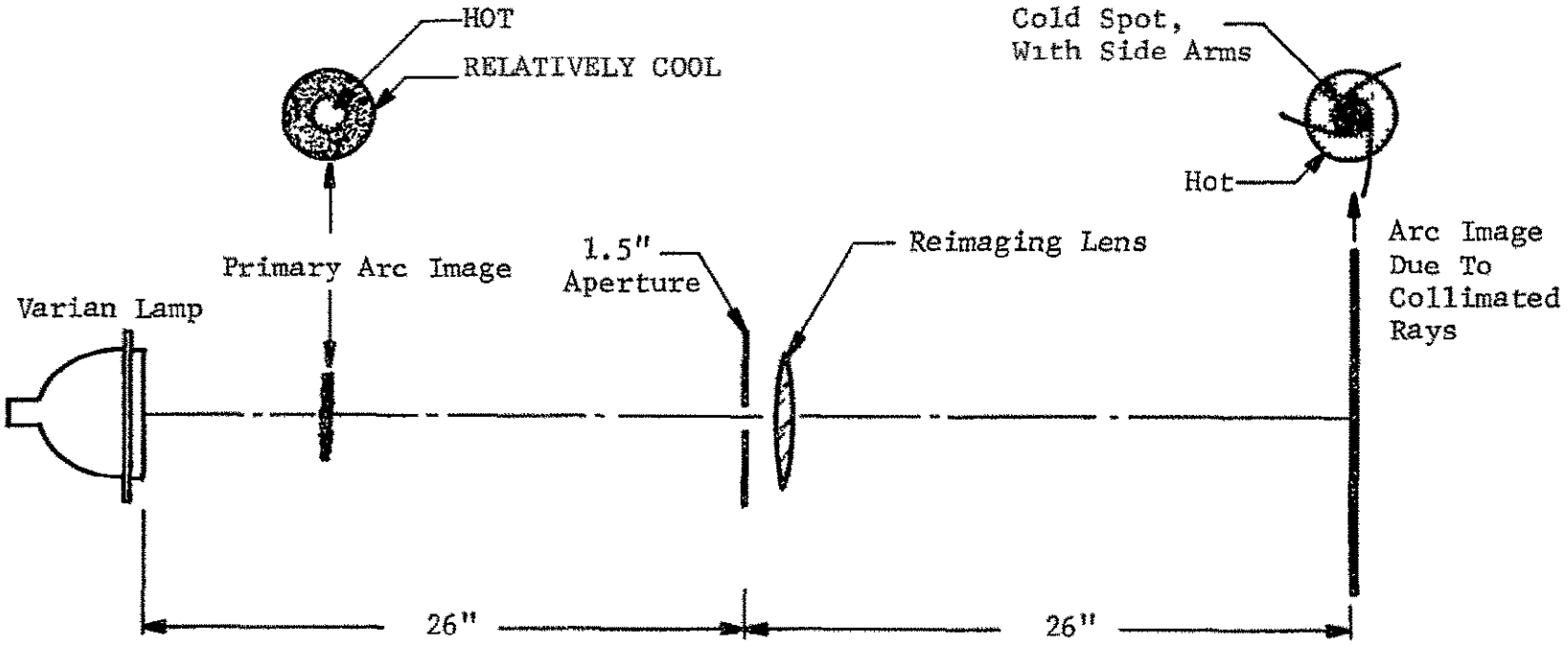

Figure 46.--Testing Collimated Rays

Intensity measurements.--The intensity at the arc image was measured with the experimental arrangement as shown in Figure 47. The arc image (at the ellipse secondary focus) was itself imaged by a lens onto the entrance slit of a monochromator. The exit slit of the monochromator was imaged onto the detector element of an EG&G light mike. The relative intensity of the arc image was measured (at λ = 8715Å) and is shown in Figure 48. The relative spectral distribution was measured and is shown in Figure 49.

The relative intensity measurements were converted to absolute intensity measurements by two independent calibration techniques:

1) A filter of known transmission characteristics was used to restrict the bandpass of the EG&G light mike, which was placed before the monochromator (Figure 47).

2) A tungsten filament source of known spectral irradiance was substituted for the xenon lamp in the arrangement as shown in Figure 47.

The calibration factors (in effect, defining the transmission factor of the monochromator) obtained by these two independent methods agreed within 10% of each other. This factor was used to convert the relative intensity measurements to absolute intensity. The spectral radiance was then calculated in units of watts/cm^2/steradian/Å and plotted in Figure 50, for various points in the spectrum. Note that the left hand scale refers to the peripheral rays and the right hand scale to the central rays. The spectral radiance of the peripheral rays should probably be reduced by a factor of 2 since the divergent rays which mostly originate from the center of the arc image nevertheless contribute some intensity in the periphery of the arc image. As an additional check the spectral radiance of the arc, as imaged by collimated rays (Figure 46), was estimated using the EG&G light mike detector. Because of the relatively large area of the detector an average spectral radiance over the peripheral region was obtained of 0.5 watts/cm^2/steradian/Å at the maximum spectral peak - which is consistent with the values shown in Figure 50, reduced by a factor of two as previously discussed. Finally, it may be noted that these figures for the maximum spectral radiance of the xenon arc are reasonably consistent with the estimates given in Reference 2 (0.5 watts/cm^2/steradian/Å maximum spectral radiance).

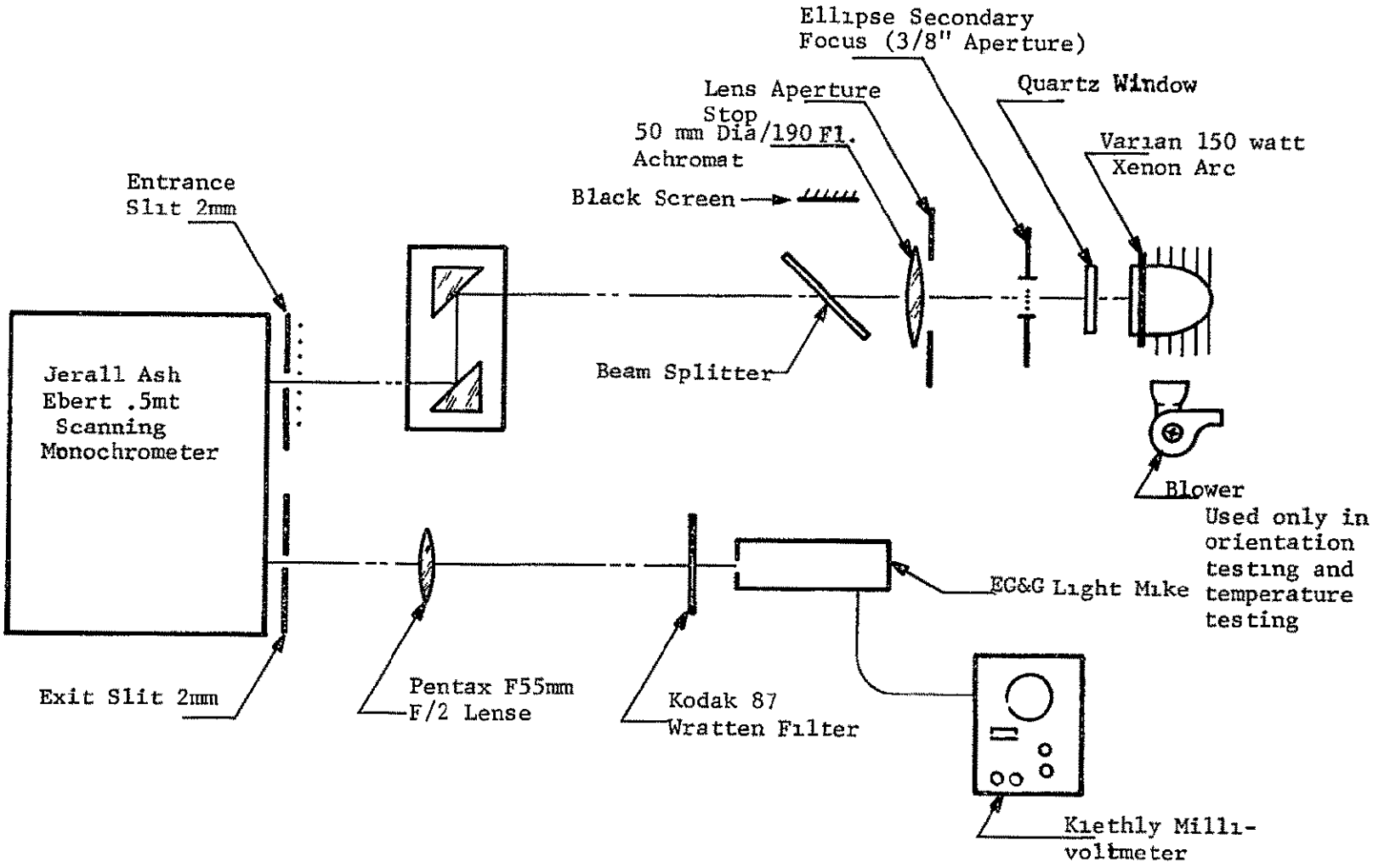

Figure 47.--Experimental Arrangement For Varian Lamp Study

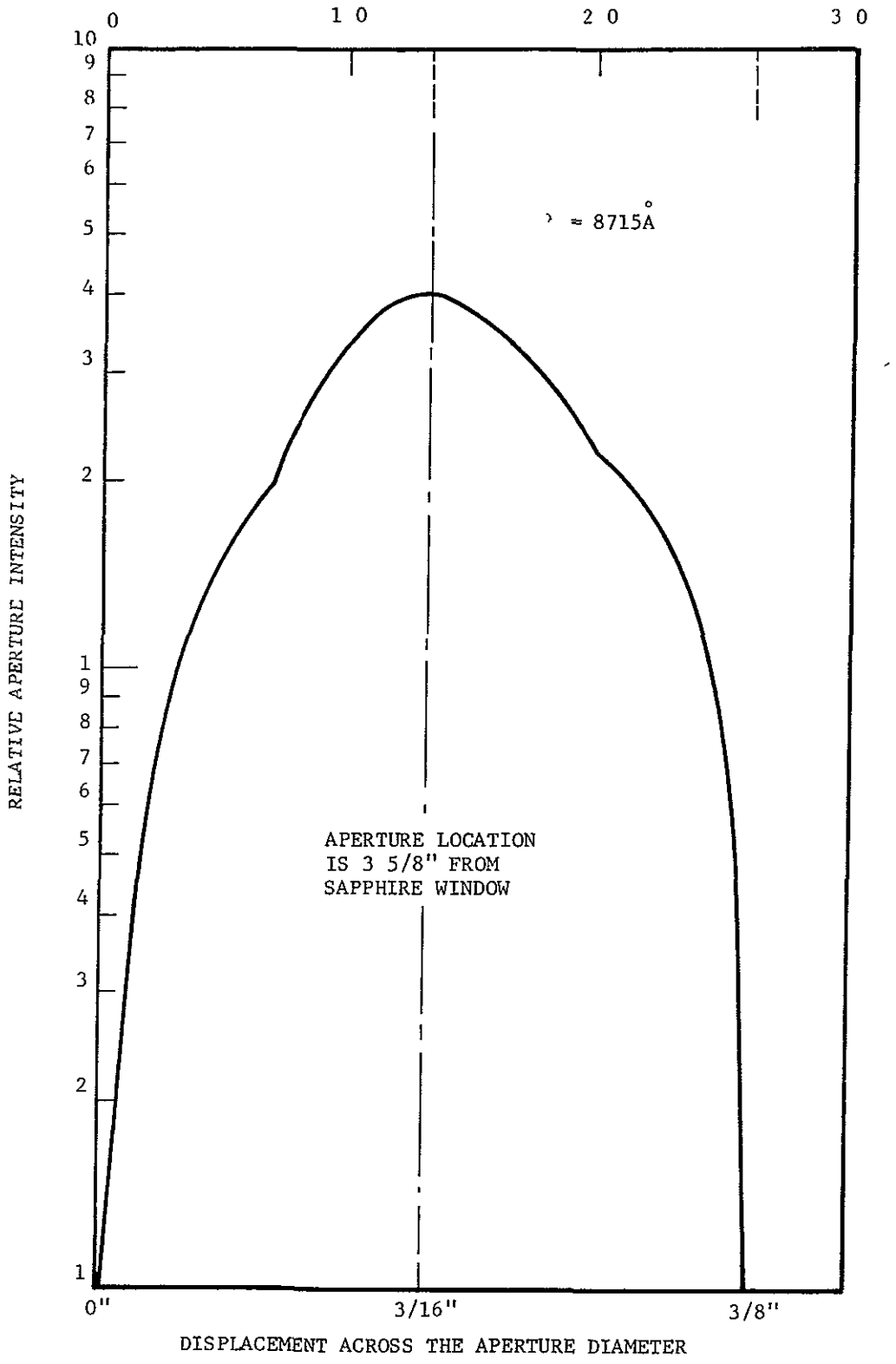

Figure 48.--Relative Intensity Of Varian Short Arc

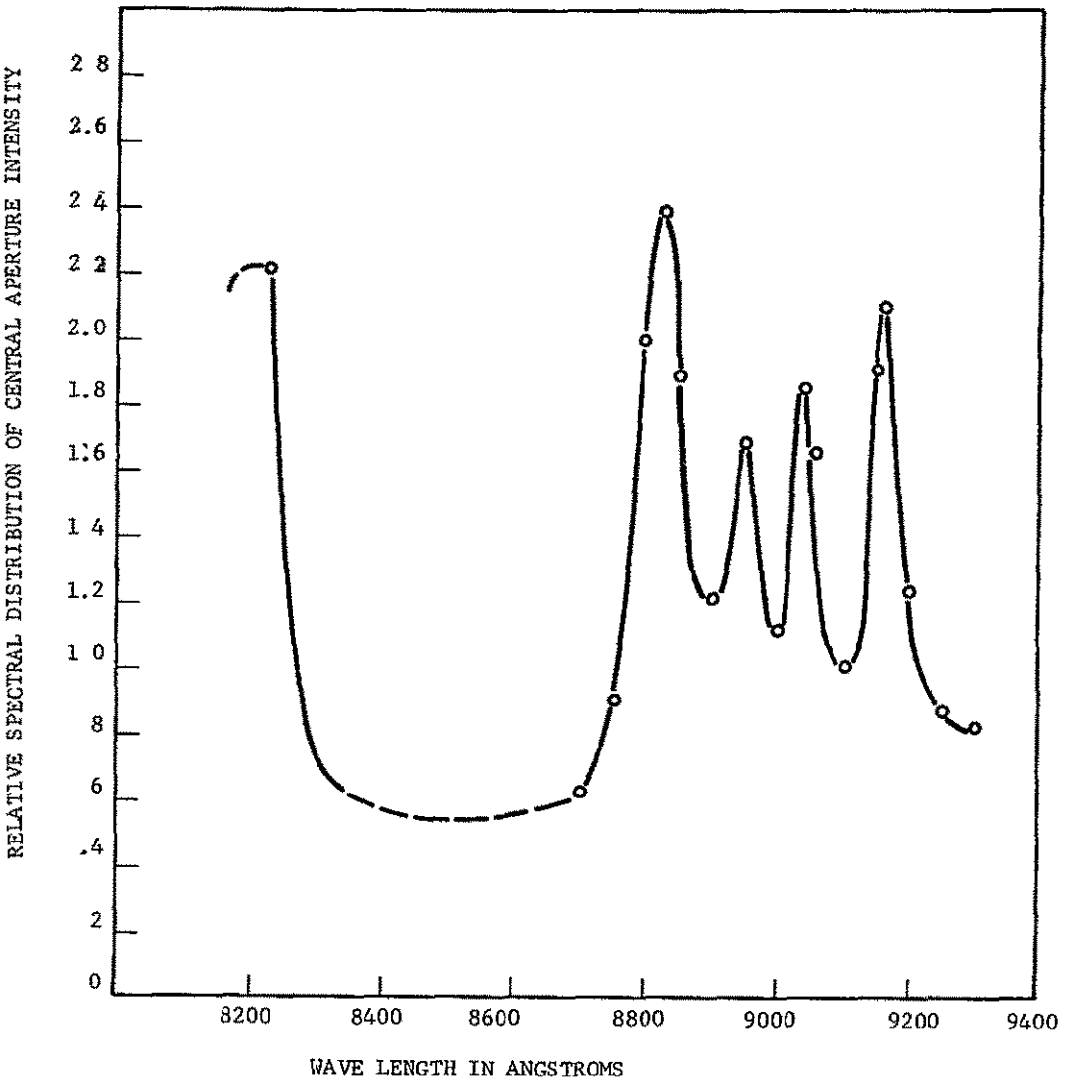

Figure 49.--Relative Spectral Distribution

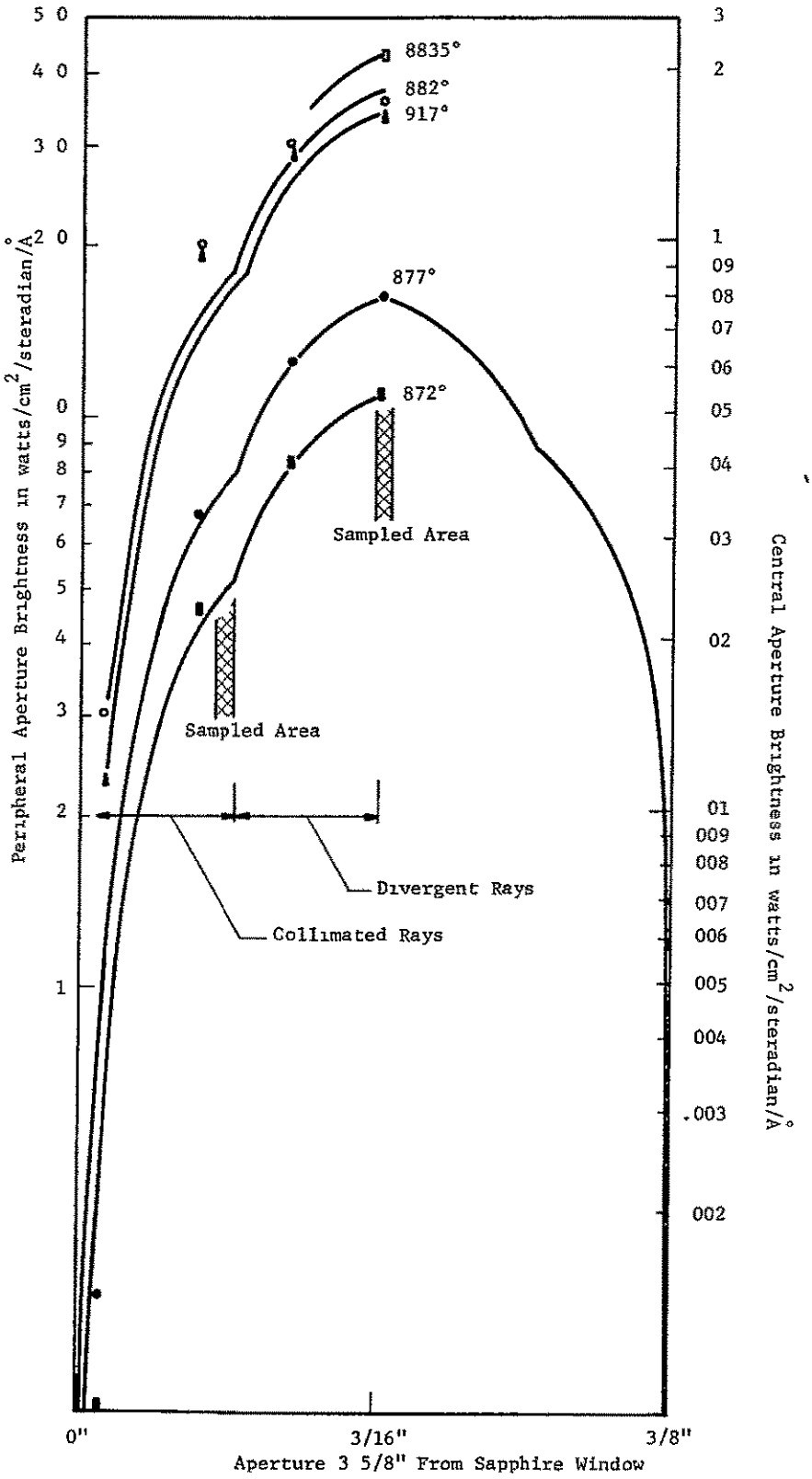

Figure 50.--Radiance Of Varian Xenon Arc At Specified Wavelengths

However, the maximum spectral radiance of the 150-watt Varian lamp cannot directly be utilized in the Oculometer. Referring to Figure 45, it can be seen that an annular region of the arc image of diameter 0.25 inch contributes the low divergence rays over a 3-degree angular spread. The Oculometer source aperture should be about 1 inch in diameter with a 1-degree spread. There is, therefore, not quite sufficient 'quantity' of the low divergence (high radiance) rays to supply the Oculometer. It may be inferred, however, that a 500-watt Varian lamp would be capable of supplying the necessary quantity of high radiance rays due to the larger physical size of the arc.

As a conservative estimate, it will be specified that the Varian lamp will provide radiation at a peak spectral radiance of 0.2 watts/cm/steradian/Å.

Arc stability.--The nominal operating orientation by the lamp was taken to be horizontal in this study (the manufacturer specifies that the lamp can be operated in any position). The effect of other lamp orientations was investigated. Apart from convective jitter when oriented vertically, the orientation of the lamp had no effect on the relative position or stability of the arc. The convective jitter would be almost entirely smoothed out by the fiber optics relay and in any event would not have any significant effect on the operation of the Oculometer.

The stability of the arc image for various values of the lamp current was investigated. At 12 amps (the rated value) the arc image was stable and the central hot spot moved about less than 1/20 inch in the image plane. At 7.5 amps the central hot spot moved generally down, occasionally to one side, by about 0.3 inch.

The wavelength of the 8819 Å line was observed to decrease by 6 Å as the lamp power was reduced from 12 amps to 7.5 amps.

Lamp temperature.--The temperatures of the lamp housing and various optical elements near the lamp were measured. The results are shown in Figures 51, 52 and 53.

Operating life.--The manufacturer claims an average life of 1000 hours. The first lamp received developed a gas leak (and thus became inoperative) after less than one hour of use. The second lamp received showed no signs of deterioration after an estimated 80 hours of operation.

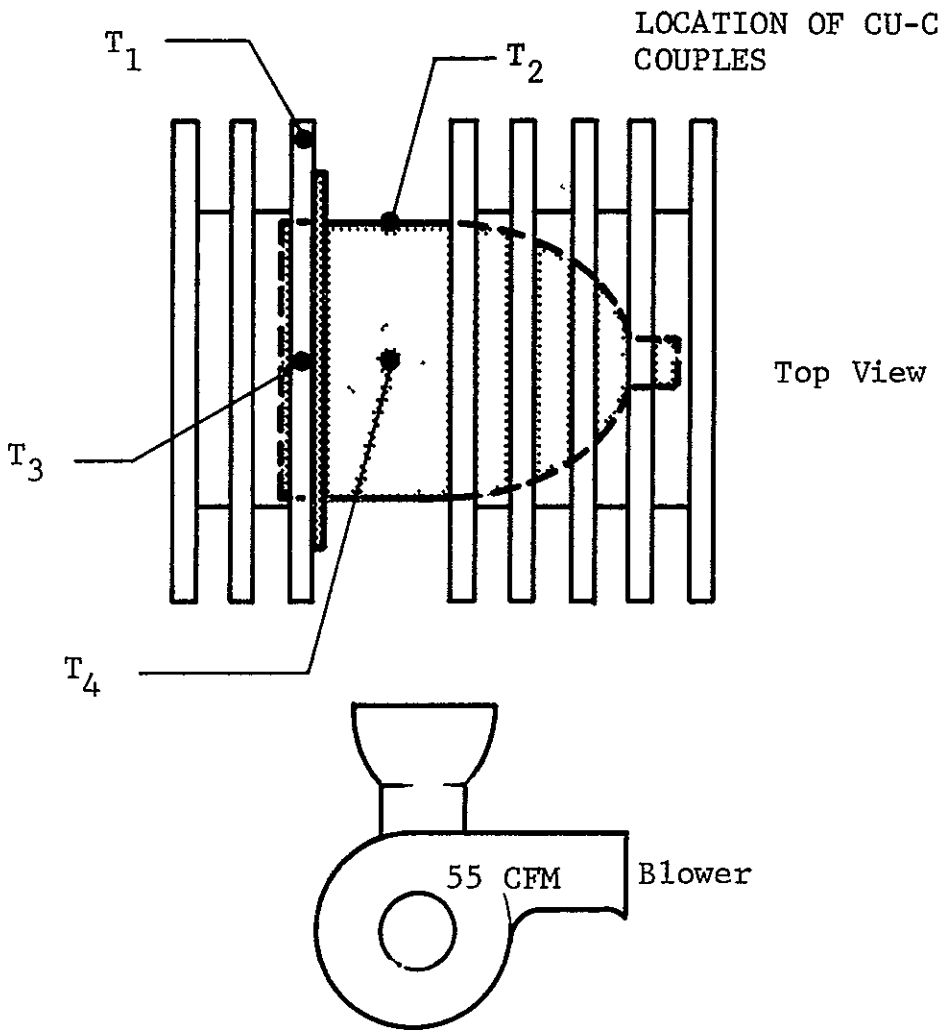

Convection Cooled	T_1 = 380 °F	Aluminum
	T_2 = 380 °F	Ceramic
	T_3 = 390 °F	Aluminum
	T_4 = >400 °F	Ceramic
Blower Cooled	T_1 = 120 °F	
	T_2 = 185 °F	
	T_3 = 110 °F	
	T_4 = 155 °F	

Figure 51.--Temperature Of Lamp (With Radiator)

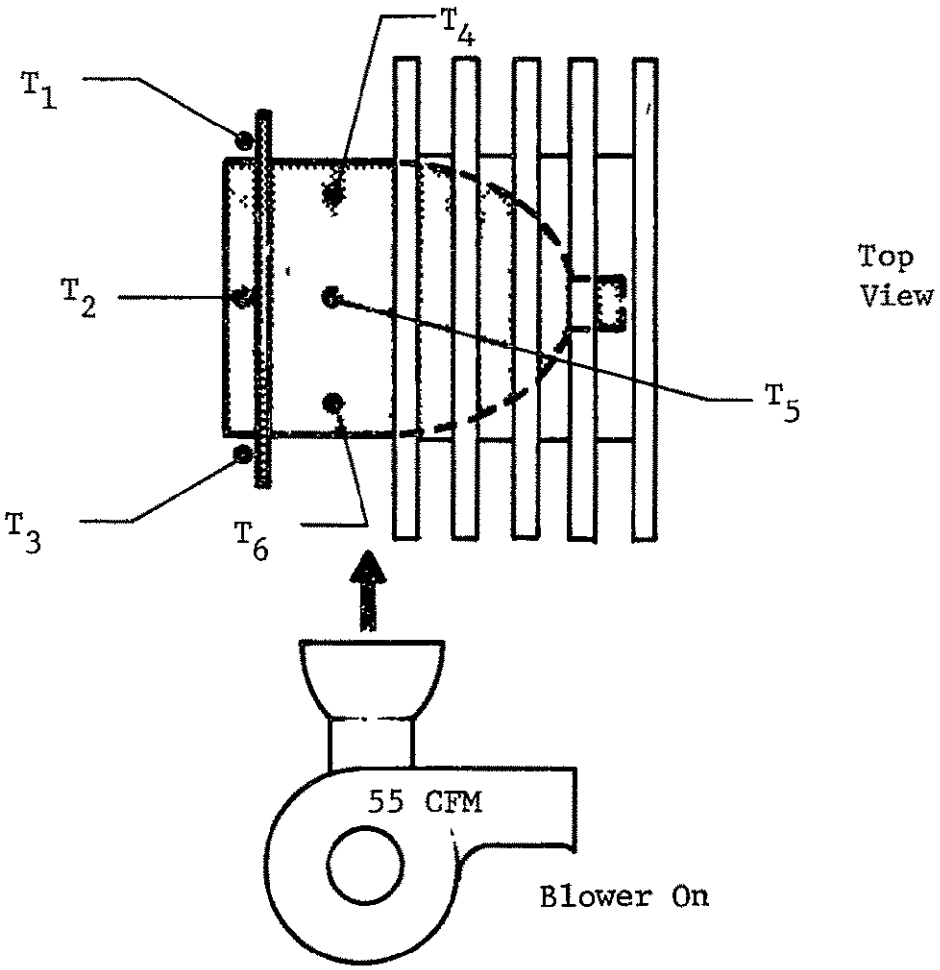

T_1	= 160 °F	Aluminum
T_2	= 160 °F	Aluminum
T_3	= 140 °F	Aluminum
T_4	= 175 °F	Ceramic
T_5	= 150 °F	Ceramic
T_6	= 145 °F	Ceramic

Figure 52.--Temperature Of Lamp (Without Radiator)

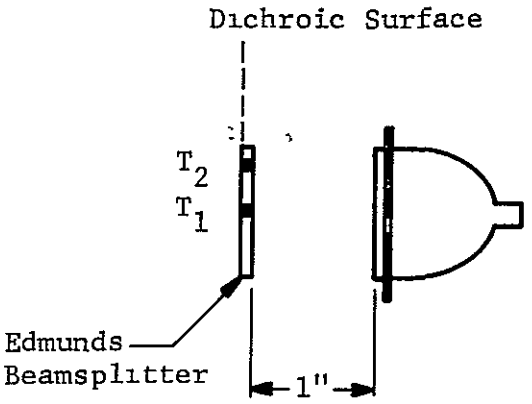

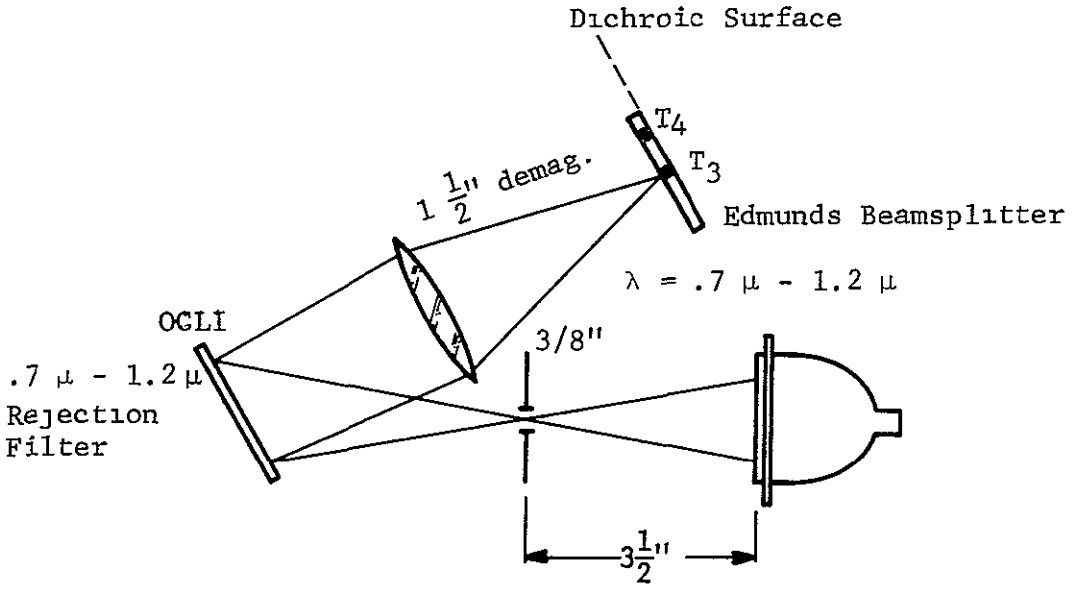

EXPECTED* TEMPERATURE OF FILTER

T_1 = 110 °F

T_2 = 110 °F

EXPECTED* TEMPERATURE OF FIBER OPTICS

T_3 = 120 °F

T_4 = 110 °F

* These measured values indicate the temperatures of critical components to be expected in the remote Oculometer.

Figure 53.--Temperatures Of Optical Elements Adjacent To Lamp

PEK Lamp

A similar experimental study was performed with a PEK 35 watt xenon short arc lamp. The experimental arrangement is shown in Figure 54. The arc image was projected onto the entrance slit of the monochromator, and the intensity measured at various parts on the arc (Figures 55, 56 and 57). The spectral radiance was determined as described for the Varian lamp experiments and the appropriate scale was then applied on the right hand side of Figures 56 and 57. The major component of the radiation has an average spectral radiance of 0.2 $W/cm^2/steradian/Å$ - as previously determined for the Varian lamp. A small fraction of the radiation has a peak spectral radiance of 0.5 $W/cm^2/steradian/Å$ - again closely corresponding to the Varian lamp results.

Assuming an F/1 arc collection system, the Oculometer needs to ulıtize about 0.016 inch of the arc. It is apparent from Figures 56 and 57 that this requirement can just be met with this PEK (35 watt) lamp, but at a spectral radiance of between 0.1 and 0.2 $W/cm^2/steradian/Å$. The maximum spectral radiance exists only over a region of about 0.004 inch. This suggests that a higher power lamp (which would have a proportionally larger arc) could supply radıation at the maximum xenon spectral radiance in sufficient quantity to meet the Oculometer requirements.

Operating life.--Three lamps were evaluated. Each failed, due to rapid electrode burn-up, after about one hour of operatión. The manufacturer claims a 200 hour average life for this lamp. The cause of the failures is not known. It is possible that the problem is associated with the low power rating (and thus small size) of the lamp.

Conclusions·

1) The 35 watt PEK lamp does not appear to be suitable, owing to short life time. Also, the size of the arc is marginal, in terms of satisfying the requirements of the Oculometer.

2) The 150-watt Varian lamp is selected for the present Oculometer. It can supply the necessary quantity of radıation at a peak spectral radiance of 0.2 $W/cm^2/steradian/Å$, it can operate in any orientation, and it has a unique, rugged construction.

3) A 500 watt lamp might be desirable if the highest possible spectral radiance is desired.

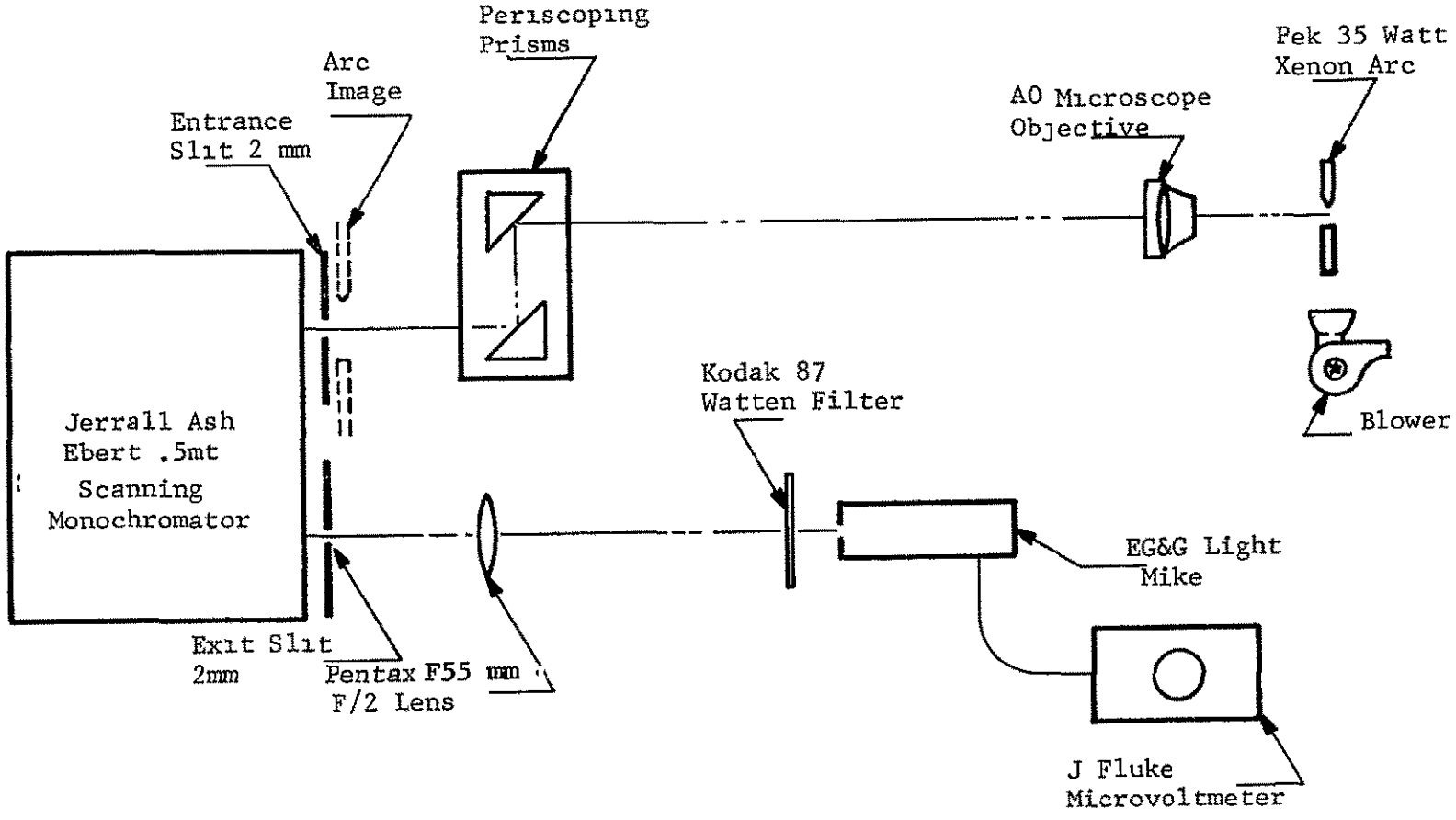

Figure 54.--Experimental Arrangement For PEK Lamp Study

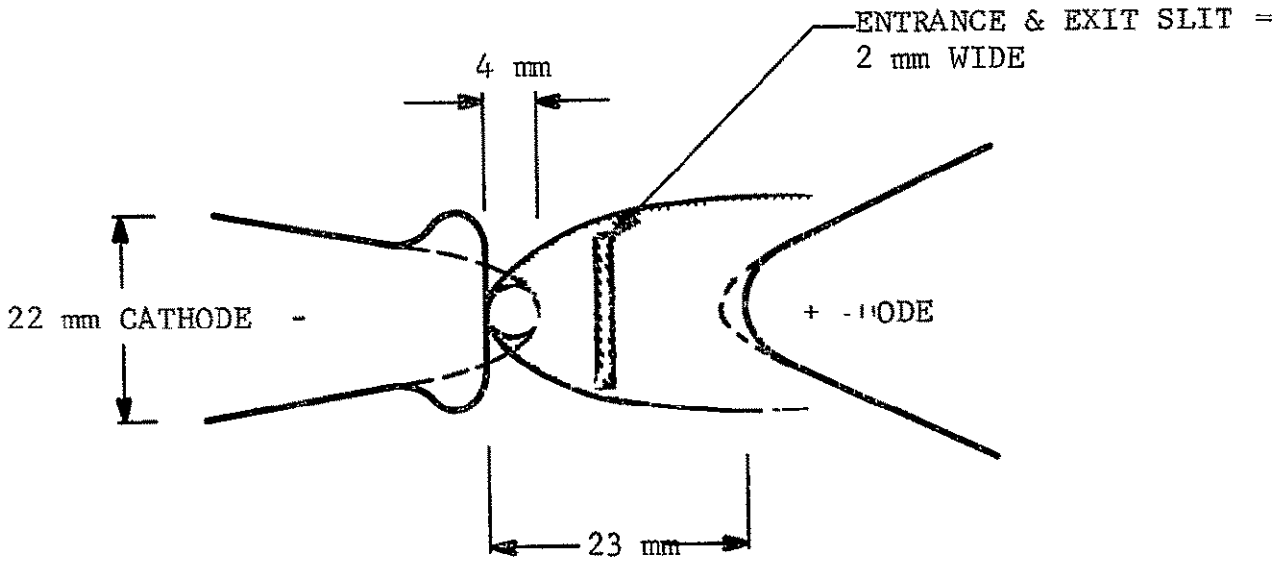

Figure 55.--Arc Image At Entrance Slit Of Monochromator (PEK Lamp)

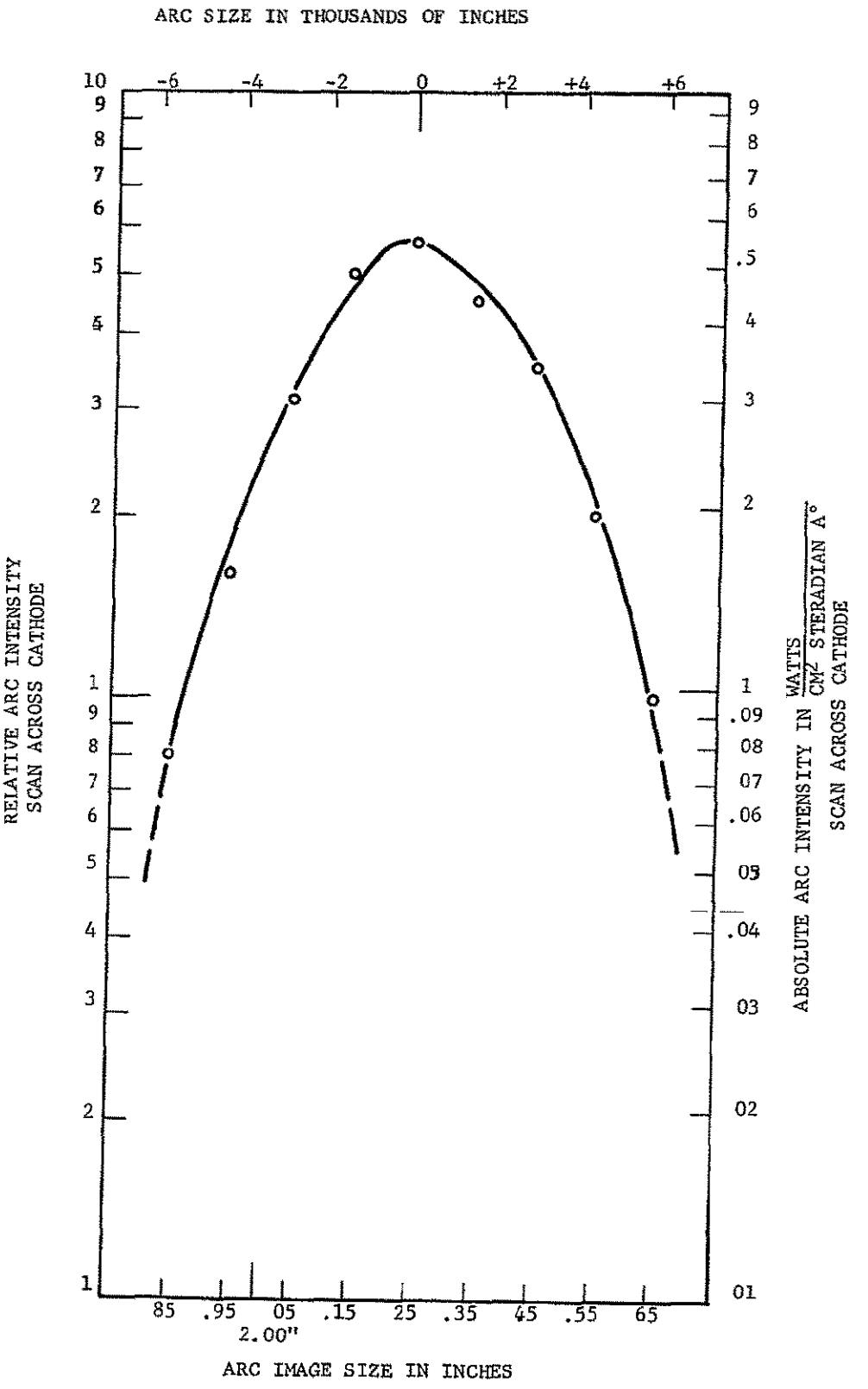

Figure 57.--Intensity Of PEK 35 W Short Arc Lamp

4) The Varian 150-watt lamps are presently made with a hydroformed reflector of relatively low optical quality. It is actually part of the envelope of the lamp. The 500-watt lamp uses a separate high quality electroformed reflector within the envelope of the lmap. The collection efficiency of this lamp, particularly for the low divergence/high spectral radiance components, may therefore by superior. A 150 watt lamp with the high quality electroformed reflector may be available, from Varian, within 6-12 months.

5) One consequence of the relatively low optical quality of the present Varian 150 watt elliptical reflector is that the arc image may be formed anywhere from 1/2 to 6 inches in front of the window (manufacturing tolerance). Varian has reclassified the elliptical reflector tubes as developmental and offers the parabolic reflector as standard. Presumably, when the high quality elliptical reflectors become available the tolerance of the arc image focal point will be tightened.

SYSTEM MODIFICATIONS

In principle, the Oculometer could be made to operate at greater nominal ranges, by simply increasing the focal length of the telephoto lens system. In the present design, however, this would not be possible (without radical change), since it would require a corresponding increase in the clear aperture diameter through the moving mirror unit in order to preserve the design system f/number. The system could, of course be designed to work at, say a 100-inch, nominal range and then operated at smaller nominal ranges than this by insertion of suitable lenses. However, the physical size of a system designed to operate at a 100-inch range would be significantly greater than the present unit design.

Operation with mirror unit demounted.--Conceptually, the mirror box could be demounted from the main unit and the system operated with the two units separated (Figure 58). The range from the eye to the mirror unit would be limited to the presently specified maximum nominal range (40 inches) (a clear aperture limitation which could be overcome by making a larger moving mirror). The range (R) from the mirror box to the (separated) main unit (Figure 58) could, in principle, have any value. Practically it is limited by the physical size of the lens attachment that has to

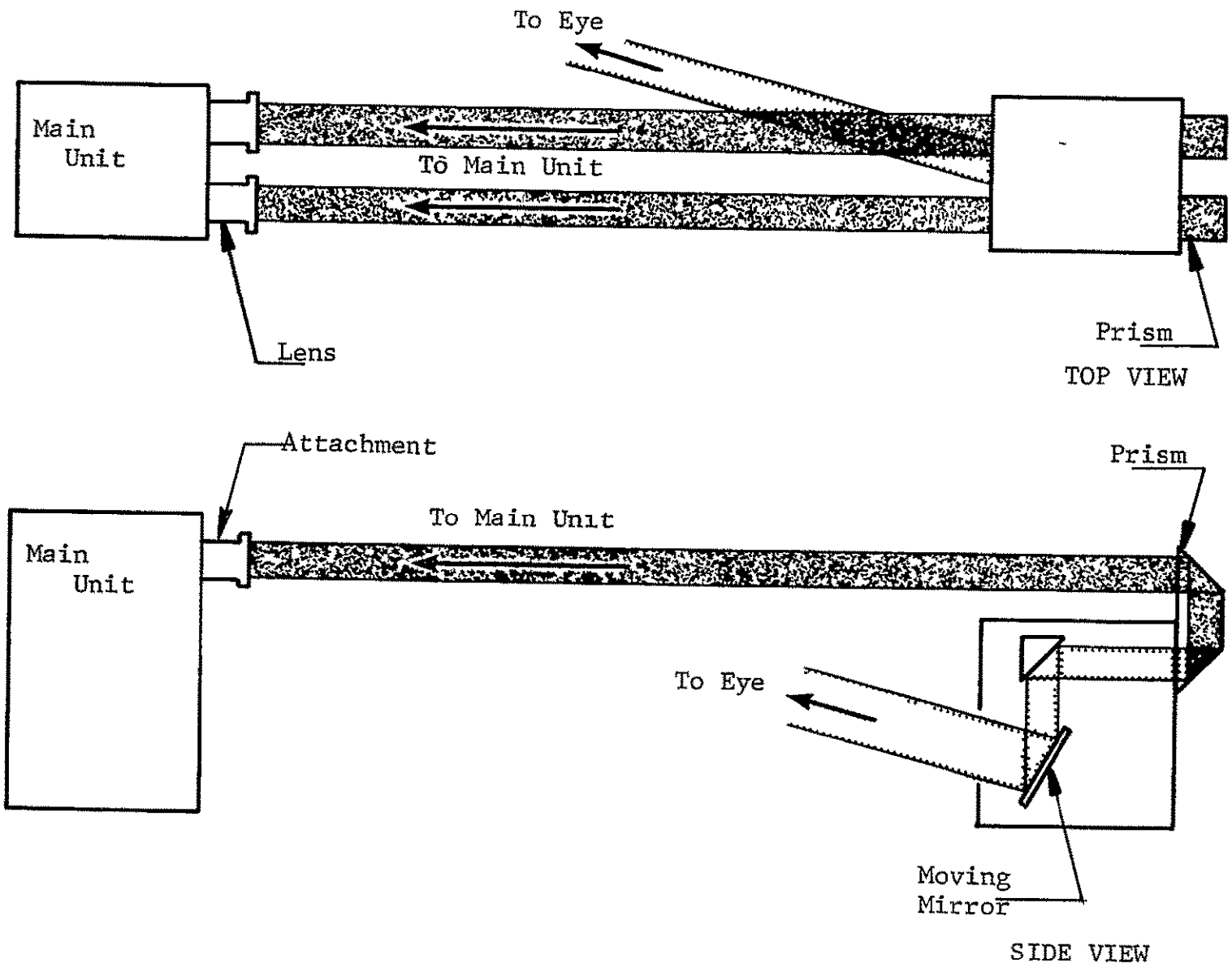

Figure 58.--Mirror Box Demounted And Operating With Separated Main Unit

be added to the remote unit and also by the optical tolerances of the surfaces in the mirror box. A value of R of up to several feet would probably be readily practical.

The lens attachment, required for the remote unit in this separated mode of operation, consists of three lenses, L1, L2 and L3, as in Figure 59. L1 is designed to image the defining aperture (A) of the mirror box onto L2. L2 is stopped down so that the image of A exactly corresponds to the clear aperture of the stop. L2 is designed to image L1 onto L3. L2 is almost at the location of the image of the eye as formed by L1, and thus has little effect upon it. L3 is designed to form a virtual image of the eye at a distance (from L3 in the negative direction) within the range 28 inches to 40 inches, and at unity magnification. The radiation received, therefore, by the main unit from L3 appears to be from a unity magnification image of the eye, located at a distance of between 28 inches and 40 inches from the main unit. The effective f/number of the system is determined by the diameter of the clear aperture, A, just as in the regular mode of operation with the mirror box mounted to the main unit. Since the lateral magnification (between the eye and the eye image as seen by the main unit) is unity, the axial magnification will also be unity. Thus, to a first order, as the eye moves axially by ±6 inches, the eye image as seen by the main unit will also move axially by ±6 inches. Thus, the lens attachment has the effect of making the eye appear, to the main unit to be in such a position that the (unmodified) optical system of the main unit can focus a correct size eye image, of the correct intensity, onto the sensor photocathodes.

The illumination system will have an identical attachment (L1, L2, L3) which, by an exactly similar argument, will correctly illuminate eye space.

Accommodation sensing.--As previously discussed the basic (unmodified) system will be capable of sensing accommodation. When the system is in the normal track mode, the sensing aperture of the scanning photomultiplier auxiliary sensor should be kept in a fixed position, close to the edge, and inside, of the pupil.

The 90-degree segment obscuring aperture, in the mirror box, will have the effect of displacing the virtual center of the collection and illuminating apertures. In a condition of accommodation error of the eye, this produces a gradient in the pupil intensity. As the 90-degree segment rotates, the pupil gradient

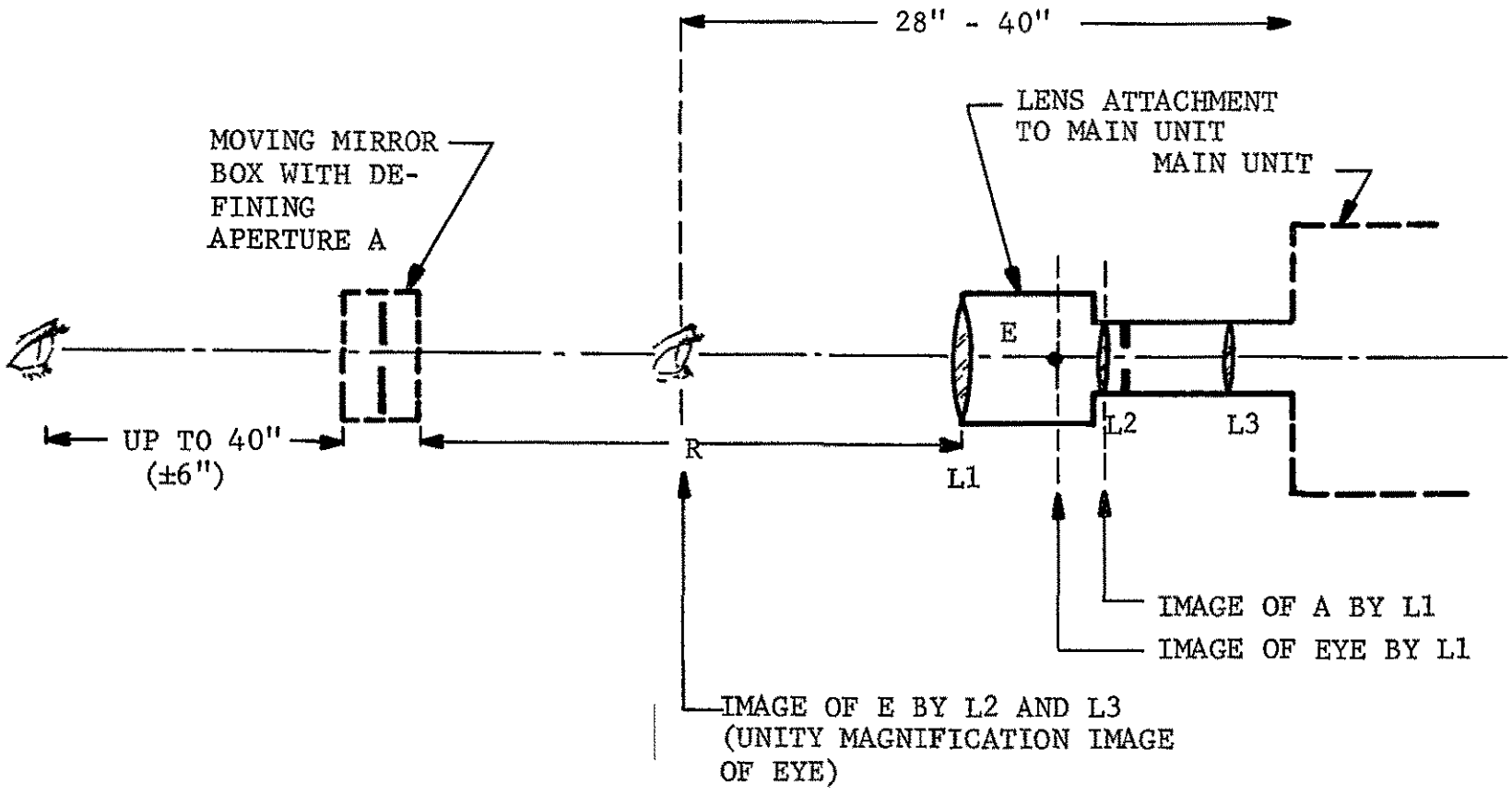

Figure 59.--Main Unit Separated From Mirror Box (Unfolded Optics)

will oscillate, and thus the video signal from the auxiliary sensor will be modulated at a frequency corresponding to the aperture rotation rate. The magnitude and phase of this modulation is proportional to the degree and sign of the accommodation error of the eye (relative to the Oculometer aperture).

REFERENCES

1. Interim Report· System Design Study for an Optimal Remote Oculometer for Use in Operational Aircraft, Honeywell Radiation Center, December 1968, Contract NAS 12-531.

2. Interim Report: Laboratory Oculometer, Honeywell Radiation Center, September 1968, Contract NAS 12-531.

3. The Eye, Volume 4, Chapter 7, edited by H. Davson, Academic Press, New York, 1962

APPENDIX A

For ideal operation of the bright pupil technique, it is clear that the eye lens should be accommodated so that the score is sharply imaged onto the retina and, correspondingly, that the source image on the retina itself be sharply imaged onto the collection aperture. In practice the eye will not, in general, be in this exact state of accommodation.

Let the eye be focussed for a range X and let the Oculometer aperture be at a range R, (Figure A.1). Consider a point source on the retina. It will form a blur circle at the collection aperture (at range R) of diameter Δ where,

$$\Delta = \frac{(R - X)d}{X}$$

where d is the diameter of the pupil in mm.

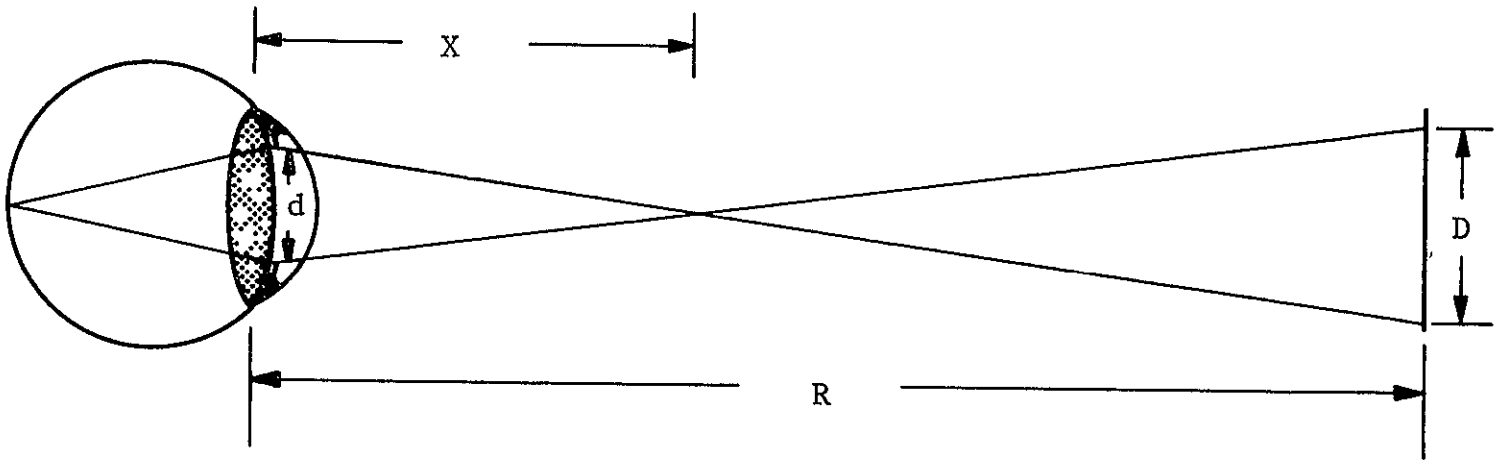

Figure A.1.--Out-Of-Focus Retinal Image Formation

The angular size of this blur is,

$$\theta_{\Delta} = \frac{\Delta}{R} = \frac{(R - X)d}{RX}$$

$$= \delta D \; d \; 10^{3}$$

where δD is the power change (in dioptres) needed to change the focus of the eye from range X to range R.

Similarly a point source at range R will produce a retinal blur circle diameter of the same angular size θ_{Δ}.

Thus, the actual image of a point source at R returned via the retina and a beam splitter to a screen at range R will be the convolution of uniform blur circle of diameter θ_{Δ} with itself. Thus the effective angular size of the blur in the retinal image can be assumed to be, approximately,

$$\theta'_{\Delta} = \sqrt{\theta_{\Delta}^{2} + \theta_{\Delta}^{2}} = \sqrt{2}\,\theta_{\Delta} = \sqrt{2}\,\delta D \; d \; 10^{-3}$$

Let F_{β} be defined as,

$$F_{\beta} = 1/\theta'_{\Delta}$$

Then,

$$F_{\beta} = \frac{1/\ 2\ 10^{3}}{\delta D d}$$

APPENDIX B

PARTS LIST REMOTE OCULOMETER OPTO-MECHANICAL ASSEMBLY

ITEM NO. | DESCRIPTION

1 Beam Splitter

OCLI Narrow Band

Reflectivity 50% ±5%
Transmissivity 50% ±5% For Both Hor. and Vert. Pol.
Band Center 8200 A°+ 750 A -250 A°
Surface-Flatness - 1/4 ring, quality - 60-40; Angle ± 2' arc
Orientation - 45° for Horizontal Pol.
- 90° for Vertical Pol.

Size 1 1/4" x 1 3/4"

2 Filter

OCLI Narrow Bandpass BPF-1

Center Frequency - 8275A°±41A°
3dB Bandwidth - 100A°
Bandwidth Tolerance
Short Wavelength End $^{+0}_{-50}$ A°
Long Wavelength End $^{+50}_{-0}$ A°

Rejection Characteristics <.5%
Transmission Outside Bandpass

Transmission >70% at band center

Orientation -0°
Surface-Flatness - 1/4 ring, Quality - 60-40, Angle ± 2' arc
Blocking Characteristics -
Short Wavelength End - .20 μ
Long Wavelength End - 1.5 μ
Diameter - 1 1/4 inches

ITEM NO. DESCRIPTION

3 Rotating Aperture
Material - Al.
90° Wedge Opaque
Diameter - 1 inch

Rotating Motor - (Motor Tach Set)

Motor - Inland Motor Corp T-0709 A
Tachometer - Inland Motor Corp T-0709H

4 Autofocussing Lens

Positive Doublet

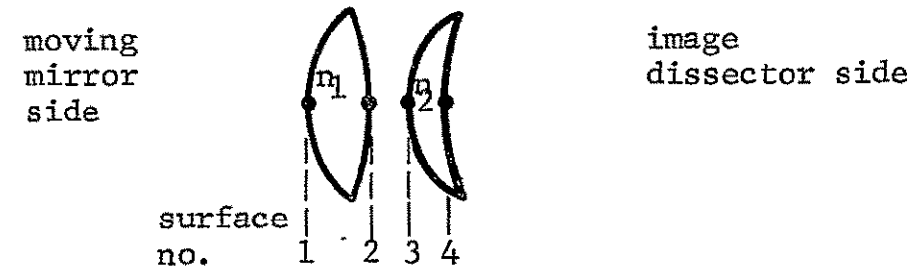

surface no.	Radius of Curvature
1	+6.811 inches ± 0.007 inches
2	-69.22 inches ± 0.3 inches
3	+5.391 inches ± 0.005 inches
4	+26.67 inches ± 0.1 inch

Element No.	DIAMETER	INDEX OF REFRACTION	THICKNESS AT VERTEX	INTERVERTEX SPACING
1	1.375	1.58	.20 inches	.05 inches
2	1.375	1.58	.20 inches	

Lense Decentration - ± 0.004 inches
Lense Thickness Tolerance - ± 0.004 inches
Surface Regularity - 1/2 ring

Coating - all element surfaces (OCLI) H.E.A. Coating Centered at 8200 Å ±1000 Å

ITEM NO.	DESCRIPTION
4 CONT.	Reflectance <1% per surface

Autofocussing Motor - (Motor Tach Set)
Inland Motor Corp T-0709-A Motor
T-0709-H Tachometer

Autofocussing Resolver
Helipot-Rectilinear Cermet 421 series 421-0300

5 Magnification Corrector Lens

Negative Singlet

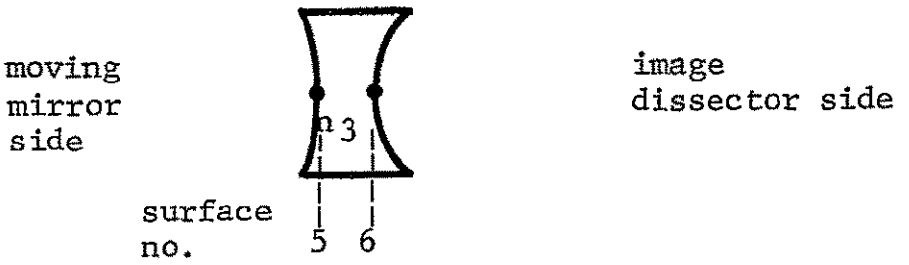

Surface No.	Radius of Curvature
1	-61.00 inches ±0.3 inches
2	1.374 inches ±0.001 inches

Element No.	Diameter	Index of Refraction	Thickness At Vertex
1	.625 inches	1.76	.15 inches

Lense Decentration - ±0.004 inches
Lense Thickness Tolerance - ±0.004 inches
Surface Regularity - 1/2 ring

Coating - Both surfaces (OCLI) H.E.A. Coating centered at 8200 Å ±1000 Å
Reflectance - < 1% per surface

ITEM NO.	DESCRIPTION
6	Beamsplitter (OCLI) Narrow Band (Page 30) Reflectivity - 25% ±5% Transmissivity - 75% ±5% -Both hor. and vertical pol. Band Center 8200 A° +750 A-250 A° Surface-Flatness - 1/4 ring, Quality - 60-40, Angle ±2' arc Orientation - 45° for horizontal pol. - 90° for vertical pol. Size 1" x 1.4"
7	Trapezoidial Prism (entrance and exit windows on the base of the trapezoid) Index of Refraction - 1.60 Surface-Flatness - 1/4 ring, Quality - 60-40, Angle ±2' arc Coating - Entrance and Exit Window (OCLI) - H.E.A. Coating Centered at 8200A° ±1000A° Reflectance - <1% per surface Size - Base - b - 3.5 inches Width - w - 1.0 inches Height - h - 1.0 inches Interior Angles (θ) - 45° ±2' arc 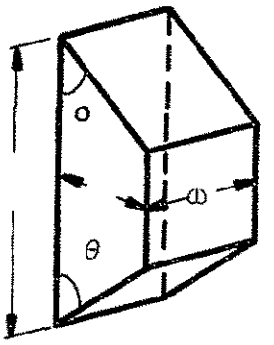
8	Image Dissector Tube Type - ITT F4012 Photocathode - S25 Aperture Width - 0.005 inches Focussing Coils Deflection Coils Cleveland Electronics VF-161-L, Cleveland Electronics VYL-198

ITEM NO.	DESCRIPTION
11	Right Angle Prism
	Size - 25 x 25 x 35 mm Material - 1.6 index glass Surface-Flatness - 1/4 ring, Quality - 60-40, Angle ±2' arc Coating on Entrance and Exit Window - (Ocli) H.E.A. Coating Center at 8200A° ±1000A° Reflectance <1% per surface Interior Angle 45° ±2' arc
12	Scanning Photomultiplier
	Type - ITT 4075 Photocathode - S25 Aperture Width - 0.100 inches Focussing - Electrostatic Deflection Coil - Cleveland Electronic VYLFA-722-PC
20	Xenon Arc Source
	Type - X6163S (Varian) Power - 150 Watts Reflector Type - Elliptical Source Focus Distance To The Window nominally 3 1/2" but Varying From 5 1/2" to 1 1/2" Window - Sapphire Window Coating - (OCLI) Wide (page 7) Band Cold Mirror 3dB cutoff 7400A° Power Supply - (Varian) P-150S-6
21	Xenon Arc Radiator
	Type - Convective, Supplemented by Forced Air Finned Section - (Varian) R-150-1 Blower - 55 C.F.M. Centrifugal

ITEM NO.	DESCRIPTION
22	SAME AS NO. 2
23	Condenser Lens Lens Type - Aspheric Pyrex (Jaegers No. 742648) Lens Shape - Plano Convex Focal Length - 30 mm Diameter - 44 mm Edged Down to 31 mm Thickness - .595 inches Coating - (OCLI) - H.E.A. Coating Centered at 8200A° ±1000A° Reflectance - <1% per surface
24	Condensing Aperture Diameter - 1/16"
25	Fiber Optics Bundle Fibers - 50 μ (American Optical) Correlation - Totally incoherent Format Circular - Diameter - 1/16" Bond - High Temperature Epoxy Numerical Aperture - .55 Length - 2 feet Sheath - Monocoil Crush Resistant Aluminum Tubing End Tips - Metal Transmission - Greater than 45% at 8275A°

ITEM NO.	DESCRIPTION
26	Expander Aperture Diameter - 1/16"
27	Expander Lens Lens Type - Aspheric Pyrex (Jaegers No. 742652) Lens Shape - Unsymmetrical Focal Length - 26 mm Diameter - 53 mm Edged Down to 25.4 mm Thickness - .680 inches Coating - (OCLI) - H.E.A. Coating Centered at 8200A° ±1000°A Reflectance - <1% per surface Spherical Surface refinished to 80-50 quality
28	Rhomboidal Prism (entrance window on the base of the Rhomboid and to exit window on the top of the Rhomboid) Index of Refraction - 1.60 Surface-Flatness - 2.5 rings, Quality - 80-50, Angle ±2' arc Coating - Entrance and Exit Window (OCLI) - H.E.A. Coating Centered at 8200A° ±1000A° Reflectance - <1% per surface Size - Base - b - 2.5 inches Width - w - 1.0 inches Height - h - 1.0 inches Interior Angles (θ) - 45° ±2' arc

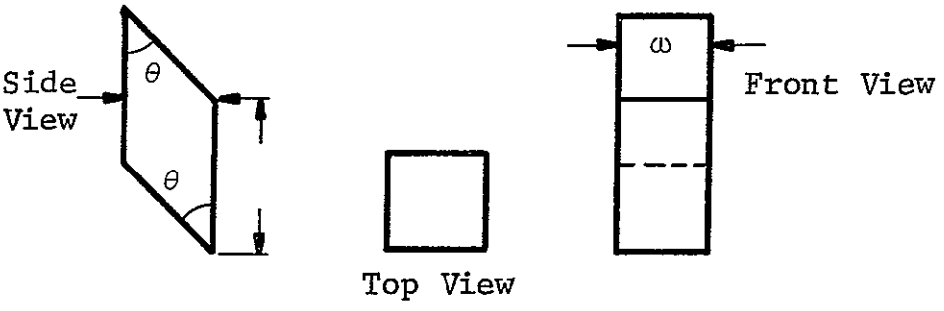

ITEM NO.	DESCRIPTION
29	Same as No. 5 Mechanically Slaved To No. 5 Surface Regularity relaxed to 2.5 rings Surface Quality relaxed to 80-50
30	Same As No. 4 Mechanically Slaved To No. 4 Surface Regularity relaxed to 2.5 rings Surface Quality relaxed to 80-50
31	Narrow Band Infrared Reflector (OCLI) Hot Mirror (page 26) Reflection - 95% at 8200A° Orientation - 45° Size - 1 1/4" x 1 3/4" Surface Regularity 2.5 rings, Quality 80-50, Angle ±2' arc
32	Broad Band Filter Circular - 1" Diameter (a) (Kodak) Wratten 89B Substrate - "B" glass, Regularity 2.5 rings, Quality 80-50, Thickness - .185" Angle ±20' arc. Total Transmission - 95% at 8200A° If Excess Brightness Requires Attention, First Utilize (b) (Corning Glass) 7-59 Substrate - 5850 glass, Regularity 2.5 rings, Quality 80-50, Thickness - 4 mm Angle ±20'arc. Total Transmission - .90 at 8200A°

ITEM NO.	DESCRIPTION
33	Narrow Band Infrared Reflector

(OCLI) Hot Mirror (page 26)
Reflection - 95% at 8200A°
Orientation - 90°
Size - 1" x 1"
Surface-Regularity 2.5 rings, Quality 80-50, Angle ±20' arc

34 Fail Safe Detector

Silicon Solar Cell (Solar System Inc)
Model SS-10
Length - 2 cm
Width - 1 cm
Thickness - .025"

40 Variable Iris Aperture

Edmund No. 40998

Outside Diameter	Aperture Maximum	Aperture Minimum	Thickness
1 57/64"	1 3/16"	3/64"	19/64"

41 Right Angle Prism

Size - 35 x 35 x 49 mm
Material - 1.6 index glass
Surface flatness - 1/4 ring, Quality 60-40, Angle ±2' arc
Coating On Entrance and Exit Window - (OCLI) H.E.A. Coating
Centered at 8200A° ±1000A°
Reflectance <1% per surface

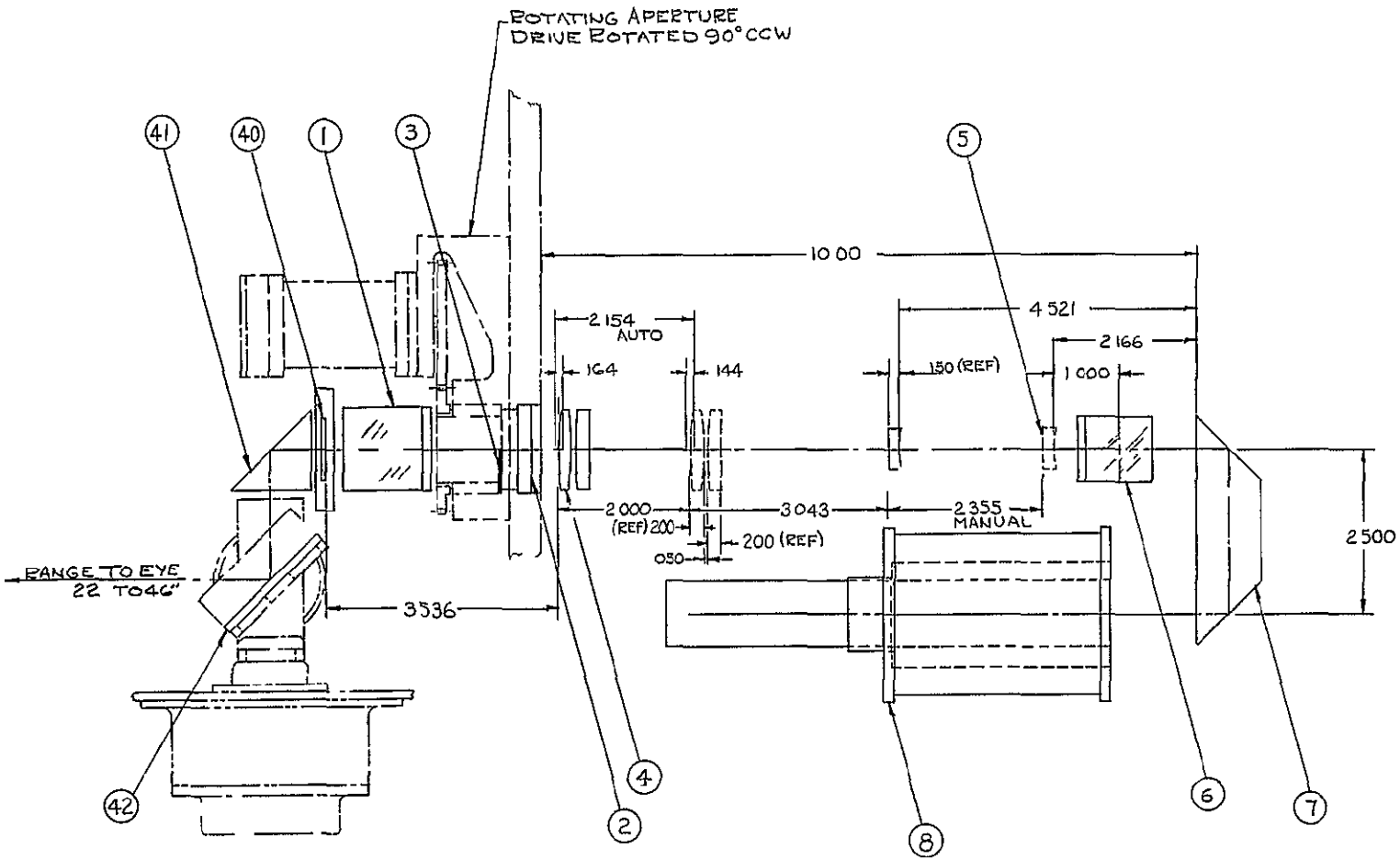

F2100-3109 Drawing Side view, collection optics.

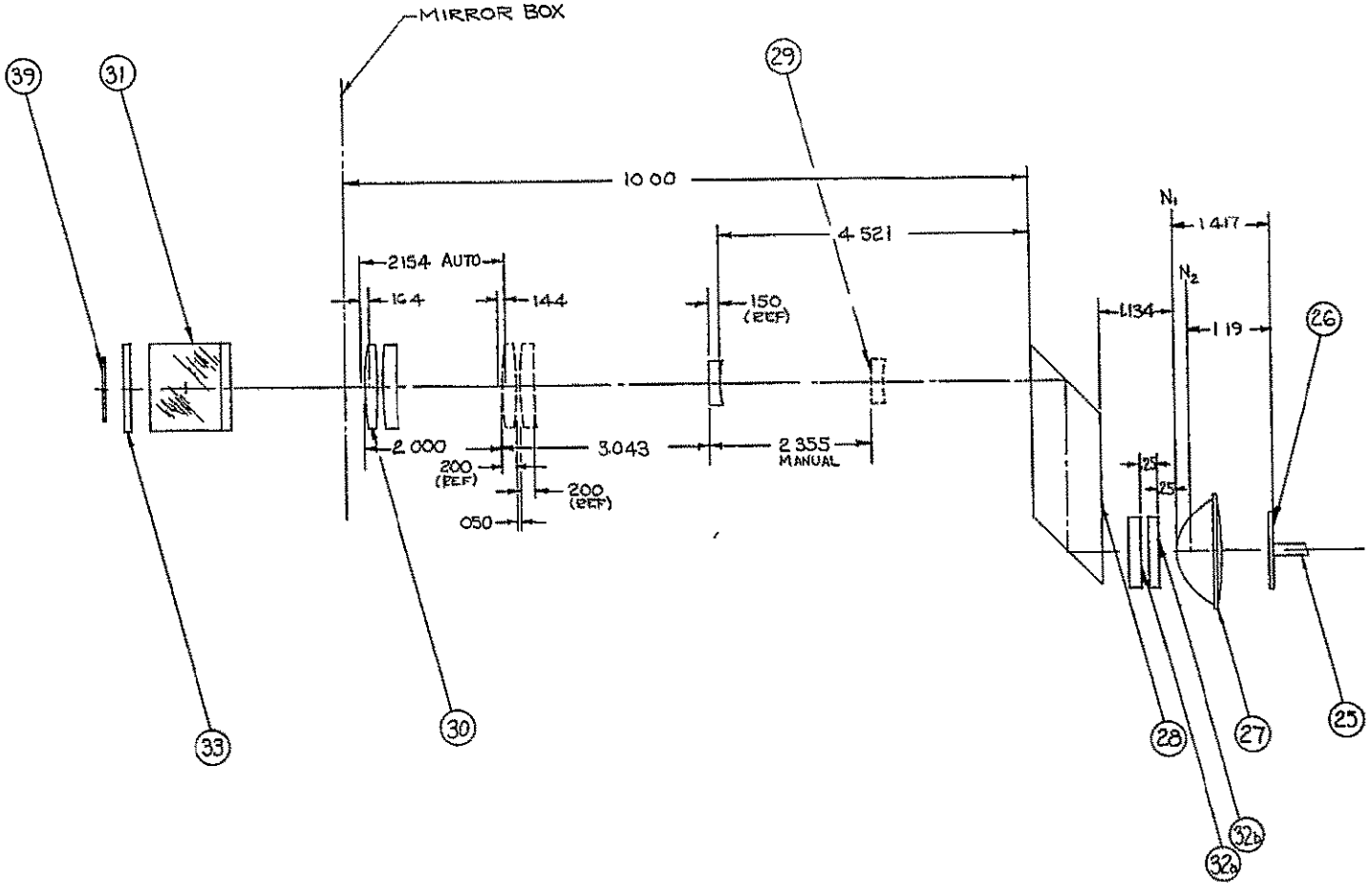

F2100-3111 Drawing Side view, illumination optics.

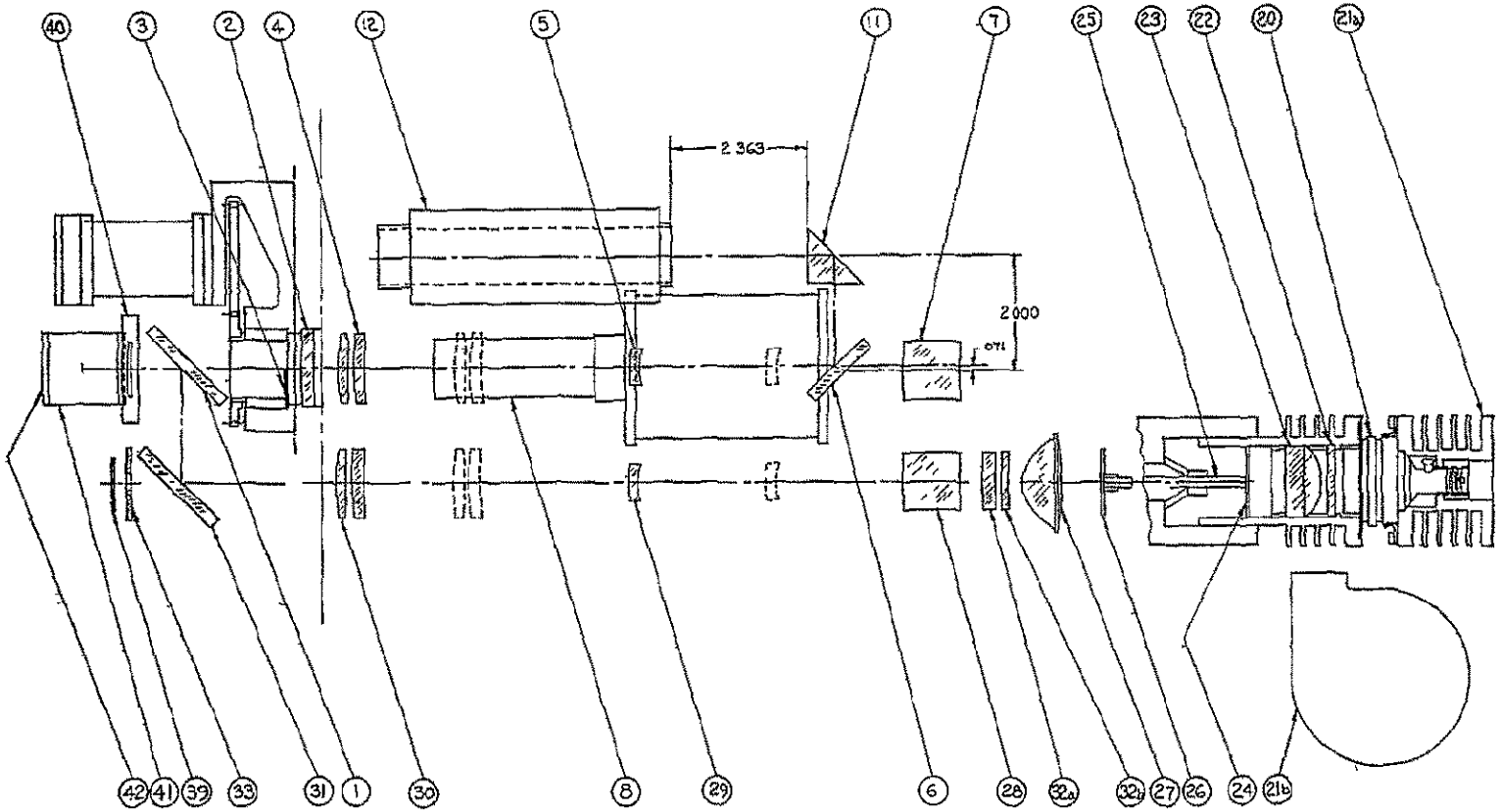

FIG 3

F2100-3112 Drawing Top view, collection and illumination optics

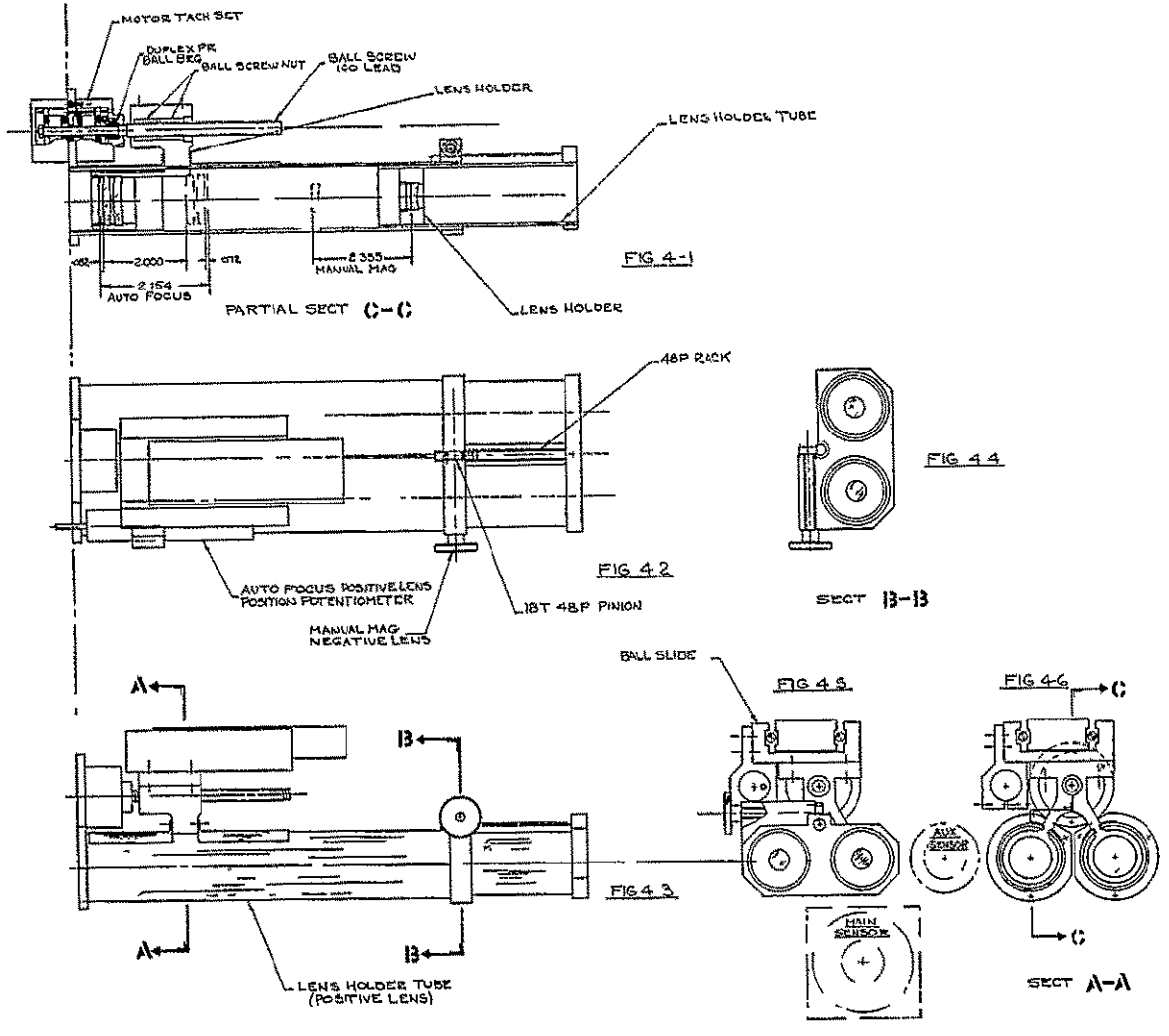

F2100-3116 Drawing Lens, and lens slide, arrangement.

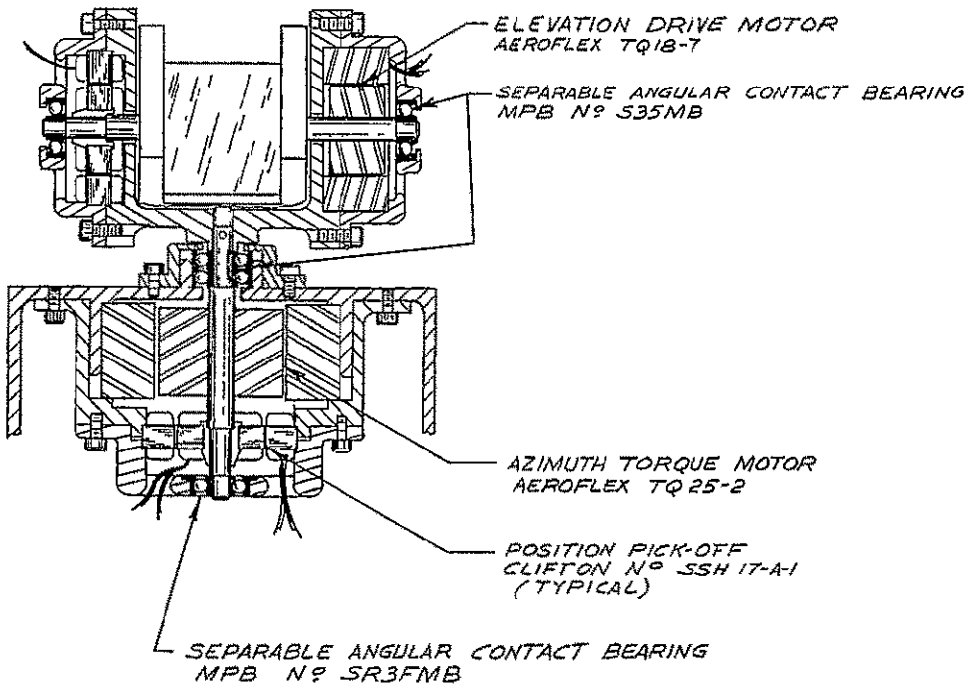

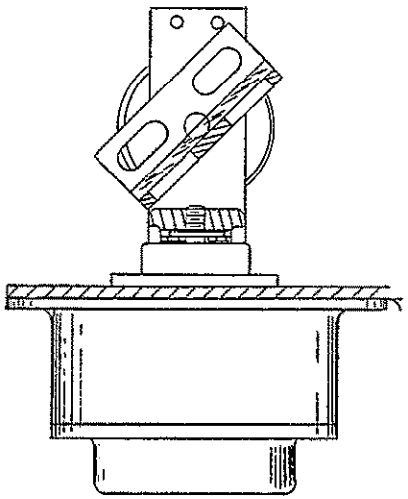

F2100-3114 Drawing Two-axis mirror.

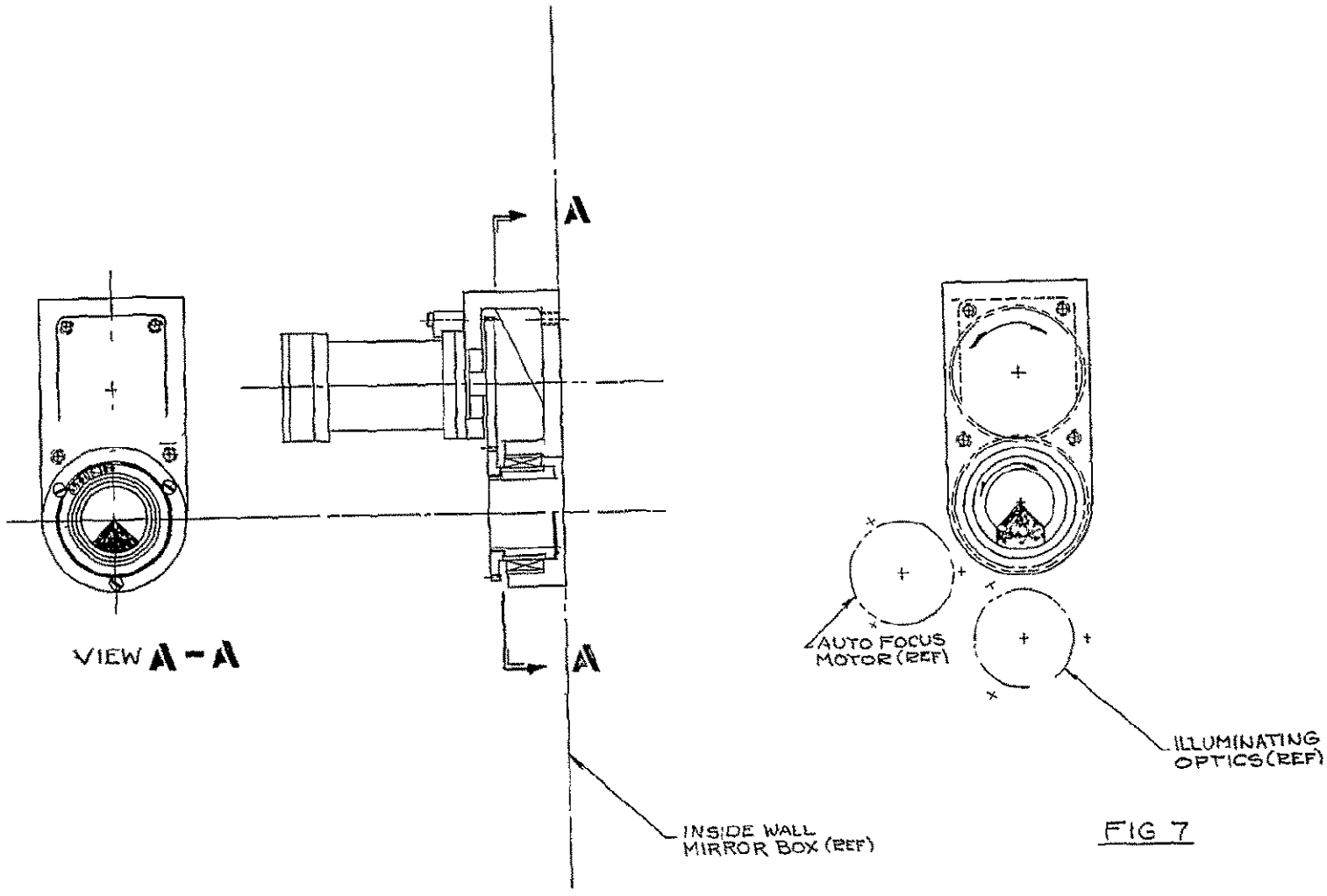

FIG 7

F2100-3113 Drawing Rotary aperture detail.

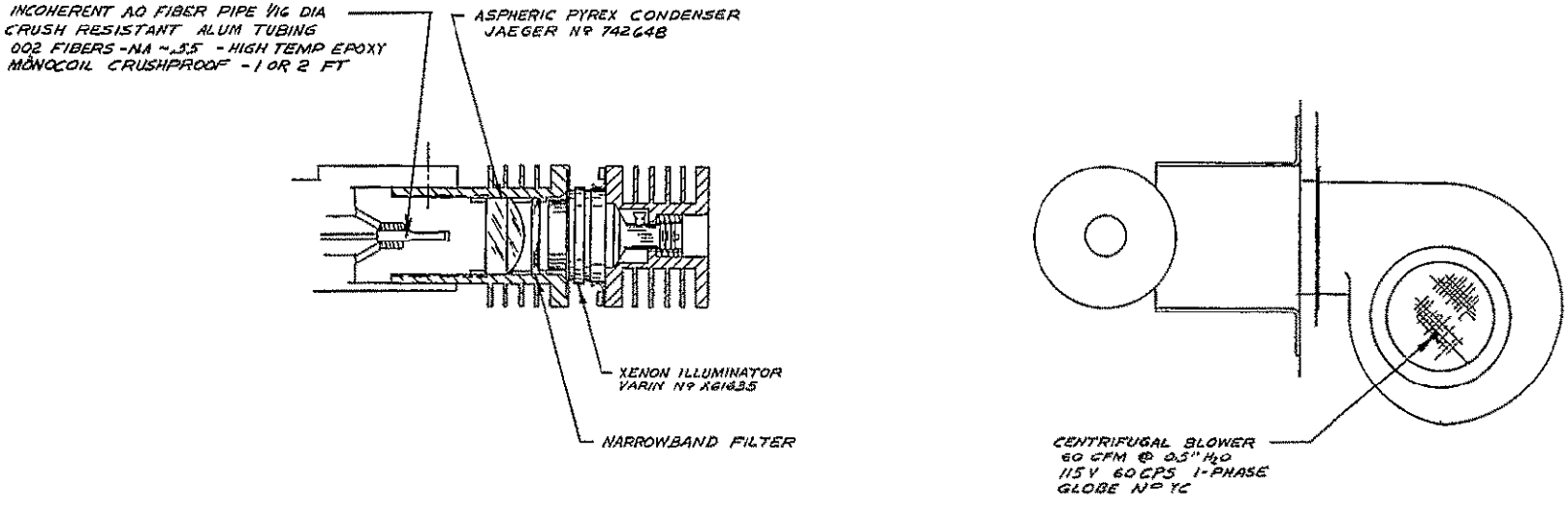

F2100-3117 Drawing Xenon lamp detail.

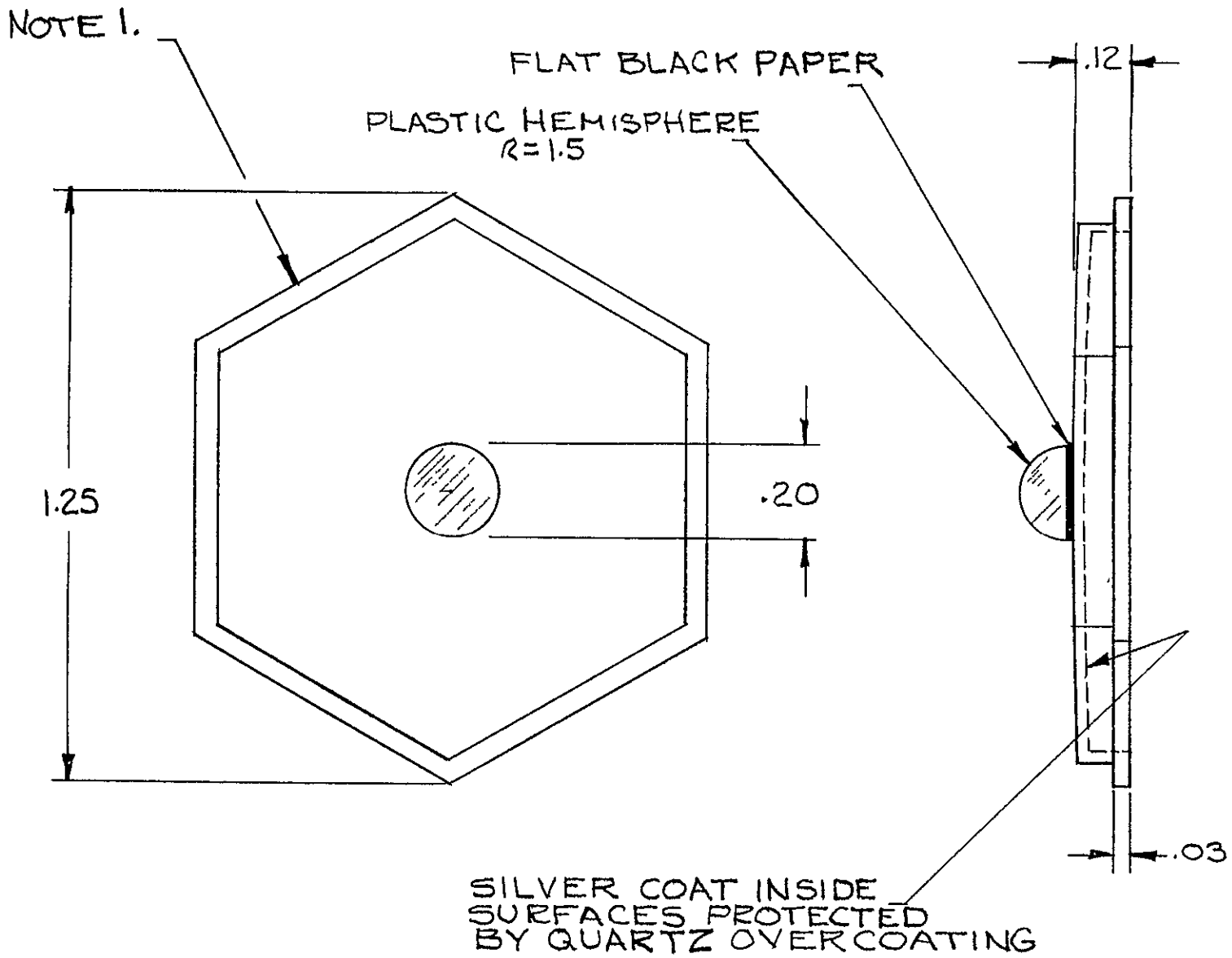

F2100-3115 Drawing Head marker detail.

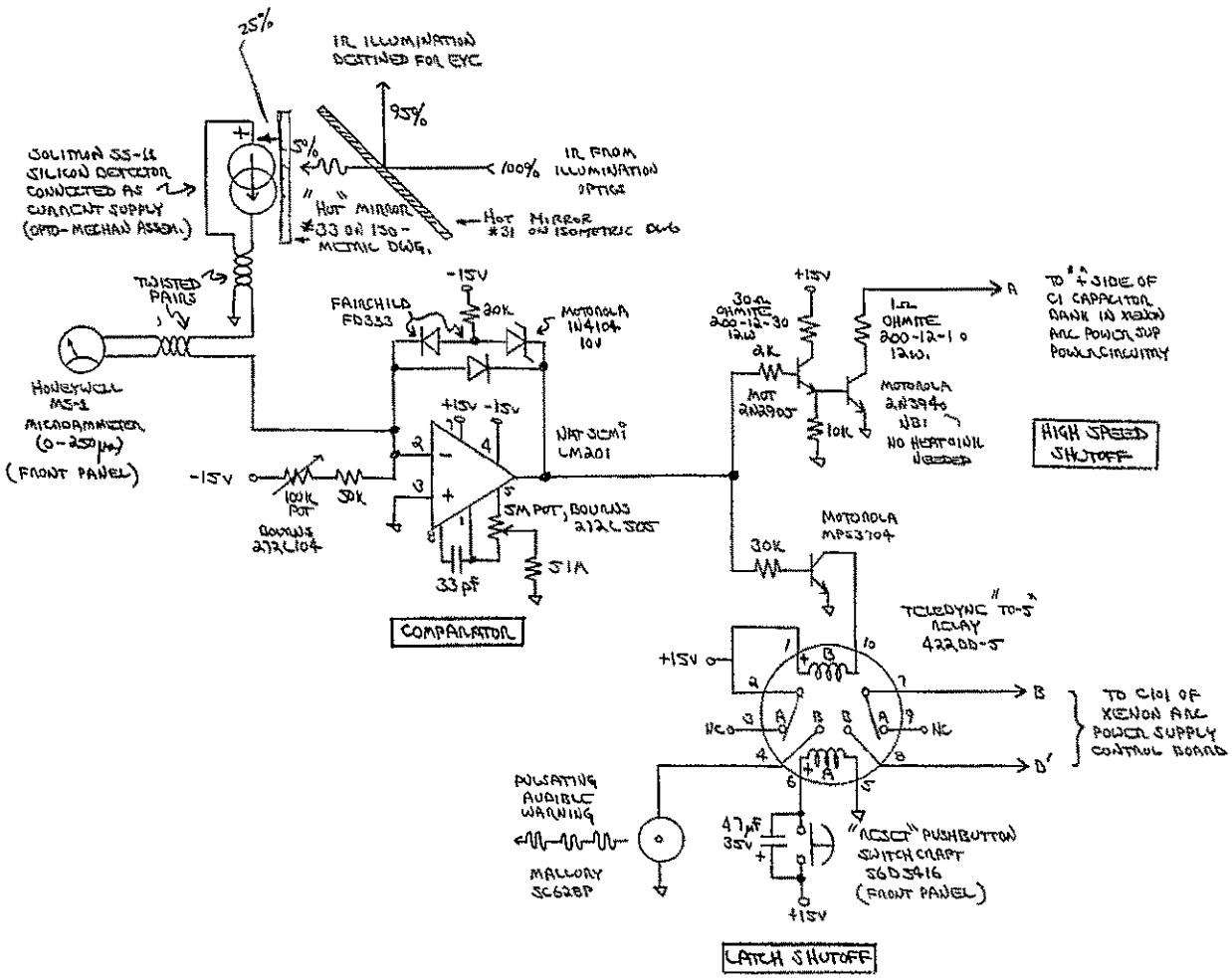

F2100-3108 Drawing Fail safe circuit

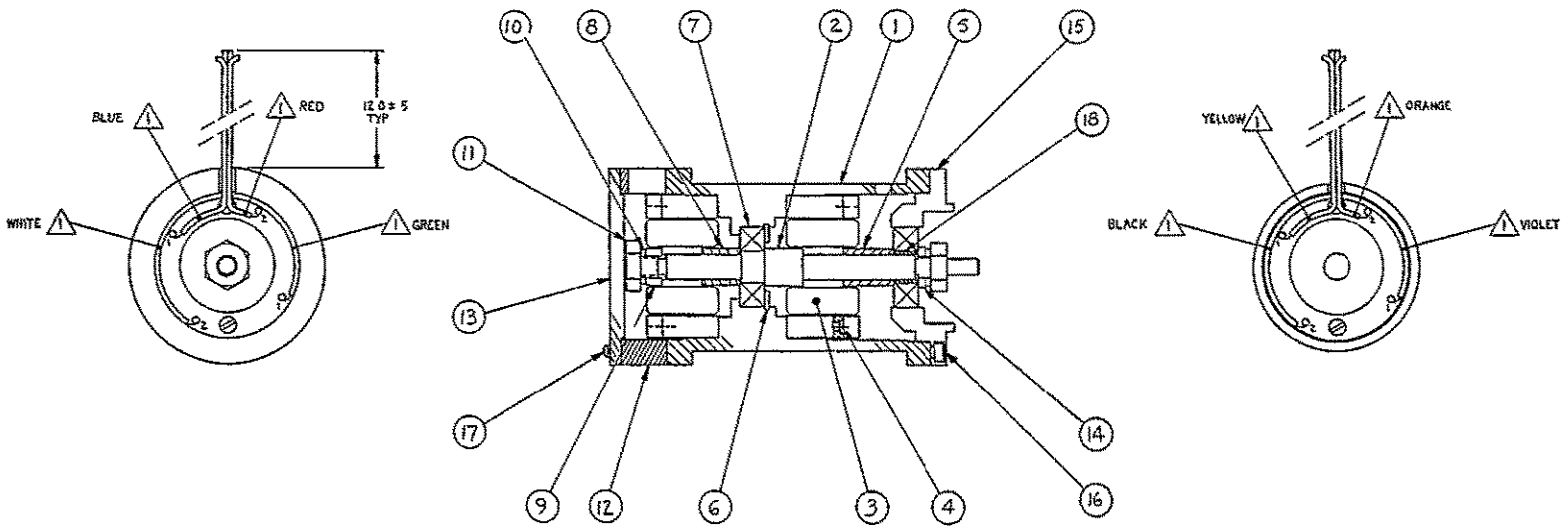

F2100-3008 Drawing Motor Assembly.

ITEM NO.	DESCRIPTION
42	Scanning Mirror
	Size - 1.2" x 1.7" x .2"
	Substrate - Aluminum
	Finish - Kanogen Treated (Nickel Phosphate)
	Coating - Silver $\approx 80 \times 10^{-6}$ inches
	Protective Finish - Quartz $\approx 80 \times 10^{-6}$ inches
	Surface-Flatness - 1/4 ring, Quality 60-40, Angle ±2' arc
	Azimuth (z axis) Motor - Aero Flex - TQ 25-2
	Azimuth (z axis) Resolver - Clifton No. SSH 17-A-1
	Elevation (x axis) Motor - Aero Flex - TQ 18-7
	Elevation (x axis) Resolver - Clifton No. SSH 17-A-1
43	Exit Window
	Size - 3" x 3"
	Material - glass
	Surface Flatness - 1/4 ring
	Quality 60-40
	Angle ±2'
	Coating both faces - OCLI HEA

APPENDIX C

OCULOMETER ACCURACY AND EYE CHARACTERISTICS: ANGLE LAMBDA

1. The angle lambda is the angle between the foveal axis and the optical axis of the eye. The average value of this angle is 5 degrees (Ref 3) (The foveal axis is displaced in visual space from the optical axis in the nasal direction).

2. The Oculometer determines the direction of the optical axis. Provided that there is no unknown rotation of the eye about the optical axis, a determination of the direction of the optical axis defines the direction of the foveal axis. However, errors will be introduced whenever there is unknown rotation of the eye about the optical axis.

Let ψ be the angle of rotation about the optical axis. The corresponding error in the determination of the direction of the foveal axis is:

$$\delta = \frac{5 \pi \psi}{180} = 8.83 \times 10^{-2} \psi$$

3. When the axis of the eye is deflected from the zero (straight ahead) position to some other position, the eyeball moves (nominally) according to Listings Law (Ref 4). This states that any displacement from the zero position is equivalent to a single rotation about an axis in the equatorial plane. (The equatorial plane is a plane in the socket, corresponding to the equatorial plane of the eye in the zero position).

Rotation of the eye about the theoretical axis may arise as follows·

(a) Rotation of the head about the optical axis of the eye.
(b) Deviations from Listings Law.
(c) Rotation of the head about any axis perpendicular to the optical axis of the eye.

These effects are considered in detail below·

3.1 Let the head rotate through an angle α about the optical axis. The ψ is equation (1), is given by

$$\psi = \alpha$$

3.2 According to Ref 5 when there is zero convergence of the two eyes, deviations from the Listings Law are small (e.g., 1/4 degree) for eye rotations of the magnitude incurred in normal vision. For eye rotations of 30 degrees, a 1 degree deviation is reported, and for very large eye rotations the deviation is 3 degrees to 5 degrees.

When the eyes are converging on an object at 30 inches the convergence is about 5 degrees and a deviation of approximately 1 degree may then occur from Listings Law due to convergence.

3.3 Let the eye rotate from the zero position (A) to position (B) (Figure C.1). Now let the head suffer a pure rotation (about one axis) to bring it to position C.

Let OX, OY be rectangular axis fixed in the plane of the pupil of the eye in position A. Let OX^1, OY^1 be the displaced axes at position B. Let θ_1 be the angle between the axis OX and the great circle path AB at A (Figure C.1a). Then, by the nature of the eye rotation (Listings Law), the axes OX', OY' will make the same angle with the great circle BD at B (Figure C.1b) as at A (Figure C.1a). Similarly let θ_2 be the angle, at B, between OX' and to great circle path BC. Then θ_2 is also the angle between OX'' and the great circle BD at C. (Head rotation between B and C).

Now, let the eye be rotated (with no head motion) from the zero position directly to C. Let the great circle angle with OX'' be θ_3, as shown in Figure C.1e and 1f.

Consider the angles in the spherical triangle ABC as in Figure C.2. Let the area of the spherical triangle be Z and the spherical radius r. Then, the sum of the angles of the spherical triangle is given by:

$$\angle A + \angle B + \angle C = \pi + \frac{Z}{r^2}$$

From Figure C.2

$$\angle A = \theta_3 - \theta_1$$

$$\angle B = \theta_1 + \theta_2$$

$$\angle C = \pi - (\epsilon + \theta_2 + \theta_3)$$

where is the angle between OX'' and OX''

$$\therefore \quad \angle A + \angle B + \angle C = \theta_3 - \theta_1 + \theta_1 + \theta_2 + \pi - (\epsilon + \theta_2 + \theta_3)$$

$$= \pi - \epsilon$$

$$= \pi + \frac{Z}{r^2}$$

$$\therefore \qquad \epsilon = \frac{Z}{r^2}$$

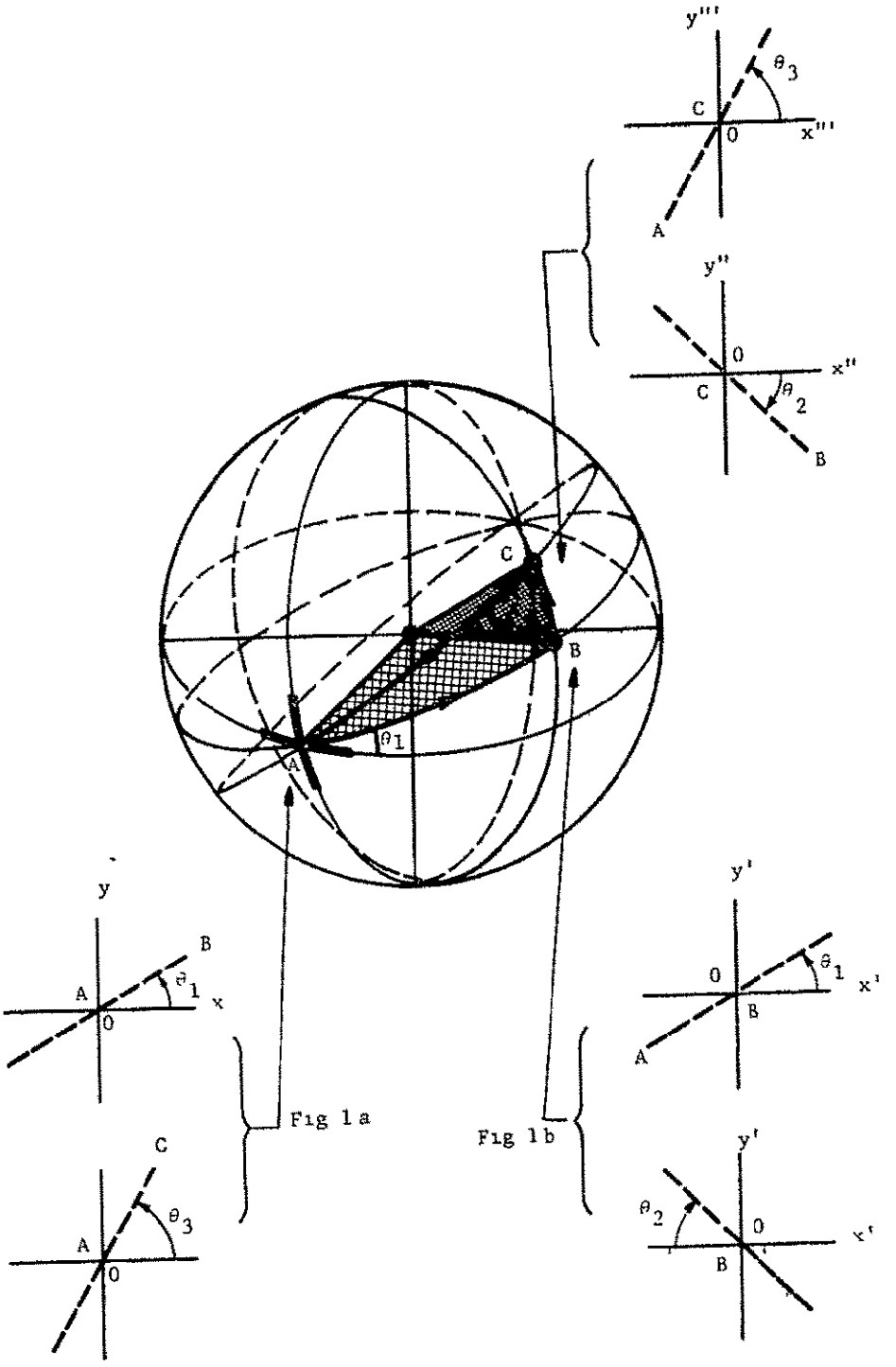

Figure C.1.--Eye and Head Rotations

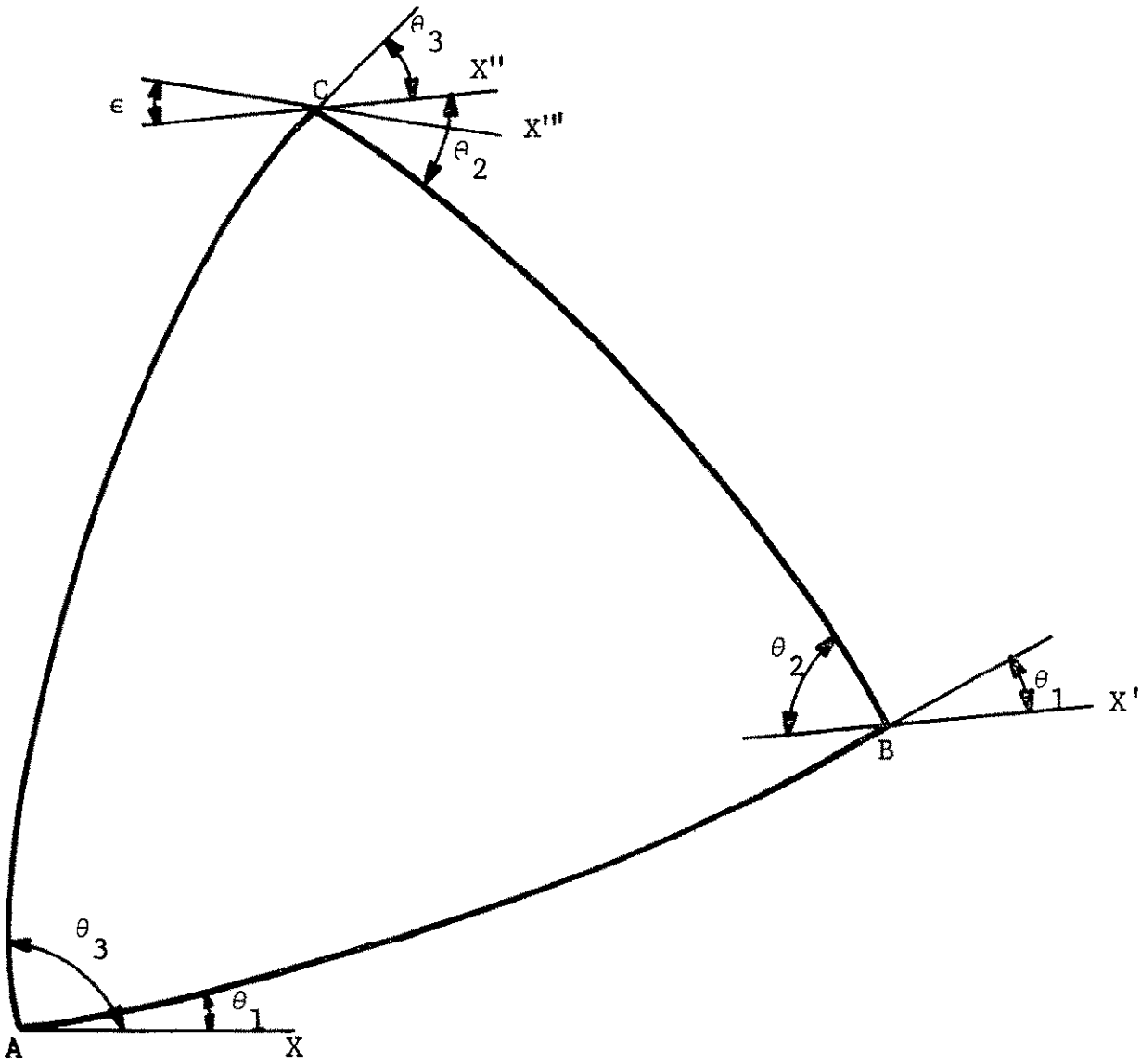

Figure C.2.--Spherical Triangle

The angle ϵ represents a relative axial rotation of the eye (at C) between two cases:

(a) Single pure eye rotation A to C
(b) An eye rotation A to B together with head rotation B to C.

The Oculometer would be calibrated in terms of a pure rotation from A to C. If, in fact, the optical axis of the eye appears at C as a result of the separate motions AB and BD, an error will be introduced, given by equation 1 where:

$$\psi = \epsilon$$

Let the eye motion θ_e° and the head rotation θ_h°. Then, approximately

$$\epsilon^\circ = \frac{\theta_e \, \theta_h}{2} \, \frac{T_1}{180}$$

$$\approx 0.01 \, \theta_e \, \theta_h$$

The corresponding error in the location of the foveal axis is·

$$\delta = 8.8 \times 10^{-2} \, \epsilon \approx 10^{-3} \, \theta_e \, \theta_h$$

The worst case eye fixation error (in degrees) as a function of head and eye rotation is given in the following table:

	Eye Angles (degrees)					
Head Angle (degrees)	5°	10°	15°	20°	25°	30°
5	.025	.05	.075	.1	.125	.150
10	.05	.1	.15	.2	.25	.3
15	.075	.15	.225	.3	.35	.45
20	.1	.2	.3	.4	.5	.6

For Reference, 3 mils is equal to approximately 0.17 degrees.

4. Summarizing the Errors:

(a) Rotation of the head about the optical axis of the eye: 0.09 degrees error per degree of rotation of the head. (Errors due to rotations of the head about the optical axis can be corrected if both eyes are tracked, thereby defining the direction of the horizontal axis fixed in the head).

(b) Deviations from Listings Law.
0.025 degrees for moderate (normal) eye rotation
0.1 degrees due to convergence at an object 30 in. from the eye.

(c) Head rotations, other than in (a) above.

NEW TECHNOLOGY APPENDIX

The following new technology items are identified as new or innovative:

1. Coarse Acquisition Sensor

   Design of Advanced Remote Oculometer, September 1969, p. 7

2. Autofocus System

   Design of Advanced Remote Oculometer September, 1969, pp. 24-40